DOT/FAA/AR-02/103

Office of Aviation Research
Washington, D.C. 20591

Parametric Study of Crashworthy Bulkhead Designs

December 2002

Final Report

This document is available to the U.S. public through the National Technical Information Service (NTIS), Springfield, Virginia 22161.

U.S. Department of Transportation
Federal Aviation Administration

NOTICE

This document is disseminated under the sponsorship of the U.S. Department of Transportation in the interest of information exchange. The United States Government assumes no liability for the contents or use thereof. The United States Government does not endorse products or manufacturers. Trade or manufacturer's names appear herein solely because they are considered essential to the objective of this report. This document does not constitute FAA certification policy. Consult your local FAA aircraft certification office as to its use.

This report is available at the Federal Aviation Administration William J. Hughes Technical Center's Full-Text Technical Reports page: actlibrary.tc.faa.gov in Adobe Acrobat portable document format (PDF)

Technical Report Documentation Page

1. Report No.	2. Government Accession No.	3. Recipient's Catalog No.
DOT/FAA/AR-02/103		

4. Title and Subtitle	5. Report Date
PARAMETRIC STUDY OF CRASHWORTHY BULKHEAD DESIGNS	December 2002
	6. Performing Organization Code

7. Author(s)	8. Performing Organization Report No.
H. M. Lankarani and M.G. Mirza	

9. Performing Organization Name and Address	10. Work Unit No. (TRAIS)
National Institute for Aviation Research Wichita State University 1845 N. Fairmount Wichita, KS 67260-0093	11. Contract or Grant No. 96-G-019

12. Sponsoring Agency Name and Address	13. Type of Report and Period Covered
U.S. Department of Transportation Federal Aviation Administration Office of Aviation Research Washington, DC 20591	Final Report From 07/96 to 12/97
	14. Sponsoring Agency Code ANM-102

15. Supplementary Notes

Program Manager: Gary Frings, Federal Aviation Administration, William J. Hughes Technical Center
Technical Monitor: Tong Vu, Federal Aviation Administration, William J. Hughes Technical Center

16. Abstract

This study investigated the head injury criteria (HIC) compliance for front-row seating in transport class aircraft. Energy-absorbing bulkheads were designed using the analysis code MADYMO and simple static tests. The first of these designs used a simple aluminum sheet and the second used an aluminum honeycomb panel with fiberglass facesheets. Both designs satisfied the HIC requirement during 16-g dynamic sled tests. The investigation also established that foam pads are not effective HIC attenuators as the only means of energy absorption on a rigid bulkhead. The HIC value for a specific design was found to be sensitive to the following parameters: head impact velocity, head impact angle, seat setback distance, belt properties, and the panel stiffness and strength. The studies also showed that a minimum of 2-4 in. of bulkhead crush is required to attenuate the HIC values to levels below 1000 during 16-g dynamic sled tests.

17. Key Words	18. Distribution Statement
Aircraft crashworthiness, Dynamic simulation, Biodynamic simulation, Nonlinear finite element analysis, Head injury criteria	This document is available to the public through the National Technical Information Service (NTIS), Springfield, Virginia 22161.

19. Security Classif. (of this report)	20. Security Classif. (of this page)	21. No. of Pages	22. Price
Unclassified	Unclassified	74	

TABLE OF CONTENTS

LIST OF FIGURES

LIST OF TABLES

EXECUTIVE SUMMARY

This report documents an investigation into problems associated with satisfaction of the head injury criteria (HIC) for front row bulkhead seats in transport class aircraft. The study addressed two aspects of the problem. First, it investigated the performances of various padding materials, none of which were found to be satisfactory. Second, it used a MADYMO biodynamic simulation model, supported by simple static tests, in the design of energy absorbing bulkheads that effectively attenuated HIC values to noninjurious levels. The performances of these designs were verified during 16-g dynamic sled tests of modified cabin class divider panels. The MADYMO model was subsequently used in a number of parametric studies to assess the affects of the bulkhead stiffness and strength on the HIC levels.

1. INTRODUCTION.

Head injuries were first identified in some of the earliest aviation accidents. Medical officers, in World War I, observed that many of these injuries occurred when the pilot's head struck the cowl. A simple design change providing more room in front of the pilot practically eliminated these injuries in one aircraft [1]. The need for head injury protection was addressed with inclusion of the head injury criteria (HIC) in the dynamic seat test requirements specified in paragraph 562 of Title 14 Code of Federal Regulations (CFR) Parts 23, 25, 27, and 29 [2-5]. This requirement poses a significant problem for many segments of the aerospace industry. The airlines and manufacturers of jet transports have claimed high costs and significant schedule overruns during the development and certification of dynamically tested seats because of difficulties in satisfying this injury criteria [6].

The HIC evolved from the Wayne State Tolerance Curve [7]. Gadd [8] defined the severity index (SI) based on raising the time integral of head acceleration (measured in g's) to the power of 2.5; the slope of a curve fit to the Wayne State data plotted on a log-log scale. Gadd also proposed the injury criteria of 1000. Versace [9] subsequently advocated the use of an effective acceleration, which he defined as

$$\frac{1}{t}\int a^{2.5}dt$$

where t and a represent the time interval and resultant head acceleration, respectively. In 1972, this approach was adopted by the National Highway Traffic Safety Administration (NHTSA), under Federal Motor Vehicle Safety Standards FMVSS 208, as a means of evaluating crash tests [10]. This became known as the head injury criteria and is represented by the equation:

$$HIC = (t_2 - t_1)\left\{\frac{1}{t_2 - t_1}\int_{t_1}^{t_2} a(t)dt\right\}^{2.5}\Big|_{MAX}$$

where

$a(t)$ - resultant acceleration of the head center of gravity, g's
t_1 - initial integration time, seconds
t_2 - final integration time, seconds

A maximization operation is performed by identifying the time interval, $t_2 - t_1$, which results in the largest HIC value. This criterion was adapted from the Federal Motor Vehicle Safety Standard (FMVSS) No. 208 [11] in 1967. The HIC was subsequently recommended by the General Aviation Safety Panel (GASP) [12] as one injury criteria that should be considered in the design and certification of aircraft seats and restraint systems. The definition currently contained in the aerospace regulations differs from the one originally listed in FMVSS No. 208. Generally, a maximum time interval of 36 ms is used in the automotive industry, while in aerospace applications, the HIC is evaluated over the time period when the head of the anthropomorphic test dummy (ATD) is in contact with any object in the aircraft interior other

than the floor or the ATD itself. The injury criteria are defined as any HIC value exceeding 1000.

Compliance with the HIC requirements has proven to be more difficult than anticipated. Difficulties have been encountered during the certification of both front-row bulkhead and row-to-row seat installations for transport (14 CFR Part 25) class aircraft. Engineers certifying seats for general aviation (14 CFR Part 23) aircraft report similar difficulties.

While some of these difficulties can be attributed to the increasing complexities of seat designs associated with in-flight entertainment and communication equipment, it was believed that a lack of fundamental understanding regarding the physics governing the HIC performance also contributes to the certification challenge. This motivated a research project to address the bulkhead problem, believed to be the simpler of the two problems. The goal of the project was to develop a rational engineering approach to the design of energy-absorbing bulkheads to comply with the HIC requirements for the 16-g, 44 ft/sec test condition specified in 14 CFR 25.562 (b) (2).

2. BASELINE INVESTIGATION.

A baseline investigation was conducted that included a static test to characterize the performance of a production cabin class divider panel designed for Boeing 727s. The test article, provided by Continental Airlines, represented a sandwich panel design consisting of a 1-in. (2.54-cm) Nomex core honeycomb and fiberglass face sheet. The face sheets of the test article were covered with the carpet used in the airline installation.

A static test was conducted to obtain load-deflection data that contained stiffness, strength, and load hysteresis information using the test setup shown in figure 1. A contact force was applied to the bulkhead by a bowling ball mounted on the end of a hydraulic actuator at the location where the head of a 50% male ATD would strike the bulkhead. The actuator was controlled manually. A load cell and string potentiometer was used to record the actuator load and position respectively. Note that the actuator position corresponded to the face sheet deflection.

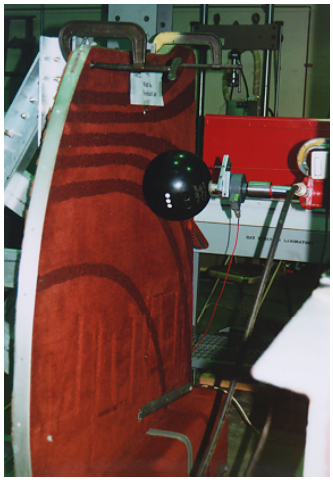

FIGURE 1. STATIC TEST SETUP FOR THE CABIN CLASS DIVIDER

The bulkhead was attached to an aluminum strongback, shown in figure 2, for the test. The instrument specifications are summarized in table 1. The data were digitized at 5 Hz using a Data Translation model 2081A analog-to-digital data acquisition board and DT VEE software [13].

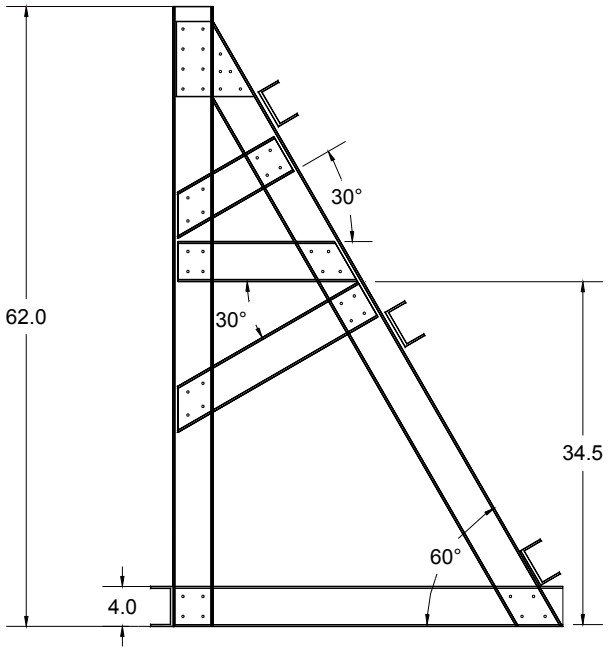

FIGURE 2. STRONGBACK FIXTURE USED IN THE STATIC AND DYNAMIC TESTS
(all dimensions in inches)

TABLE 1. INSTRUMENT SPECIFICATION FOR ALUMINUM SHEET PANEL STATIC TEST

Instrumentation	
String Pot (Linear Motion Transducer)	
Manufacturer	Magnetek Rayelco
Model No.	PV – 40B - 50G
Serial No.	111 – 8485
Position Sensitivity	Adjust ±0 - 5.0 mV/V/in. (±0 - 1.97mV/V/cm)
Load Cell (Uniaxial)	
Manufacturer	Eaton Corporation
Model No.	31 32 - 2K
Serial No.	13627
Capacity	2000 lbs (8900 N.)
Data Acquisition System	
DT VEE	
Data Translation, Marlboro, MA	

The results acquired during the static test are presented in figure 3 for the baseline test article. The irregular shape of the loading curve after the first load drop is typically exhibited by honeycomb when it is crushed.

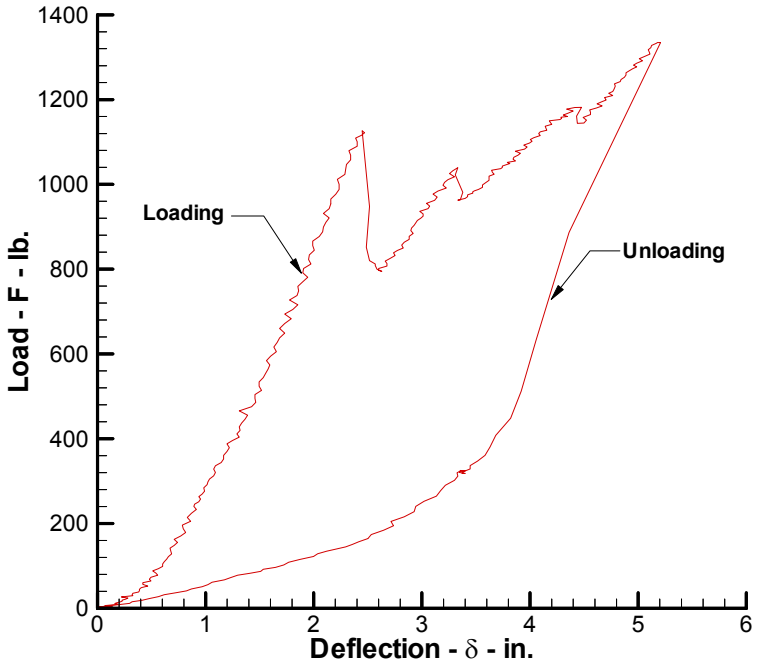

FIGURE 3. LOAD-DEFLECTION CURVE OBTAINED FROM THE STATIC TEST OF BASELINE CABIN CLASS DIVIDER PANEL

The latter portion of the unloading curve (that portion of the curve below 450 lbs.) exhibits a response that is much softer than the initial stiffness. This reduction in stiffness largely reflects the crushing damage produced in the Nomex core. A smaller portion of this stiffness loss is probably associated with damage to the face sheets.

3. DYNAMIC TEST OF BASELINE DESIGN.

A dynamic test of the baseline design was conducted to measure the accelerations in the head of a 49 CFR Part 572, Subpart B anthropomorphic test dummy. The sled is a pneumatically propelled deceleration type design and produces test pulses such as the one shown in figure 4.

An iron seat, fabricated from 2-in.-square steel tubing, was used in the dynamic test. The seat back and seat pan were constructed from 1/8-in. aluminum plate. The geometry of the seat, shown in figure 5, is representative of a typical airline economy class seat with the seat back fixed in the upright position. Seat cushions were not used during the test. A nylon seat belt (Pacific Scientific part no. 1108134-01) with a static tensile strength of 3000 lb. was used during this program.

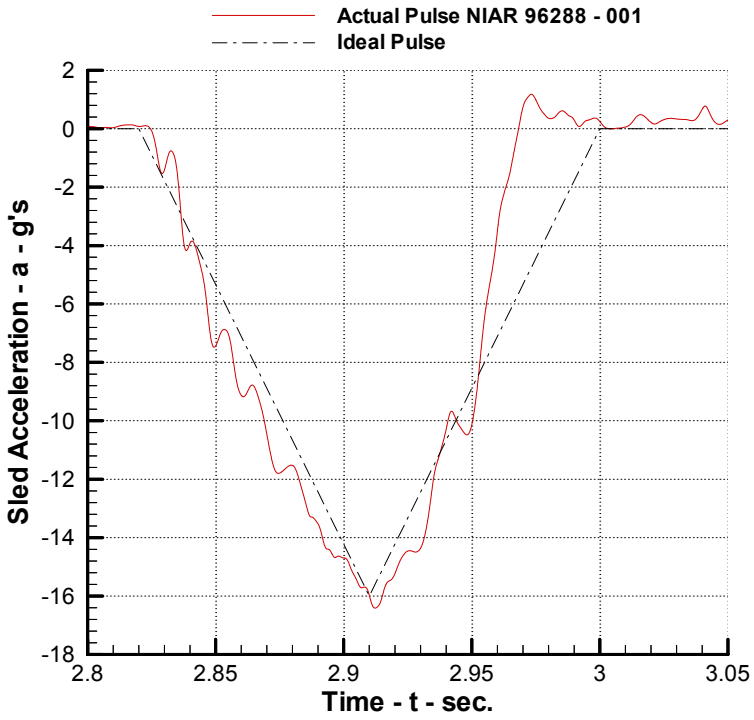

FIGURE 4. IDEALIZED TRIANGULAR PULSE AND ACTUAL DECELERATION PULSE

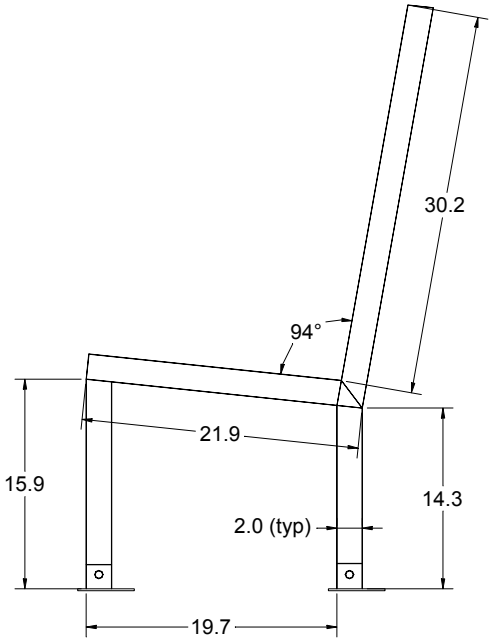

FIGURE 5. SEAT FIXTURE (all dimensions in inches)

The cabin class divider was attached to the 9-g aluminum strongback as shown in figure 6. The seat setback distance between the seat and bulkhead is shown in figure 7. The method of attachment was modified since the cabin class divider did not provide adequate strength to

withstand a 16-g test. A top-view drawing illustrating the modified method of attachment is shown in figure 8.

FIGURE 6. SETUP FOR CABIN CLASS DIVIDER PANEL TEST

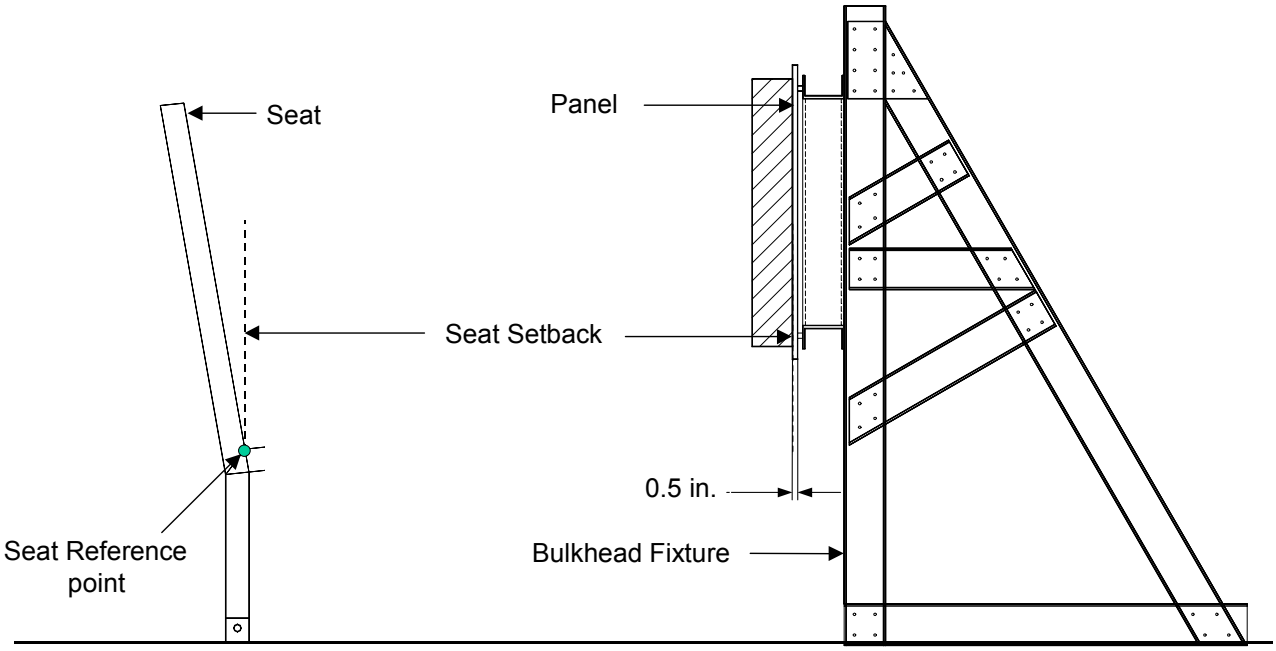

FIGURE 7. SEAT SETBACK OR SEAT-PITCH MEASUREMENT CONVENTION FOR SLED TESTS

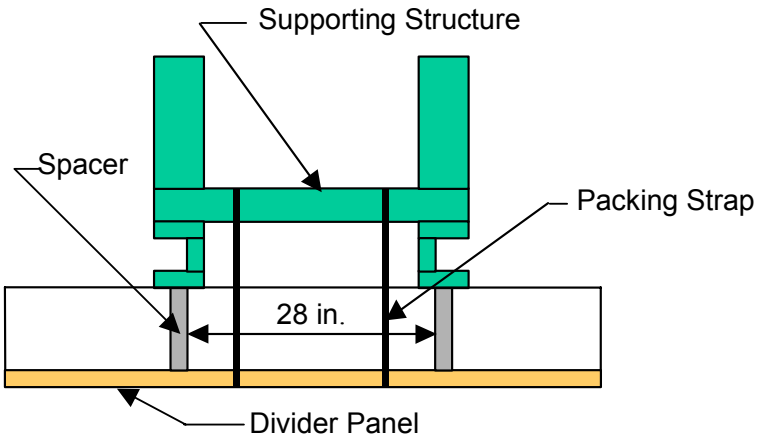

FIGURE 8. TOP VIEW OF THE PANEL ATTACHMENT TO THE SUPPORTING STRUCTURE

Three optical targets were attached to the seat to establish a moving reference frame. Four additional targets were mounted on the ATD as shown in figure 9 in order to track the dummy motion. A dynamic test was conducted at a 34-in. seat setback distance. The results from the test are shown in table 2. The procedure to obtain the results is described in appendix C.

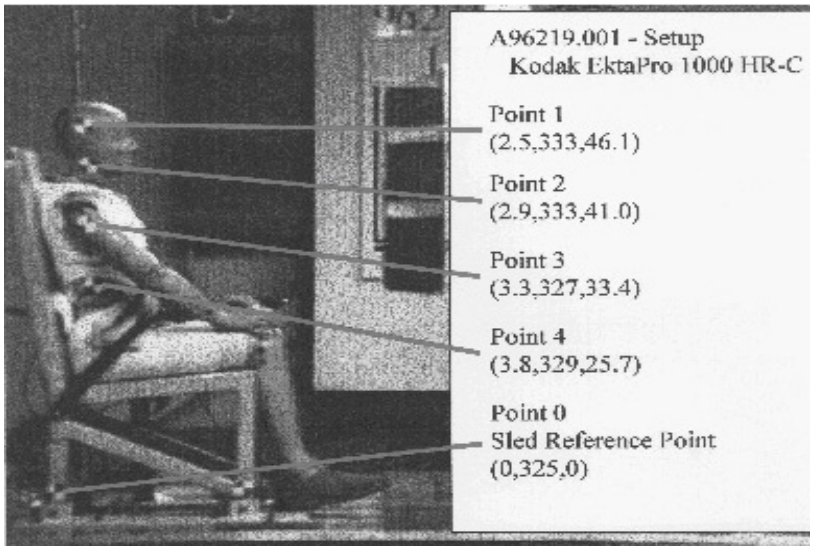

FIGURE 9. TARGET POINT LOCATIONS FOR VIDEO DATA REDUCTION

TABLE 2. DYNAMIC TEST RESULTS—BASELINE CONDITION

Test ID	Test Pulse (g's)	Head Impact Angle (degrees)	Head Impact Velocity (ft/sec)	Peak Head Acceleration (g's)	HIC Window (ms)	HIC
97191-002	16.3	42	45.3	156	11.0	1394

The head accelerations represent the data of greatest interest. A typical resultant head acceleration response, for a 34-in. setback, is shown in figure 10.

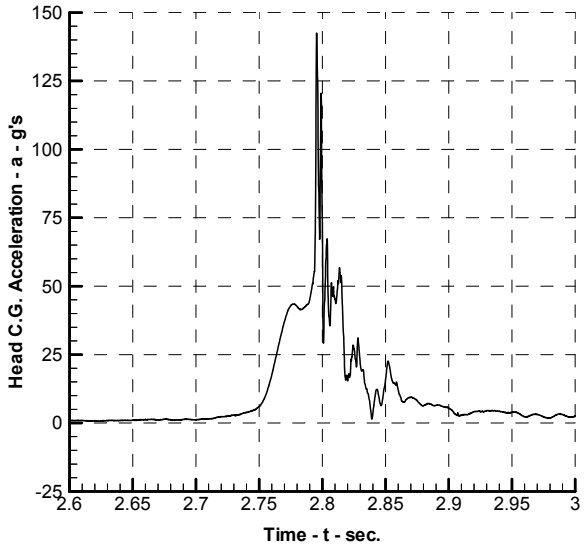

FIGURE 10. RESULTANT HEAD ACCELERATION RESPONSE FOR BASELINE BULKHEAD AT A 34-in. SEAT SETBACK

The sign convention for the head impact angle, reported in table 2, is defined in figure 11. The results were judged to be representative of hard cabin furnishings commonly installed in aircraft certified prior to promulgation of the dynamic seat test requirement. The HIC value is well in excess of the injury threshold, and the head impact velocity is slightly greater than the velocity change of the sled (typically 44 ft/sec).

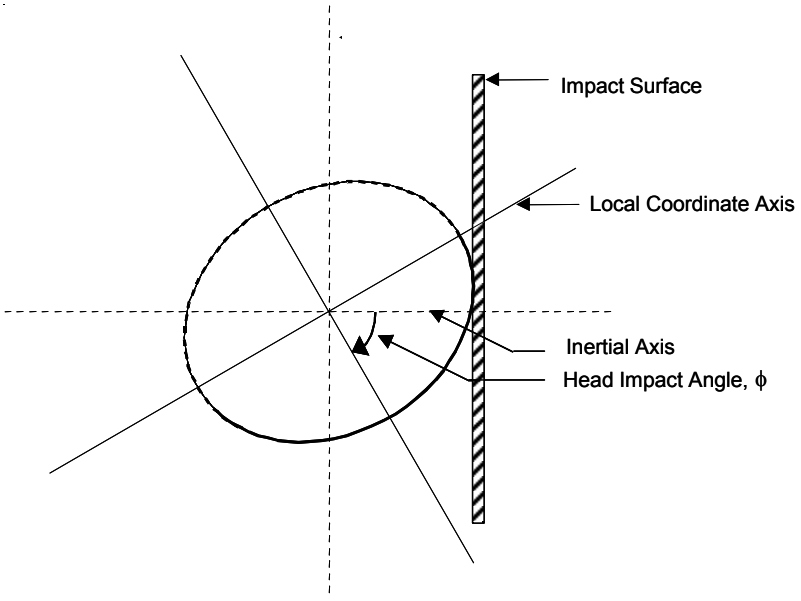

FIGURE 11. CONVENTION FOR HEAD IMPACT ANGLE MEASUREMENT

4. HEAD IMPACT TESTS OF A PADDED BULKHEAD STUDY.

A series of dynamic sled tests were conducted to assess the effectiveness of padding materials in reducing HIC values produced during 16-g tests. The same strong back fixture and test conditions were used in these tests as in the baseline tests. The foam pads were mounted on a 1/2-in. aluminum plate that served as a rigid bulkhead.

Several pad designs were evaluated during this study, a number of which were fabricated from General Plastics LAST-A-FOAM. Two densities of this rigid polyurethane foam were tested, 2 and 3 lb./in.^{3}. The contact surface of the pads constructed from this foam were covered by a heavy cotton fabric since these rigid foams have a very grainy texture that would never be left exposed in an aircraft installation. Most of the pads used in this study measured 24 x 24 in., except for three tests where 18 x 19 in. Ensolite pads were used. The nominal densities of the Ensolite II and Ensolite III pads were 4.0 and 8.0 lb./ft.^{3} respectively.

The dynamic tests were conducted at seat setback distances ranging from 32-36 in. A representative head path envelope obtained during one of these tests is shown in figure 12 and typical accelerometer data are presented in figure 13. These data reflect the fact that the x and z acceleration components provide the greatest contributions to the resultant head acceleration. The y component is much smaller, a fact that is consistent with the unyawed test condition.

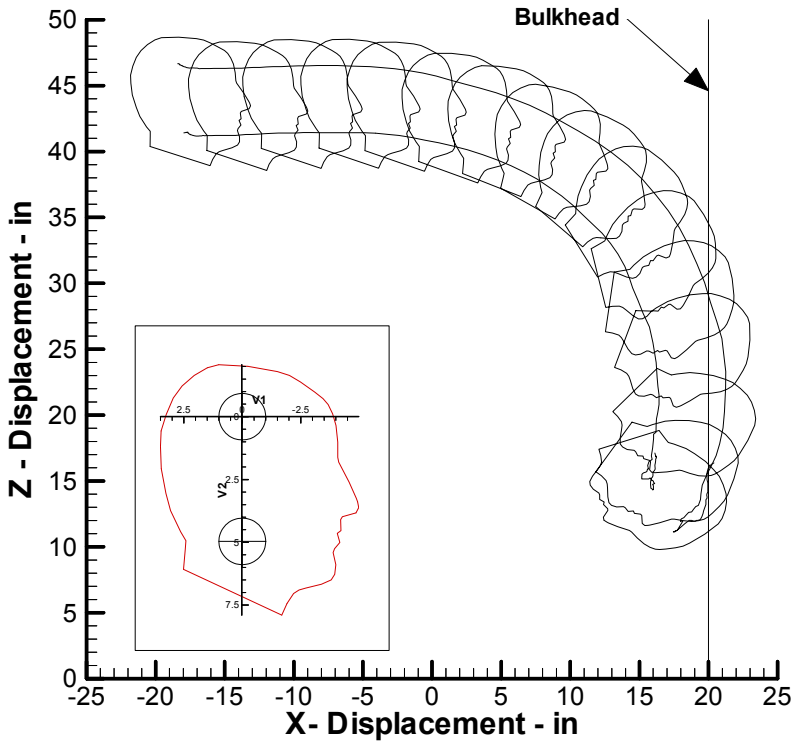

FIGURE 12. A SAMPLE HEAD PATH ENVELOPE OF SEAT/ATD/BULKHEAD SLED TESTS

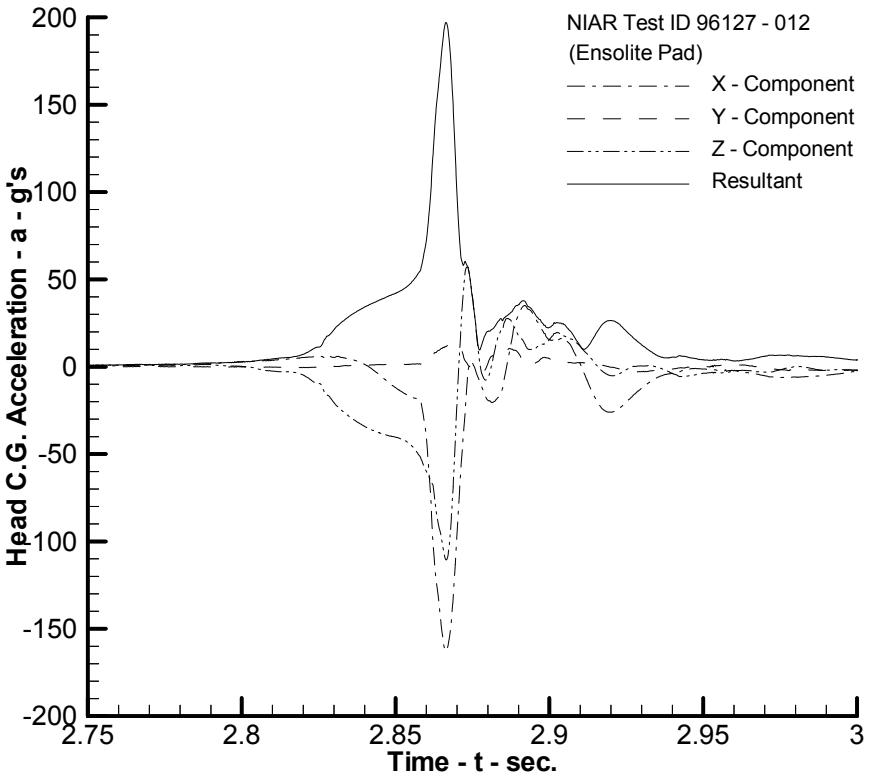

FIGURE 13. TYPICAL HEAD C.G. ACCELERATION TIME HISTORY

The results of these tests are summarized in table 3. Reviewing these data, it is seen that the data collected far exceeded the injury criteria by a large margin. In view of the high HIC values computed for these tests, it was concluded that a simple cushion design on the bulkhead would not produce the desired level of head injury protection. Further consideration of these results led to the additional conclusion that the high-HIC values were a result of the high stiffness of the pads.

Therefore, two perforated pads made of LAST-A-FOAM were designed in an effort to reduce the impact force levels. The first of these designs contained a rectangular pattern of 3/4-in.-diameter holes on a 3-in. pitch, and the second contained 2-in.-diameter holes on a 3-in. pitch. The results from dynamic bulkhead tests of these pads are presented at the bottom of table 3 and were as disappointing as the earlier results. The posttest photos of the pads with 3/4-in.-diameter holes, shown in figure 14, reveal that the impact zone exhibited minimal damage following the tests. The high HIC values of all configurations tested pointed to the need for even weaker pads. However, the pad stiffness could not be reduced further, since the pads containing 2-in.-diameter holes were already quite fragile and difficult to handle.

TABLE 3. TEST RESULTS FROM THE SEAT/ATD/BULKHEAD SLED TESTS

Test No.	Padding Material	Padding Thickness (in.)	Seat Setback (in.)	Peak Sled Acc.[*1] (g's)	Head Impact Velocity (ft/sec)	Head Impact Angle (deg.)	Head c.g. Peak Acc. (g's)	HIC	Δt (ms)
96127-001	No Bulkhead	-	-	17.0	-	-	-	-	-
96127-002	No Bulkhead	-	-	17.0	-	-	-	-	-
96127-003	FR 3703[*2]	2.00	32.0	16.9	-	-	-	-	-
96127-004	FR 3502[*3]	2.00	32.0	16.6	-[*4]	-	-	-[*4]	-
96127-005	FR 3703	3.12	32.0	15.6	43.1	18	274	4645	6.7
96127-006	FR 3502	3.00	32.0	15.6	42.1	10	203	2647	7.4
96127-007	FR 3502	2.00	36.0	15.6	46.8	48	251	2537	6.3
96127-008	FR 3703	3.00	35.0	16.4	46.6	32	276	3400	3.9
96127-009	FR 3502	3.00	35.0	16.4	49.0	27	188	2601	9.2
96127-010	FR 3502+ 3703[*5]	1.00+2.00	35.0	16.6	48.5	25	245	3709	6.7
96127-011	Ensolite II+III[*6]	1.00+1.00	36.0	16.3	49.0	36	231	2715	7.1
96127-012	Ensolite II+III	2.00+1.00	35.0	16.4	49.2	29	197	2719	8.8
96219-001	FR 3502[*7]	2.00+2.00+2.00	34.0	16.7	45.9	32	191	2850	9.5
96219-002	(FR 3502+ 3503) [*7]	(1.00+2.00)+3.00	34.0	15.6	46.4	29	168	2481	10.8
96219-003	FR 3502	1.00+2.00	34.0	17.0	47.1	29	196	2691	7.7
96219-004	Ensolite II+III	2.00+1.00	34.0	16.9	47.0	24	193	2352	8.5
96219-005	FR 3703[*8]	3.00+3.00	34.0	17.0	47.3	31	190	2937	9.4
96219-006	FR 3502+ 3703	1.00+3.00	34.0	16.1	45.9	28	198	2624	8.8

Comments:
[*1] A minimum of 16.0 g is required for 14 CFR Part 25.
[*2] Unmodified General Plastic LAST-A-FOAM 3 lb./cu. ft. [14].
[*3] Unmodified General Plastic LAST-A-FOAM 2 lb./cu. ft.
[*4] Accelerometer cable failed. No HIC data recorded.
[*5] Outer layer comprised of softer FR 3502 while the inner layer comprised of FR 3703.
[*6] For Ensolite, the lower number corresponds to softer (lower density) material.
[*7] Three, 2-inch thick foams are glued together and perforated by 3/4-inch-diameter holes at a 3-inch pitch.
[*8] Foam is perforated by 2-inch-diameter holes at a 3-inch pitch.

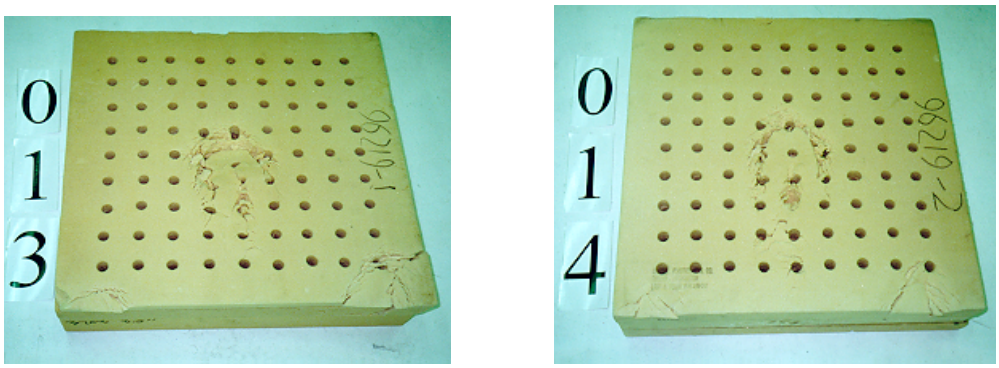

FIGURE 14. POSTTEST CONDITION OF RIGID FOAM PADDING MATERIAL

5. MADYMO ANALYSIS OF BASELINE TESTS.

A MADYMO biodynamic model was created to support the design of an acceptable bulkhead. MADYMO [15] is a computer program that possesses multibody dynamic analysis and nonlinear finite element analysis capabilities. It possesses robust tools to model restraint systems and contact surfaces that include the capability to represent arbitrary force-deflection characteristics of lap belts and shoulder harnesses. The contact algorithm allows the belts to slide over the occupant body and also generates friction forces and normal forces in addition to the kinematics constraints.

The model of the baseline problem represented the standard 50% male ATD model and bulkhead geometry evaluated during the baseline dynamic tests as shown in figure 15. The pelvic restraint was represented by a simple one-dimensional, cable-type structural representation. The load elongation curve used for the lap belt is shown in figure 16. The bulkhead was modeled by a combination of a rigid plane and the load-deflection response measured during the static tests. The load is defined as the force acting on the head of the ATD in a direction normal to the bulkhead. The deflection is defined as the distance that the head penetrates the bulkhead. An additional plane was defined to represent the fixture beam positioned directly in front of the ATD's feet during the dynamic tests and provided the boundary condition for the ATD's lower extremities.

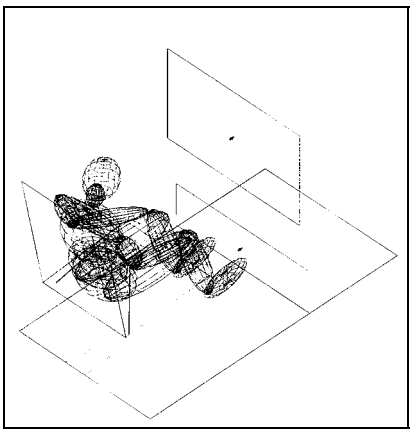

FIGURE 15. ANALYSIS MODEL OF SLED TEST SETUP

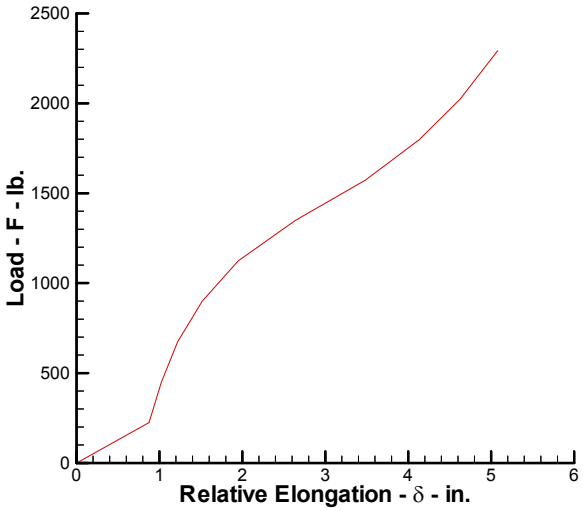

FIGURE 16. RELATIVE ELONGATION CHARACTERISTICS OF SEAT BELTS

The predicted response of the dummy and panel are shown in figure 17 for one instant in time. The acceleration data is compared with experimental data in figure 18. These data have been filtered to CFC 1000 as specified in SAE Recommended Practice J-211 [16]. The corresponding experimental accelerometer data were also filtered using this signal-processing algorithm. Additional results are presented in table 4. A comparison of the analysis results reveals that the MADYMO model produced reasonable predictions of these experimental results.

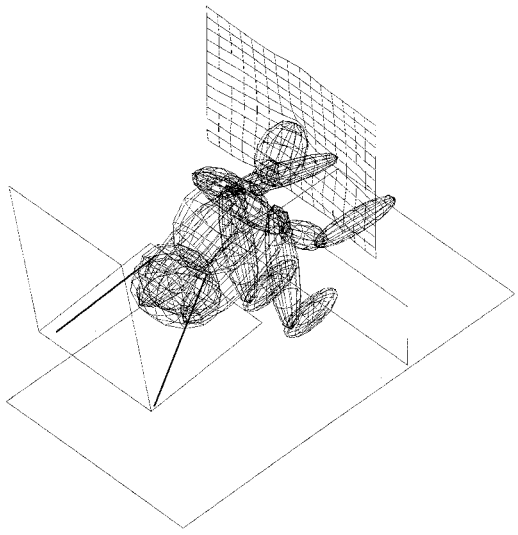

FIGURE 17. PANEL CONDITION AT HEAD STRIKE

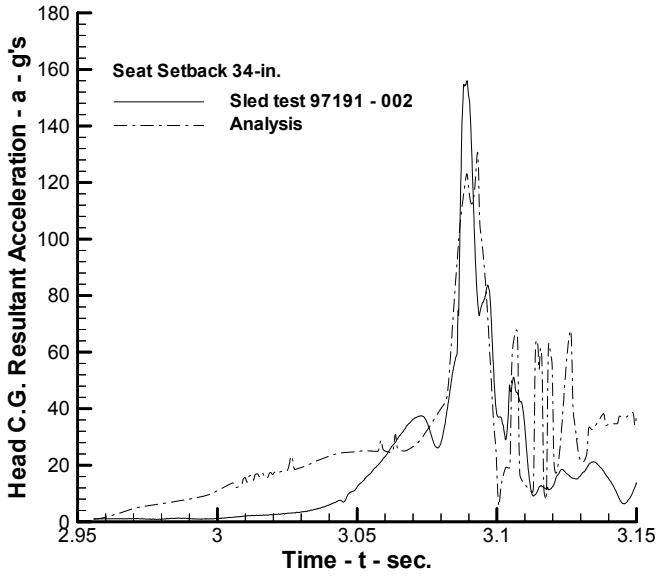

FIGURE 18. HEAD c.g. ACCELERATION TIME HISTORIES FOR UNMODIFIED BULKHEAD PANEL

TABLE 4. DATA COMPARISON FOR THE DIVIDER PANEL WITHOUT MODIFICATION

	Head Impact Angle (degrees)	Head Impact Velocity (ft/sec)	Peak Head Acceleration (g's)	HIC	HIC Window $\Delta t = t_2 - t_1$ (ms)
Analysis Result	45	45.9	133	1443	13.8
Sled Test (97191-002)	42	45.3	156	1394	12.5

As mentioned earlier, the high HIC values gives rise to two possibilities, either the bulkhead is too stiff or it is too strong. To determine which is the case, an energy-absorbing panel was considered that possesses the load-deflection curve shown in figure 19. In this system, the load increases in a linear-elastic fashion until the system strength, denoted by F_{cr}, is reached. This is followed by a perfectly plastic response until the system is unloaded. Note that the unloading response follows an offset path with the same slope as the stiffness K of the initial linear-elastic curve.

Since the area under this curve represents the energy absorbed by the panel, it is apparent that the most effective energy absorber is one with infinite stiffness, a large strength value, and a large deflection capability before failure. Since the goal is to reduce the HIC value to a level that is below the injury threshold and since the HIC is a function of acceleration, it seems that a reduction in the resultant head acceleration will produce a corresponding reduction in the HIC value. This should be achieved if the strength of the panel, F_{cr}, is reduced, since this would reduce the magnitude of the force applied to the head.

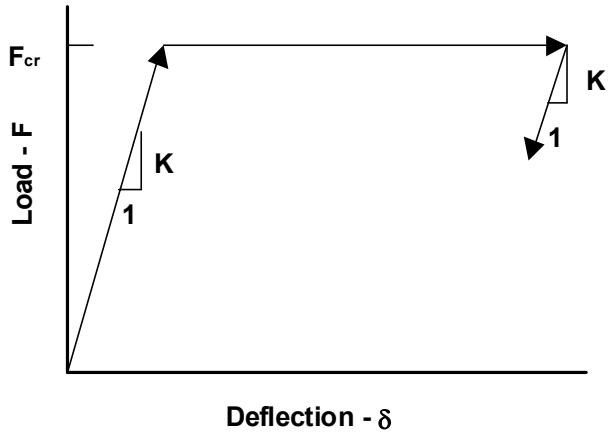

FIGURE 19. LOAD-DEFLECTION CURVE FOR AN ENERGY-ABSORBING PANEL

For a given occupant size and initial conditions, the amount of displacement required at a specified strength level is dictated by the kinetic energy imparted to the panel by the ATD or occupant. Since for the dissipation of a given kinetic energy (given area under the load-deflection curve), the displacement requirement or crush needs to be increased if the force level is decreased, or vise versa (to keep the area the same), it is possible that the energy-absorbing system may either fail structurally or consume all of the available space. Both possibilities must be considered when designing a HIC-compliant bulkhead.

In any event, the ATD response in a front row bulkhead seat is far more complicated than the simple model just described. The design of an energy-absorbing bulkhead requires a more sophisticated analysis for two reasons. First, the dynamic response of an ATD or human occupant cannot, in general, be accurately represented by a single degree-of-freedom system. Second, the response of a typical bulkhead panel is not accurately represented by the ideal elastic-plastic load-deflection curve presented here.

6. PRELIMINARY DESIGN STUDY.

The baseline MADYMO model was used in a preliminary design study to identify a simple but effective solution to the front row HIC problem. This problem is challenging at a fundamental level, since the structural response of panels, such as presented in figure 3, does not approach the ideal elastic-plastic response desired from an energy absorber. Based on the thoughts presented in the previous section, the deformations required to successfully attenuate HIC values to noninjurious levels were believed to be beyond that which is achievable from conventional honeycomb panel designs. Specifically, the displacements required were expected to exceed any reasonable core thickness. Therefore, consideration of honeycomb materials was ruled out for the preliminary design study in favor of a monolithic panel design.

It was also recognized, from the outset, that the response of monolithic panels does not provide the stiff elastic-plastic response exhibited by the efficient energy absorber described previously. Rather, these panels will exhibit a membrane-type response that is very soft initially and stiffens as the panel deforms. This stiffness increase is produced by the increased in-plane stresses and is the so-called geometric stiffening or stress stiffening effect.

The low cost and simplicity of these designs were judged to have significant benefits leading to the selection of this concept for the preliminary design study. Not only were these designs inexpensive, they were also easy to fabricate and quickly mounted to the aluminum fixture fabricated for the baseline study.

The preliminary design study used the MADYMO model shown in figure 20. The analysis used the same representation of the seat, occupant, and restraint system used in the baseline study; however, the bulkhead was represented by a finite element model. The seat setback distance between the bulkhead and the occupant was varied between 32 and 37 inches during parametric studies of this system.

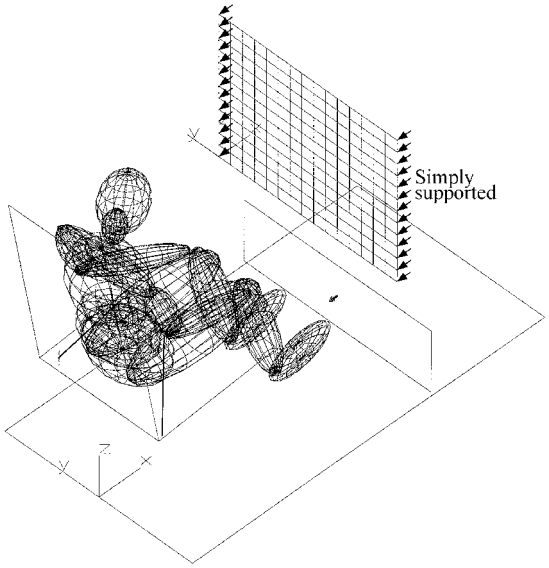

FIGURE 20. SIMULATION MODEL WITH ALUMINUM SHEET PANEL

The bulkhead finite element model contained 180 shell elements and was able to accurately represent large out-of-plane displacements in addition to the linear response. This model also included the effects of nonlinear material properties by using an elastic-plastic model to represent the behavior of 2024-O aluminum. Material properties for this alloy were obtained from tensile tests, using a servo-hydraulic test stand, since these data were not available in the literature.

The initial conditions and dynamic load conditions used in this design study represented the test conditions defined in 14 CFR 25.562 (b)(2). However, the model was not yawed 10° with respect to the velocity vector as specified in the regulation. The panel's displacement boundary conditions were defined in a way to approximate a typical installation of a cabin class divider panel. The vertical edges of the panel were simply supported, while the top and bottom edges were free.

The computer model was used in a parametric study to investigate the effect of panel thickness on the system response for a 34-in. seat setback distance. These results are presented in figures 21 and 22 and summarized in table 5. They show that this system is effective in attenuating the HIC value and also indicates that this performance is associated with panel deflections in excess of 2 in.

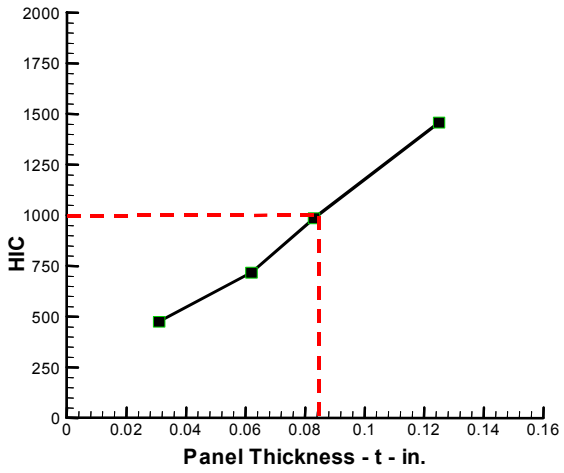

FIGURE 21. HIC VS PANEL THICKNESS

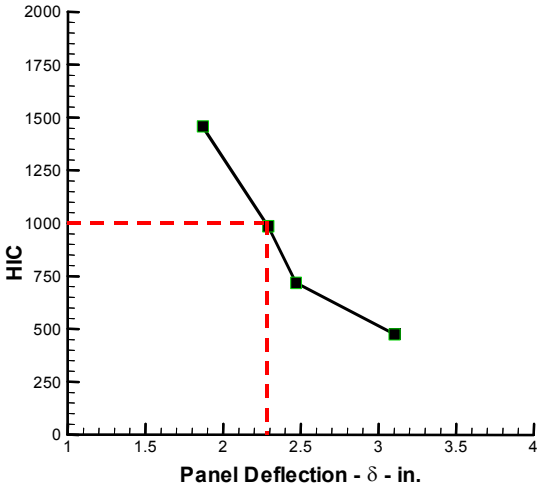

FIGURE 22. HIC VS PANEL DEFLECTION

TABLE 5. PREDICTED HIC RESULTS FOR MONOLITHIC PANELS AT A 34-in. SEAT SETBACK

Case No.	Peak Sled Acceleration Test Pulse (g's)	Sheet Thickness (in.)	Sled Velocity (ft/sec)	Maximum Panel Deflection (in.)	HIC Values From Analysis
1	16.7	0.03	45.9	2.8	475
2	16.7	0.063	45.9	2.5	718
3	16.7	0.08	45.9	2.3	986
4	16.7	0.12	45.9	1.9	1458

The results of a parametric study for a 0.063-in. panel, where the seat setback distance was varied, are presented in figure 23.

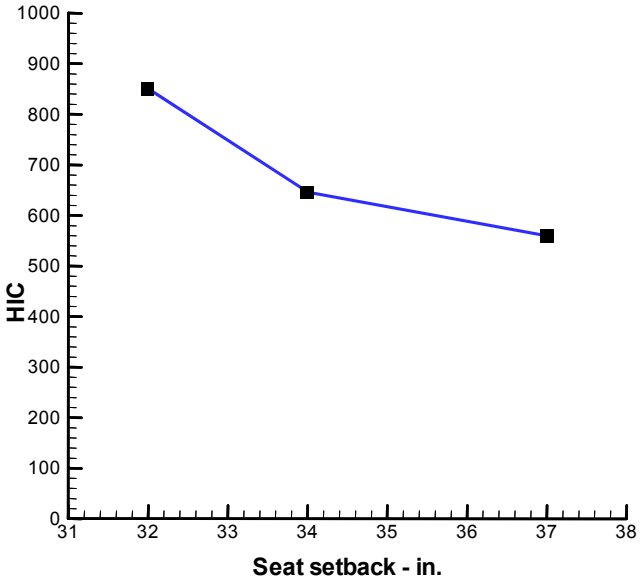

FIGURE 23. HIC VS SEAT SETBACK DISTANCE

7. VALIDATION OF HIC ATTENUATION.

A series of dynamic sled tests were conducted to validate the predictions of the aluminum panels designed using the MADYMO model. The test setup for this series of tests was the same as used in the baseline tests. The aluminum specimens were attached to the fixture, shown in figure 24, which was then mounted on the sled.

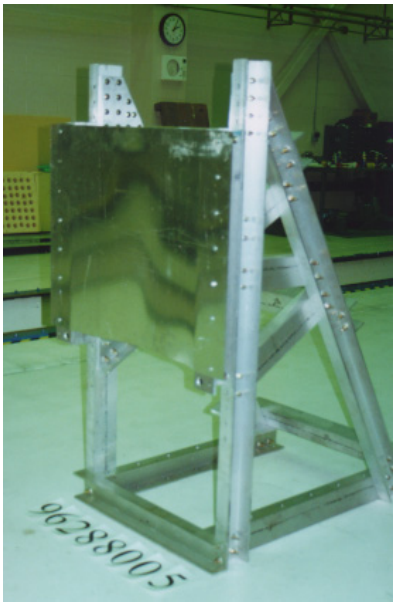

FIGURE 24. MODIFIED BULKHEAD WITH ALUMINUM SHEET PANEL

Tests were conducted at three seat setback distances ranging from 32 to 37 in. Each test was conducted with a new aluminum test article because they were permanently deformed as shown in figure 25.

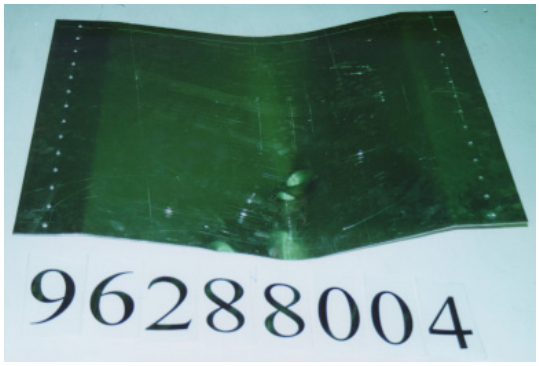

FIGURE 25. PERMANENT DEFORMATION OF ALUMINUM SHEET PANEL AFTER SLED TEST

The results of these tests are presented in table 6 and figure 26.

TABLE 6. RESULTS OF SLED TESTS WITH SEAT SETBACK VARIATION*

Test ID*	Seat Setback (in.)	Test g (g's)	Head Impact Velocity (ft/sec)	Head Impact Angle (degrees)	Head c.g. Peak Acceleration (g's)	HIC
96288-004	34	16.6	45.1	38	142.5	694
96288-006[1]	34	17.0	-	-	111.5	653
96288-007	34	17.3	46.6	33	167.8	397
96288-008	32	16.4	45.3	32	171.8	832
96288-009	32	15.9	46.1	32	201.7	882
96288-010	37	16.7	46.5	67	66.5	528
96288-011	37	17.1	47.3	67	101.7	515
96288-012	37	17.1	50.4	67	73.6	614
96288-013[1]	32	16.6	-	-	130.8	792

[1]Video data not available
*All the tests were conducted using 0.063-in.-bare Al 2024-O sheet panel

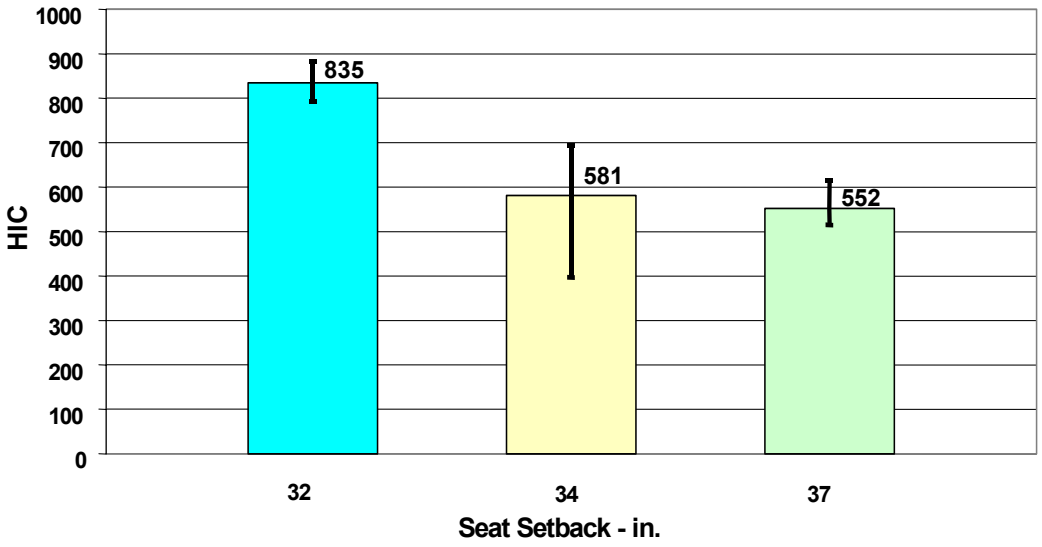

FIGURE 26. HIC VARIATION FOR DIFFERENT SEAT SETBACKS

The head path, predicted using MADYMO, is presented in figure 27 along with the corresponding head path digitized from the high-speed video data. From this figure, it is seen that the predicted results are in good agreement until well past the point where the head initially contacts the wall.

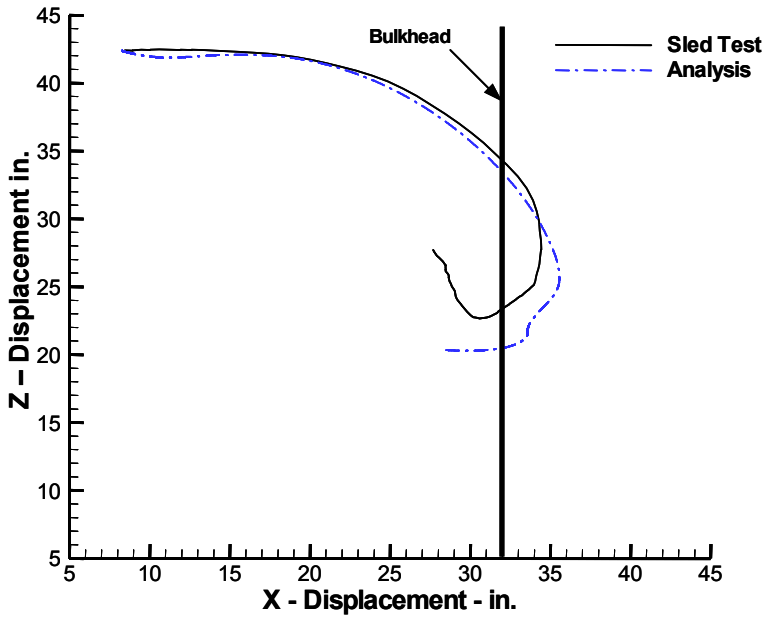

FIGURE 27. HEAD TRAJECTORY COMPARISON BETWEEN SLED TEST VS ANALYSIS AT A 32-in. SEAT SETBACK DISTANCE

The ATD positions predicted by the MADYMO simulations are presented with the corresponding frames from the video data and are seen to be in close agreement at different seat setbacks, as shown in figure 28.

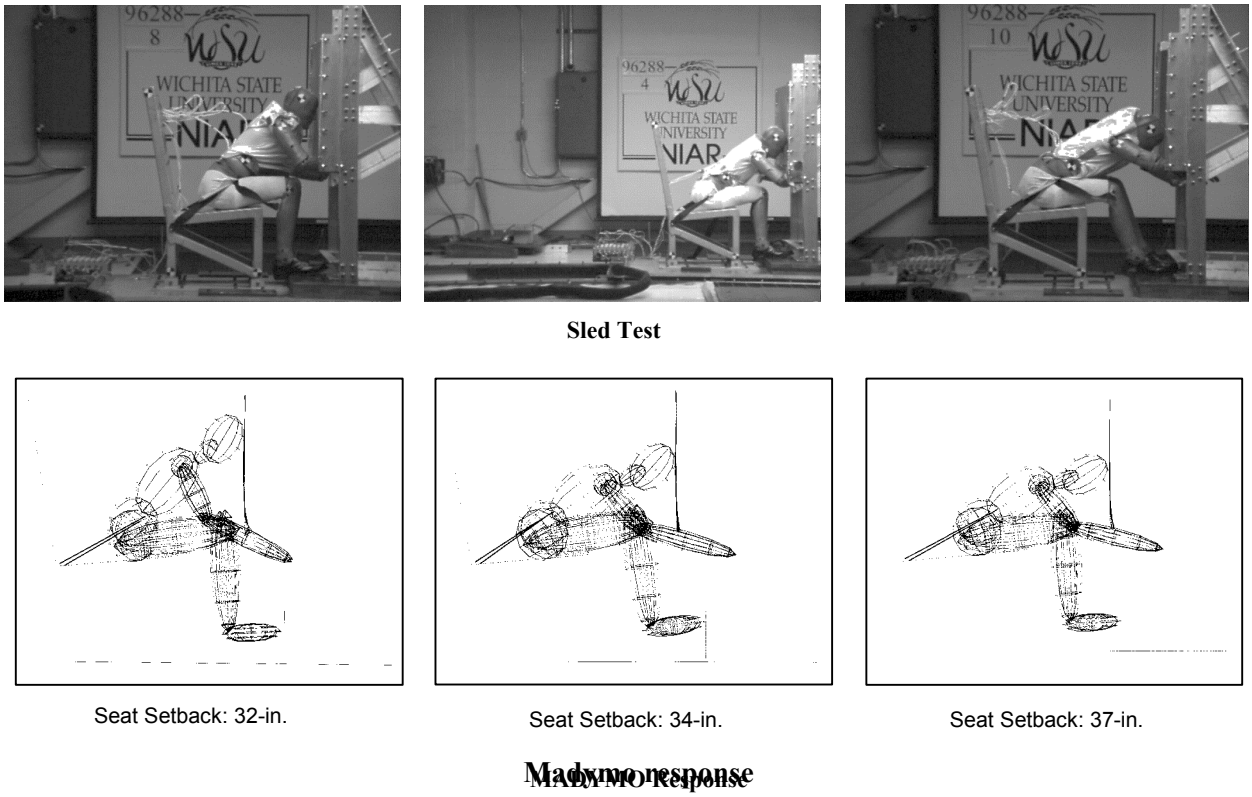

FIGURE 28. ATD RESPONSE FOR DIFFERENT SEAT SETBACKS

The data presented in table 7 compares results recorded during test series 96288 and MADYMO predictions. The data from MADYMO models correspond to the ATD model seated at the same seat setback distance and given the same deceleration pulse as in the sled test. Table 7 shows that the MADYMO results predict the same trend in the data, although they are somewhat conservative.

TABLE 7. COMPARISON OF MADYMO RESULTS WITH EXPERIMENTAL RESULTS

	Seat Setback (in.)	Head Impact Velocity (ft/sec)	Head Impact Angle (degrees)	Head c.g. Peak Acceleration (g's)	HIC
Sled Test	32	45.7	32	168	835
MADYMO	32	44.9	32	166	918
Sled Test	34	46.1	34	141	581
MADYMO	34	46.6	40	140	620
Sled Test	37	48.1	67	81	552
MADYMO	37	47.6	60	80	560

The average HIC and the scatter band for the tests at each of the seat setback distances are shown in figure 26. The trends in these data are clearly consistent with that shown in figure 23. The peak head acceleration data (figure 29) reflects the same trend as the HIC data.

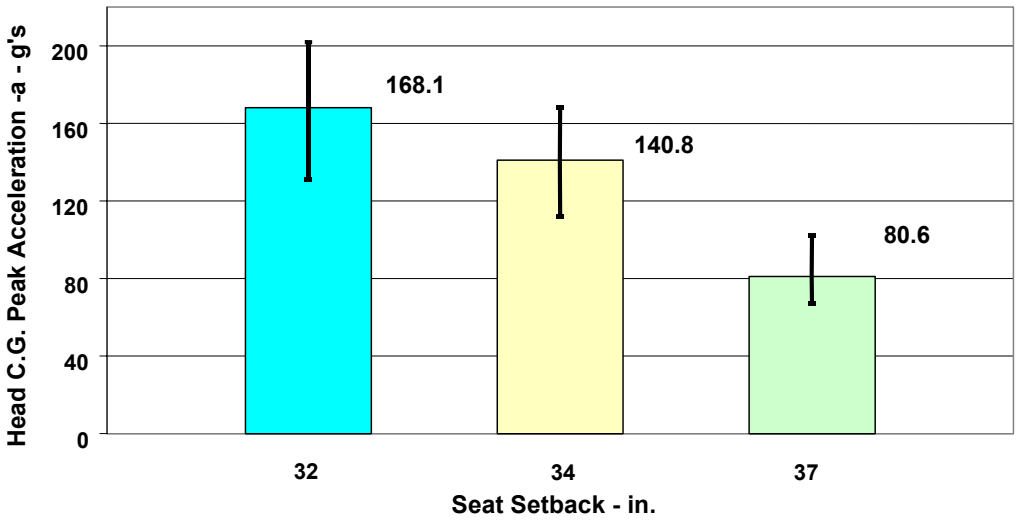

FIGURE 29. EFFECT OF SEAT SETBACK ON PEAK HEAD ACCELERATIONS

A series of sled tests were conducted at a seat setback distance of 34 in. in which the panel thickness was varied. The resultant head acceleration for a 0.063-in.-thick panel is presented in figure 30 along with data acquired during the baseline test. These results show that the aluminum panel produces a response with a lower amplitude and longer duration than the honeycomb panel did during the baseline test.

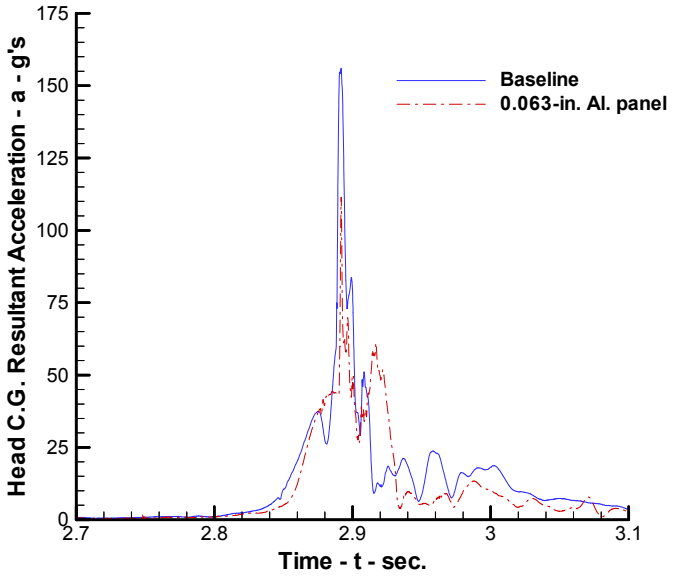

FIGURE 30. HEAD ACCELERATION TIME DISTANCES FOR BASELINE AND 0.063-in. PANEL TESTS

The variation of the HIC values calculated from the experimental data for different panel thicknesses is shown in figure 31. The same trend is observed in these data as predicted using the MADYMO model, as shown in figure 21.

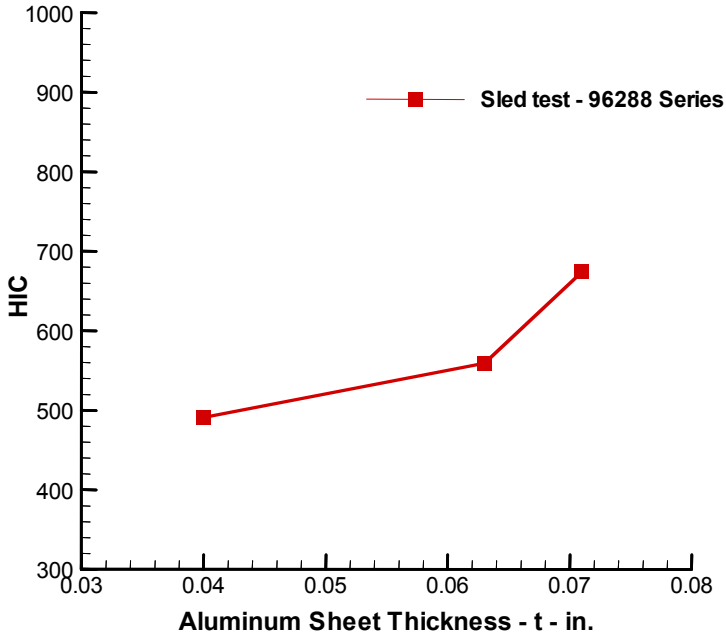

FIGURE 31. VARIATION OF HIC WITH PANEL THICKNESS

An examination of the photographs and the MADYMO-graphical output presented in figure 28 provides some insight into the mechanisms governing HIC values. It is apparent that the head motion is arrested earlier for the smaller seat setback distances. For larger seat setback distances, such as the 37-in. case, the head of the ATD exhibited a sweeping motion past the bulkhead. In this case, only a portion of the ATD's kinetic energy was imparted into the bulkhead, and the friction force produced during this contact can be significant. A careful review of the motion recorded on the video data revealed that for some of these cases, the friction force produced a stick-slip phenomenon wherein the motion of the head was arrested, broke free, was arrested again, and so on. The head accelerations produced during this kind of head motion are significantly different from that measured during tests that do not exhibit the stick-slip behavior. These differences can produce a significant affect on the corresponding HIC values.

8. STATIC TESTS—ALUMINUM PANELS.

The aluminum panels produced acceptable HIC values; however, an aluminum sheet may not be acceptable in the design of all cabin furnishings. The panels themselves do not possess a great deal of strength and, thus, may not be suitable for galleys, lavatories, and service cart storage cabinets. Their structural characteristics, however, are useful in the design of these interior furnishings.

The structural performance of the aluminum panels is not rate-sensitive; therefore, the engineering data of most importance to the HIC problem is their force-deflection response. These data relate the applied force to the deflection at the point where the head of the ATD contacts the panel.

The load-deflection behavior was measured during static tests of the aluminum panels; the same fixture was used as for the dynamic sled tests. The same actuator, load cell, and string potentiometer used in these tests were also used in the earlier baseline static test of the cabin class divider panel. Two panels were tested to establish the repeatability of the results.

The results of these tests are shown in figure 32 where it is seen that the data is in close agreement for the loading portions of the curves. The difference seen during the start of the unloading portions was caused by manual control used during these tests.

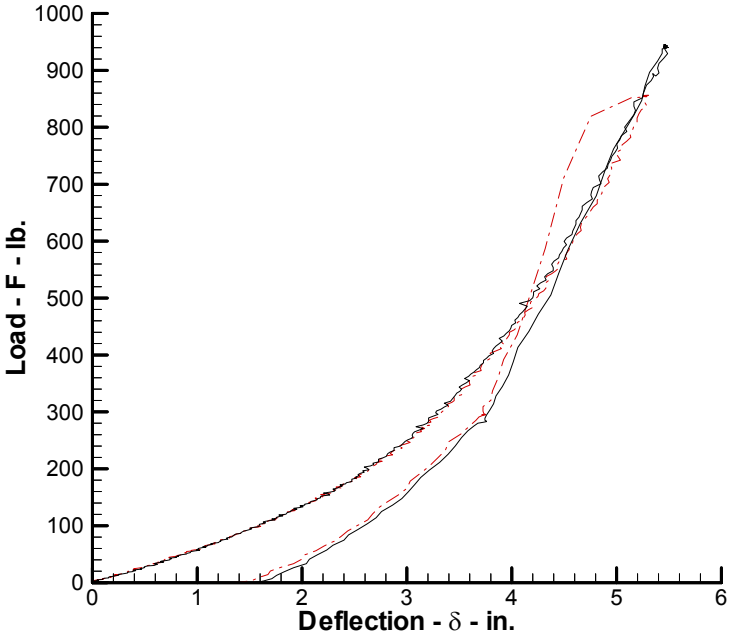

FIGURE 32. CONSISTENCY OF THE STATIC TESTS
(Test 1 and Test 2 Superimposed)

The stiffening response exhibited by the aluminum panel is characteristic of transversely loaded membranes and cable lattices and reveals that it is not an efficient energy absorbing system. Therefore, a requirement exists to preserve space behind the panel.

9. STATIC AND DYNAMIC TESTS OF MODIFIED CABIN CLASS DIVIDER PANELS.

Based on the results of the tests of the thin aluminum panels, it was decided to study whether the original cabin class divider panel could be modified to produce similar results. Thus, a modification was sought that would reduce the strength of the honeycomb panel.

It was recognized that the successful modification must reconcile the fundamental difference between the two types of structures. That is, the honeycomb panels are plates, whereas the aluminum panels are membranes. In view of this, a hypothesis was developed that a membrane-type response could be obtained by introducing "damage" to the face sheets of the sandwich panel. The so-called damage consisted of a pattern of vertical slits that were cut into both front and back face sheets. The first pattern contained three slits spaced 6 in. apart, while the second pattern contained five slits with a 4-in. spacing. These slits were cut into the panel face sheets with care to avoid damaging the honeycomb core.

Static tests of these modified panels were conducted to measure their load-deflection characteristics using the same test setup and procedure described earlier. The results of these tests are presented in figure 33 where it is seen that the slits primarily reduce the stiffness of the structure. A significant difference between the responses of the honeycomb panels compared to the aluminum panels is the significant hysteresis behavior exhibited by the honeycomb panels, as they are unloaded. This type of effect was expected to be beneficial since it indicates that much of the energy imparted to the panel by the ATD during the initial part of the impact is not returned to the ATD during its rebound.

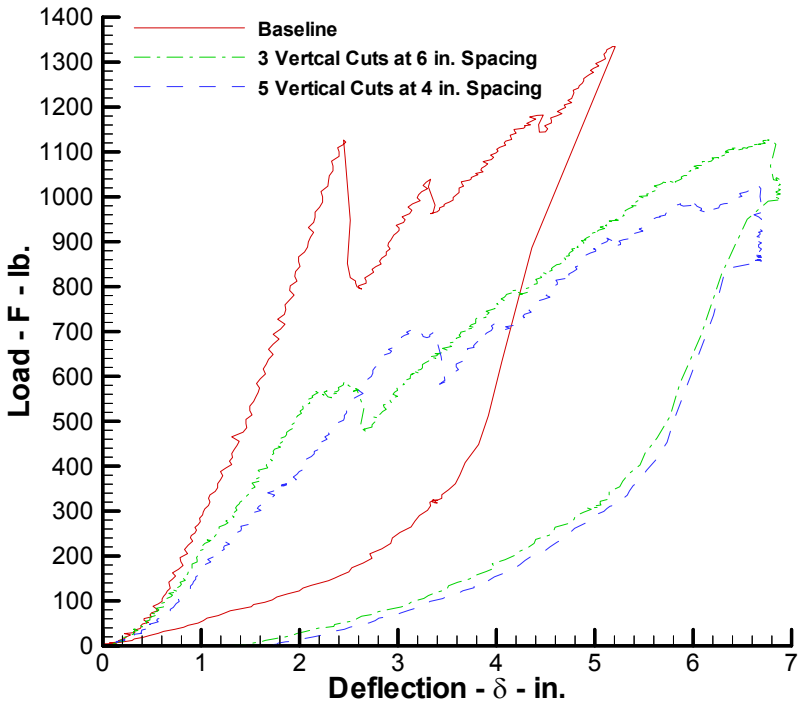

FIGURE 33. LOAD-DEFLECTION CURVES OBTAINED FROM THE STATIC TEST OF THE CABIN CLASS DIVIDER PANELS

These load-deflection data were used in a MADYMO model to predict the dynamic response of the ATD for the ideal 16-g deceleration. The model was similar to the baseline model. However, it contained a rigid plane grounding a nonlinear spring that was defined using the empirical load-deflection data for the panel with five slits. The panel with three slits was not modeled since its response was not significantly different than the one with five slits.

The results of this analysis are presented in the table 8 along with the results predicted for the baseline model. These predictions indicate that the modified panel should produce a significant improvement in the HIC values compared to the baseline design.

TABLE 8. ANALYSIS PREDICTED RESULTS USING THE STATIC LOAD DEFLECTION CHARACTERISTICS

Simulation Case	Head Impact Angle (degrees)	Head Impact Velocity (ft/sec)	Head c.g. Peak Acceleration (g's)	HIC	HIC Window $\Delta t = t_2 - t_1$ (ms)
Unmodified panel	45	46	133	1443	13.8
Modified panel with 5 vertical slits	45	46	80	831	27.8

Dynamic tests were conducted to confirm this improvement, using the same test setup used during dynamic testing of the aluminum panel. Four sled tests were conducted during this series of tests. It was not possible to maintain a constant seat setback distance for these tests due to a fixture limitation, thus this distance varied from 33-35 in. The results for these tests are summarized in table 9. Comparing the results for the 34-in. seat setback shows that the modification did reduce the HIC value by a significant amount. A comparison of the head acceleration response for these tests, figure 34, reveals a corresponding reduction in the peak g level to almost half. However, the time interval for the HIC integral is nearly three times greater than for the unmodified panel (31.1 ms vs 11.0 ms for the 34-in. seat setback tests).

TABLE 9. SLED TEST RESULTS USING MODIFIED CABIN CLASS DIVIDER PANELS

Test ID	Test Pulse (g's)	Divider Panel Modification	Seat Setback (in.)	Head Impact Angle (degrees)	Head Impact Velocity (ft/sec)	HIC	HIC Window $\Delta t = t_2 - t_1$ (ms)
97191-001	16.7	No	35	53	44.9	823	19.0
97191-002	16.3	No	34	42	45.3	1394	12.5
97191-003	17.1	Slit pattern 2	33	40	45.6	1132	22.7
97204-002	16.2	Slit pattern 2	34	44	41.3	882	31.1

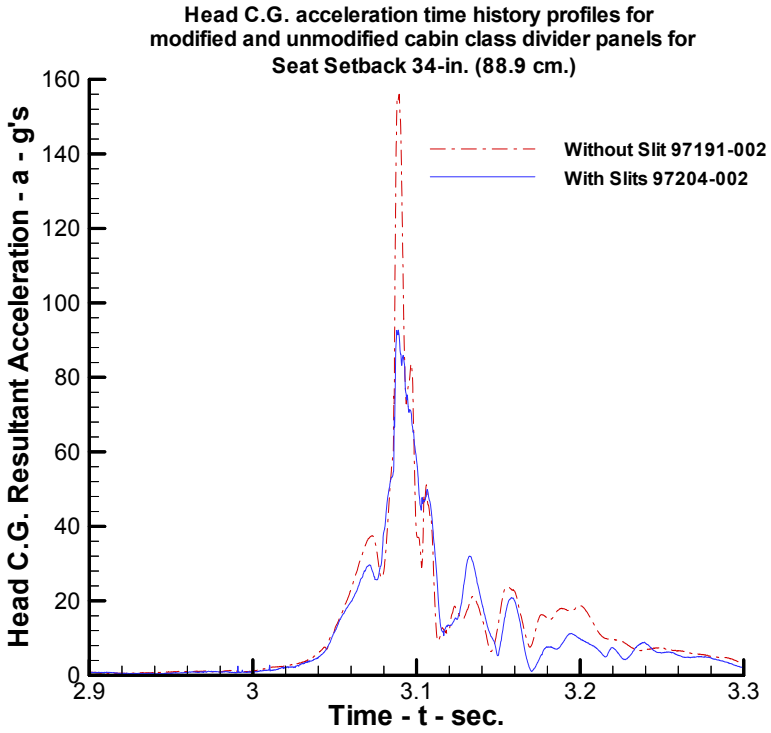

FIGURE 34. HEAD ACCELERATION TIME HISTORY FOR TESTS 97191-002 AND 97204-002

The baseline and modified bulkhead designs were analyzed at the 34-in. seat setback position for the experimental test pulses. The HIC results computed from these data are summarized in table 10.

TABLE 10. COMPARISON OF RESULTS FOR MODIFIED AND UNMODIFIED HONEYCOMB PANELS

Panel	Test Pulse (g's)	Head Impact Velocity (ft/sec)	Peak Head Acceleration (g's)	HIC	HIC Window $\Delta t = t_2 - t_1$ (ms)
Baseline Test	16.3	45.3	156	1394	12.5
Baseline Analysis	16.3	45.9	133	1443	13.8
5 Slits Test	16.2	41.3	93	882	31.1
5 Slits Analysis	16.2	45.9	80	831	27.8

These results confirm the improvement in the HIC level produced by modifying the panel design and illustrate another characteristic of the HIC formula. Although the modified panel attenuated the peak head acceleration, the maximization operator in the HIC formula produced a much longer time interval for the critical HIC value. This increased the HIC level over what it would be had the time interval been constant.

10. DESIGN GUIDELINES FOR HIC-COMPLIANT BULKHEADS.

One of the fundamental questions facing designers of cabin furnishings is whether HIC performance is governed by stiffness or strength. This issue was identified in section 5. This question was addressed by two additional MADYMO studies. The first of these considered a linear-elastic system defined by the stiffness, K, and associated with the load-deflection curve shown in figure 35. Note that no energy is absorbed in such a system. Since it is elastic, all of the energy is returned to the system (probably through the head of the ATD).

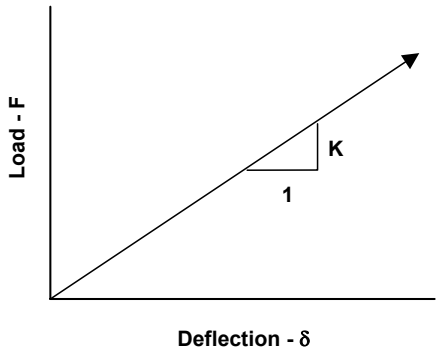

FIGURE 35. LINEAR-ELASTIC SYSTEM

An ideal energy absorber was considered as the second system. This perfectly plastic system was defined in terms of the strength parameter, F_{cr}, and is associated with the load-deflection curve shown in figure 36.

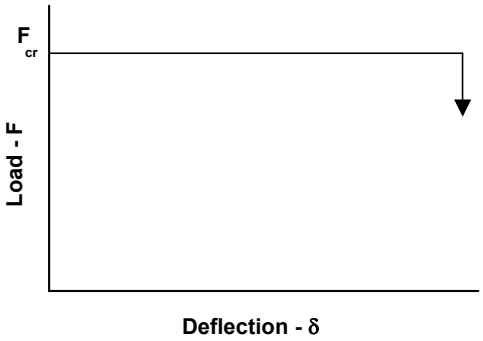

FIGURE 36. IDEAL PLASTIC SYSTEM

It may be noted that such a system would produce a lower HIC value than the linear-elastic system.

Parameter studies were performed to determine the critical values, i.e., the values producing HIC levels of 1000, for the two models. These studies used the ideal test pulse and a 32-in. seat setback distance. The HIC values and peak head accelerations are presented in figures 37 and 38 for the linear-elastic and plastic systems respectively. These figures show that the HIC criteria is satisfied if the stiffness of the elastic system is less than 485 lb./in. and if the strength of the plastic system is less than 1760 lb.

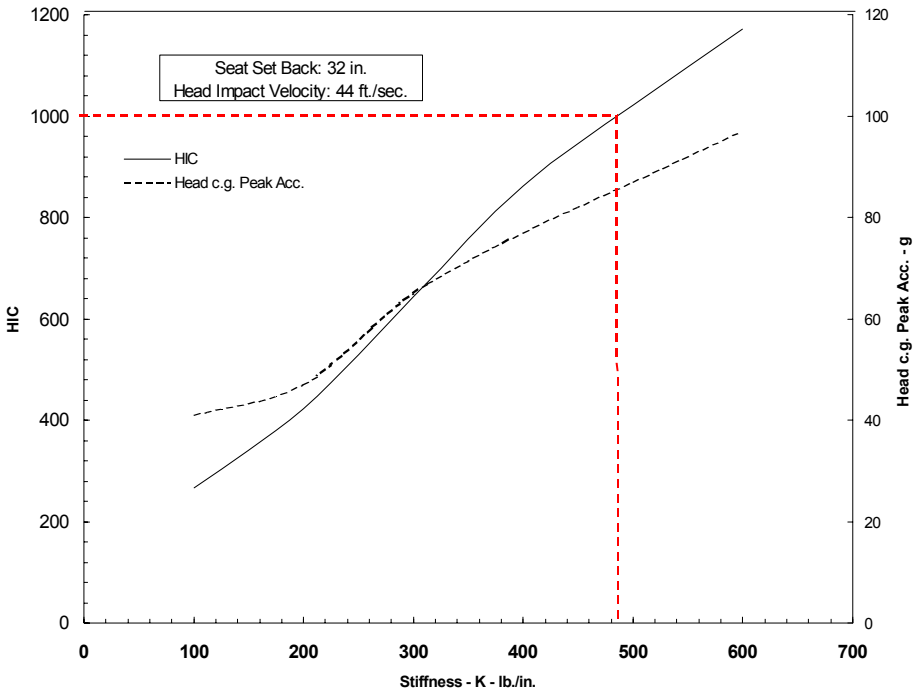

FIGURE 37. HIC AND MAXIMUM HEAD ACCELERATION VS STIFFNESS

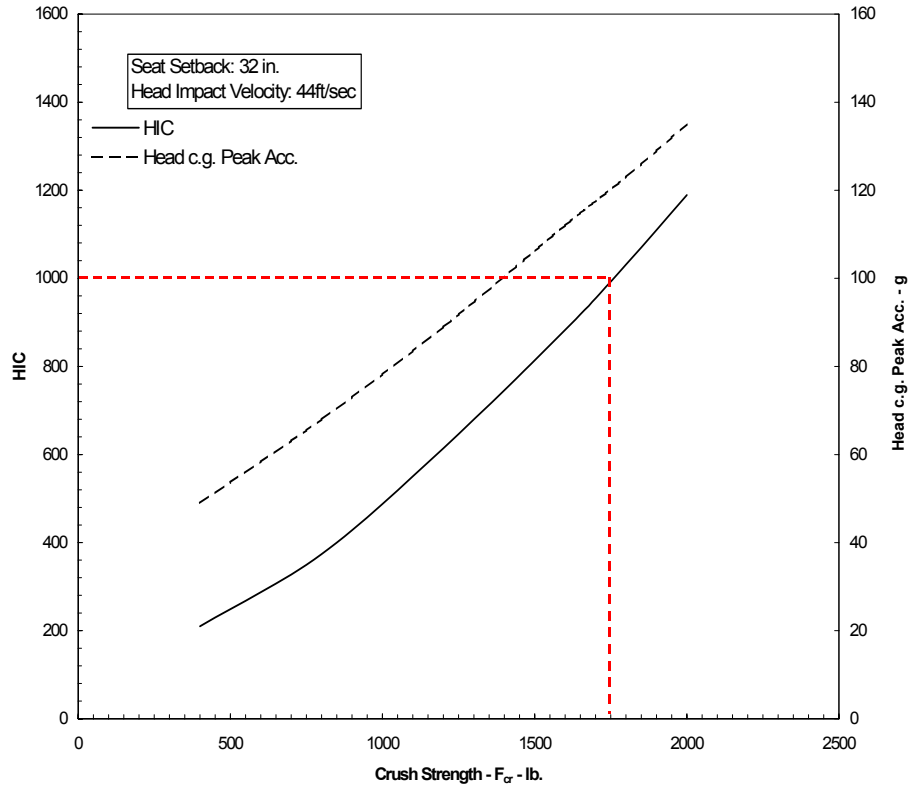

FIGURE 38. HIC AND MAXIMUM HEAD ACCELERATION VS CRUSH STRENGTH

The deflections for HIC = 1000 were respectively computed as 1.94 and 3.45 in. for the perfectly plastic and linear-elastic systems. So, in spite of the fact that it is possible for the linear-elastic system to return all the energy to the ATD, the stroke required for this system is only 78% more than the stroke required for the perfectly plastic system.

The parameter studies were extended to determine how much stroke is required if the stiffness (or strength) is less than the critical value. The results of the stiffness study are shown in figure 39 and those for the strength study in figure 40.

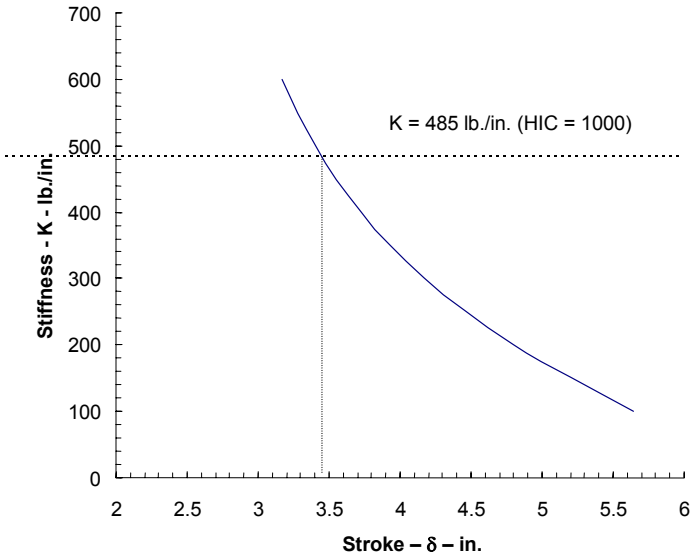

FIGURE 39. STROKE REQUIRED AS A FUNCTION OF BULKHEAD STIFFNESS

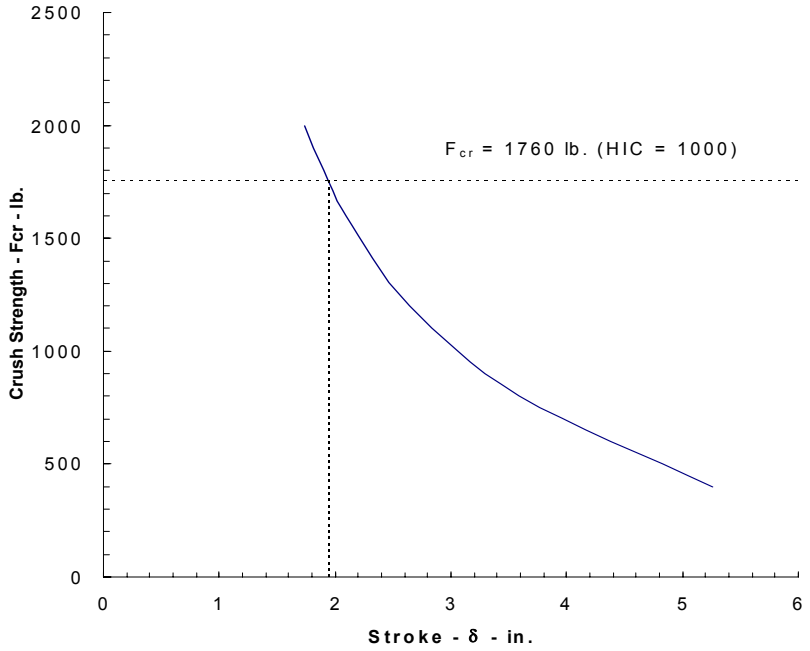

FIGURE 40. STROKE REQUIRED AS A FUNCTION OF BULKHEAD STRENGTH

These figures illustrate the fact that the required panel deflections increase as the strength or stiffness is reduced below the critical values. The implication of these data is that the response of a structure exhibiting an elastic-plastic response will fall between the linear-elastic and perfectly plastic responses. Thus, these structures will have to be designed with the capability to deform 2-4 in. in order to satisfy the HIC requirement.

11. CONCLUSIONS.

This study investigated the head injury criteria (HIC) compliance for front-row seating in transport class aircraft. Bulkheads were designed, fabricated, and tested to successfully demonstrate compliance with this requirement. The first of these designs used a simple aluminum sheet and the second used a weakened honeycomb panel. An analytical study of these designs showed that the HIC levels are very sensitive to the magnitude of the force applied to the ATD's head. The results also established that HIC attenuation requires a minimum of 2 in. of panel deflection for an ideal energy absorbing panel and as much as 3.5 in. of deflection for an elastic panel. Tests of soft aluminum panels demonstrated satisfaction of the head injury criteria and produced deflections of approximately 2.4 in. Tests of modified honeycomb panels produced similar results. Thus, it is concluded that compliance with the head injury criteria requires provisions for 2-4 in. of panel deflection at appropriate force levels.

12. REFERENCES.

1. Anon., "Air Service Medical, War Department," ARMY, Washington, D.C. 1919.

2. Title 14 Code of Federal Regulations, Part 23, Amendment 23-36, Section 562, published in the Federal Register, August 15, 1988.

3. Title 14 Code of Federal Regulations, Part 25, Amendment 25-64, Section 562, published in the Federal Register, May 17, 1988.

4. Title 14 Code of Federal Regulations, Part 27, Amendment 27-25, Section 562, published in the Federal Register, November 13, 1989.

5. Title 14 Code of Federal Regulations, Part 29, Amendment 29-29, Section 562, published in the Federal Register, November 13, 1989.

6. Chandler, R.F., "Human Injury Criteria Relative to Civil Aircraft Seat and Restraint Systems," SAE Paper 851847, Society of Automotive Engineers, Warrendale, PA, 1985.

7. Lissner, H.R., Lebow, M., and Evans, F.G., "Experimental Studies on the Relation Between Acceleration and Intracranial Pressure Changes in Man," *Surgery, Gynecology, and Obstetrics*, Vol. 111, p 329-338, 1960.

8. Gadd, C.W., "Use of a Weighted Impulse Criterion for Estimating Injury Hazard," SAE Paper 660793, Proceedings of the Tenth Stapp Car Crash Conference, pp. 16-174, Society of Automotive Engineers, Warrendale, Pennsylvania, 1966.

9. Versace, J., “A Review of the Severity Index,” SAE Paper 710881, Proceedings of the Fifteenth Stapp Car Crash Conference, pp. 771-796, Society of Automotive Engineers, Warrendale, Pennsylvania, 1971.

10. Motor Vehicle Safety Standard 208: Occupant Crash Protection 49 CFR 571-208, vs Code of Federal Regulation, National Highway Traffic Safety Administration, Washington, D.C., 1972.

11. Department of Transportation (1971) Occupant Crash Protection – Head Injury Criterion, NHTSA Doc Number 69-7, Notice 19, S6.2 of FMVSS 208, March 1971.

12. Chandler, J.S., “Development of Crash Injury Protection in Civil Aviation,” Accidental Injury: Biomechanics and Prevention, Springer-Verlag, A.M. Nahum, J.W. Melvin eds., 1993, pp. 70.

13. DT VEE Program Reference Manual, Data Translation Inc., Marlboro, MA, March 1995.

14. LAST-A-FOAM, General Plastics Inc., Tacoma, Washington.

15. MADYMO Users Manual, Version 5.4, TNO Automotive, May 1999.

16. Anon., “Instrumentation for Impact Test,” SAE Surface Vehicle, Society of Automotive Engineers, Recommended Practice J211/1, Warrendale, PA, March 1995.

APPENDIX A—DATA ANALYSIS FOR BULKHEAD SLED TEST SERIES 96127, 96219, AND 96288

SLED TEST 96127-005

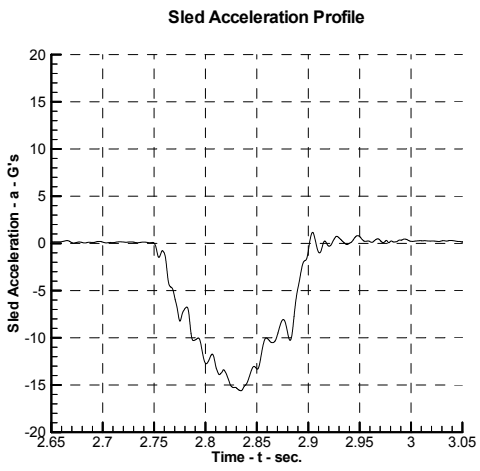

(a)

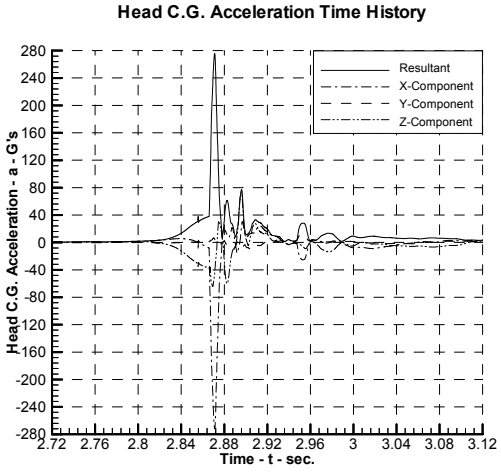

(b)

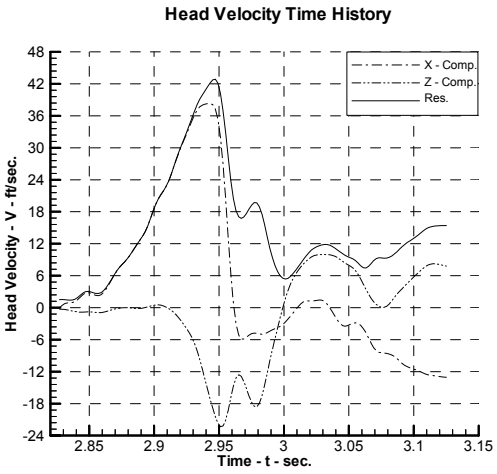

(c)

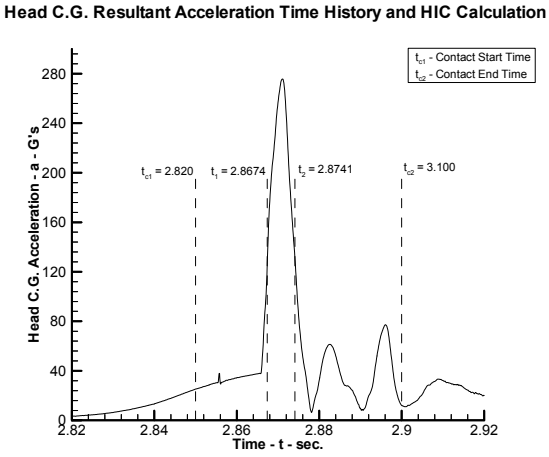

(d)

Results of Sled Test 96127-005

Figure – (a)

Panel – Rigid panel with 3.125-in. (7.94-cm) Rigid Foam FR 3703
Seat setback – 32 in. (81.28 cm)
Peak sled deceleration – 15.6 g
Rise time – 74.8 ms
Velocity change – 29.9 ft/s (9.80 m/s)
Velocity change total – 45.8 ft/s (13.96 m/s)

Figure – (d)

Head impact velocity – 43.1 ft/s (13.14 m/s)
Head impact angle – 18°
Head c.g. peak acceleration – 274.5 g
HIC – 4645
$\Delta t = t_2 - t_1 = 6.7$ ms

SLED TEST 96127-006

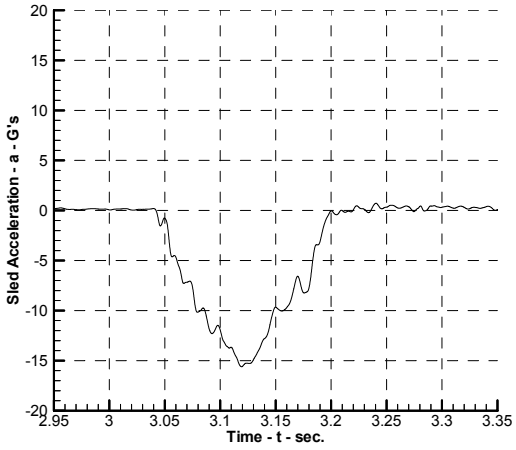

(a)

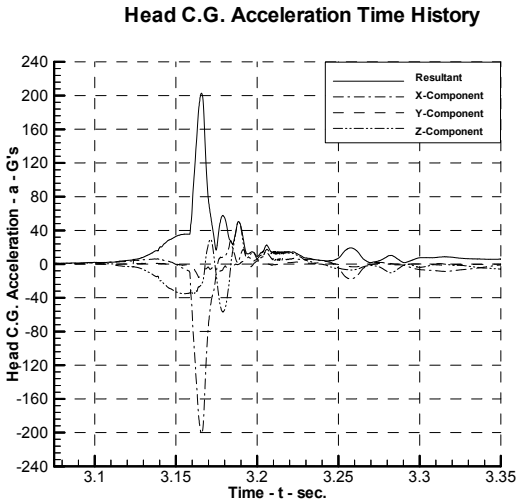

(b)

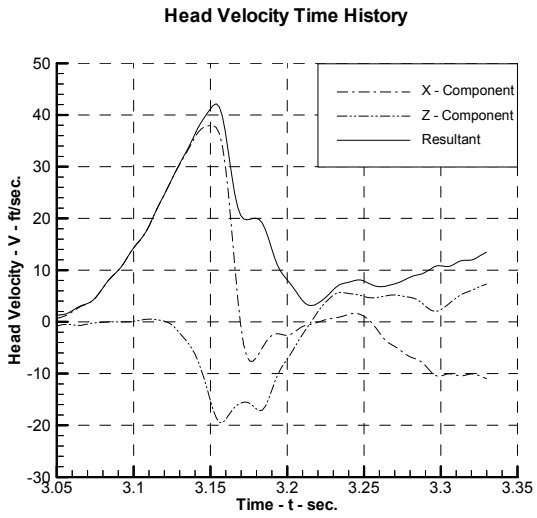

(c)

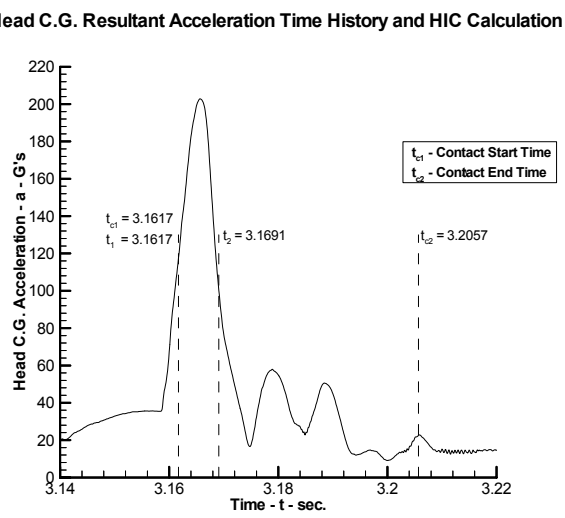

(d)

Results of Sled Test 96127-006

Figure – (d)

Panel – Rigid panel with 3-in. (7.62-cm) Rigid Foam FR 3502
Seat setback – 32 in. (81.28 cm)
Peak sled deceleration – 15.6 g
Rise time – 74.3 ms
Velocity change – 29.4 ft/s (8.96 m/s)
Velocity change total – 45.4 ft/s (13.84 m/s)

Figure – (d)

Head impact velocity – 42.14 ft/s (12.84 m/s)
Head impact angle – 10°
Head c.g. peak acceleration – 203 g
HIC – 2647
$\Delta t = t_2 - t_1 = 7.4$ ms

SLED TEST 96127-007

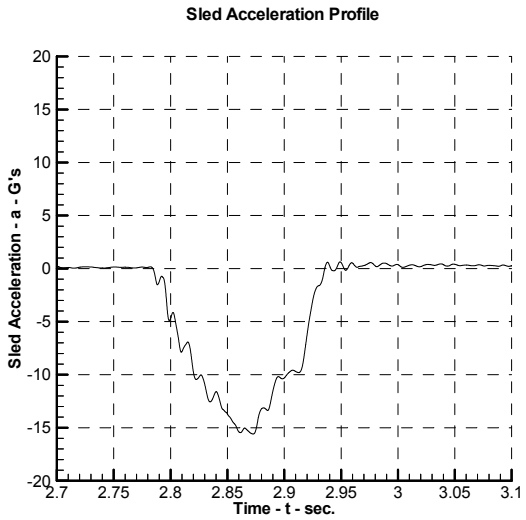

(a)

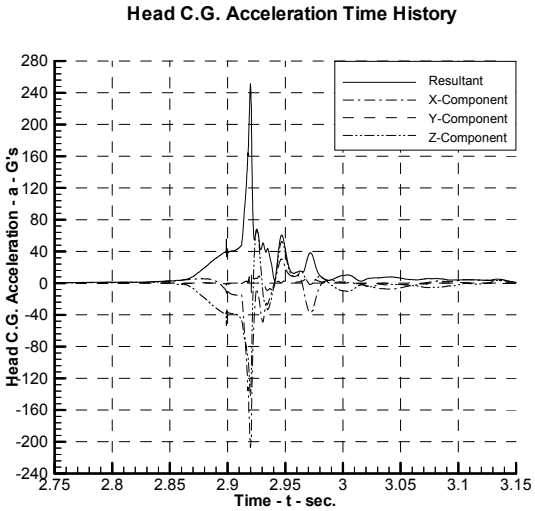

(b)

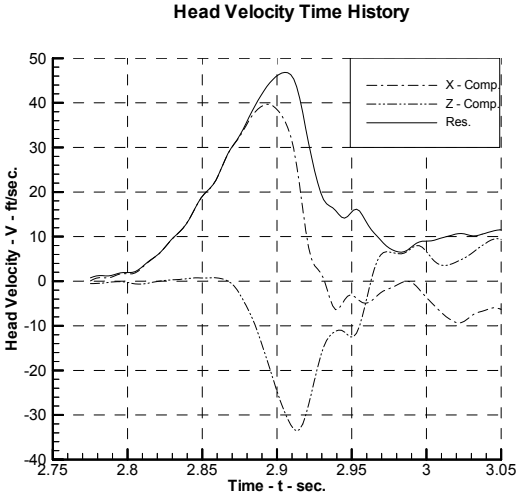

(c)

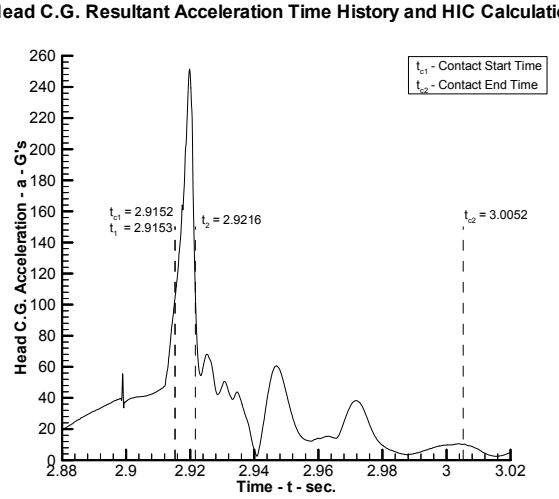

(d)

Results of Sled Test 96127-007

Figure – (a)

Panel – Rigid panel with 2-in. (5.08-cm) Rigid Foam FR 3502
Seat setback – 36 in. (91.44 cm)
Peak sled deceleration – 15.6 g
Rise time – 71.6 ms
Velocity change – 29.9 ft/s (9.12 m/s)
Velocity change total – 45.6 ft/s (13.90 m/s)

Figure – (d)

Head impact velocity – 46.82 ft/s (14.27 m/s)
Head impact angle – 48°
Head c.g. peak acceleration – 251.5 g
HIC – 2537
$\Delta t = t_2 - t_1 = 6.3$ ms

SLED TEST 96127-008

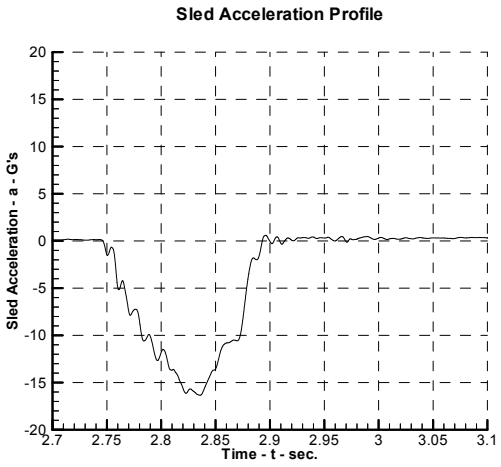

(a)

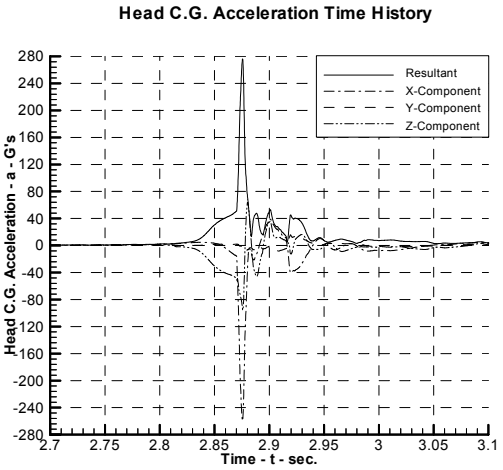

(b)

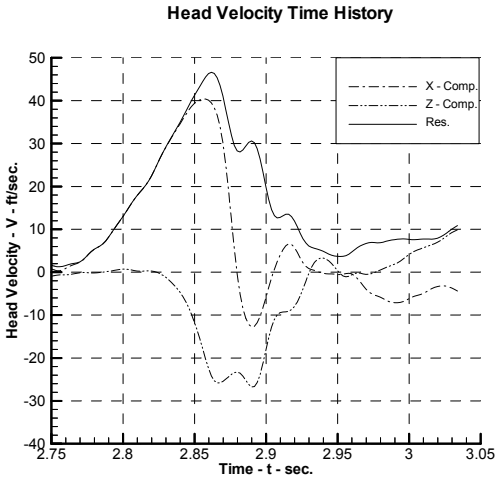

(c)

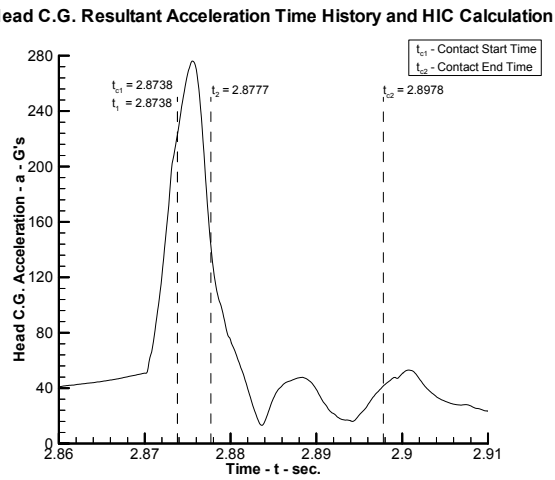

(d)

Results of Sled Test 96127-008

Figure – (a)

Panel – Rigid panel with 3 in. (7.62 cm) Rigid Foam FR 3703
Seat setback – 35 in. (88.9 cm)
Peak sled deceleration – 16.4 g
Rise time – 74.3 ms
Velocity change – 30.6 ft/s (9.93 m/s)
Velocity change total – 45.9 ft/s (14.0 m/s)

Figure – (d)

Head impact velocity – 46.63 ft/s (14.21 m/s)
Head impact angle – 32°
Head c.g. peak acceleration – 276.1 g
HIC – 3400
$\Delta t = t_2 - t_1 = 3.9$ ms

SLED TEST 96127-009

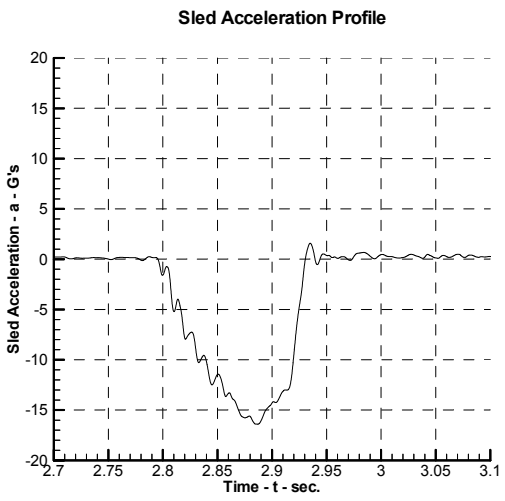

(a)

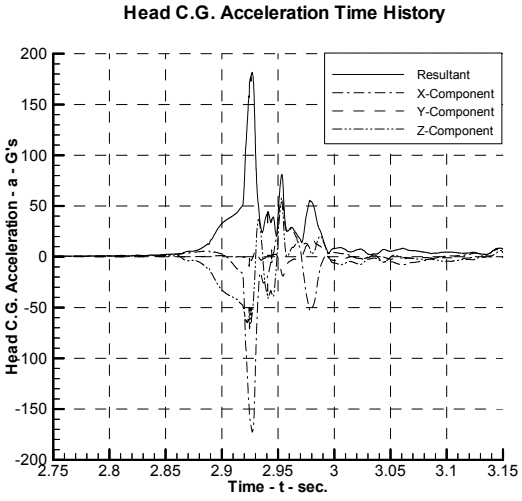

(b)

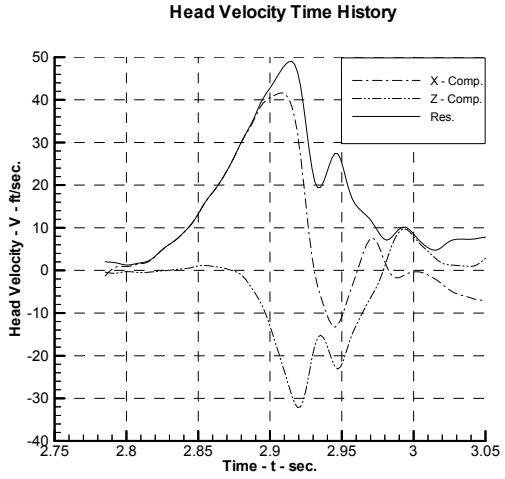

(c)

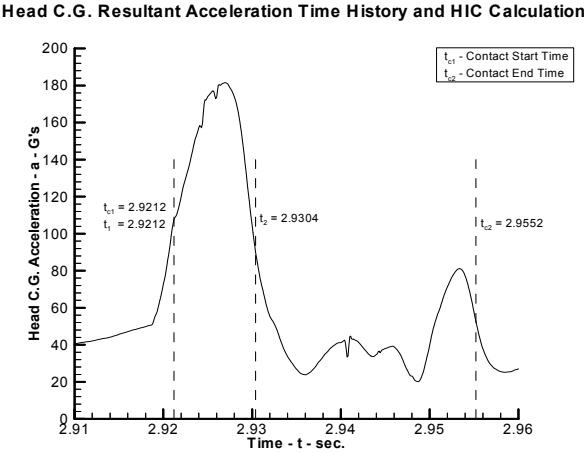

(d)

Results of Sled Test 96127-009

Figure – (a)

Panel – Rigid panel with 3-in. (7.62-cm) Rigid Foam FR 3502
Seat setback – 35 in. (88.9 cm)
Peak sled deceleration – 16.4 g
Rise time – 77.8 ms
Velocity change – 29.9 ft/s (9.16 m/s)
Velocity change total – 45.5 ft/s (13.87 m/s)

Figure – (d)

Head impact velocity – 49 ft/s (14.94 m/s)
Head impact angle – 27°
Head c.g. peak acceleration – 188.5G
HIC – 2601
$\Delta t = t_2 - t_1 = 9.2$ ms

SLED TEST 96127-010

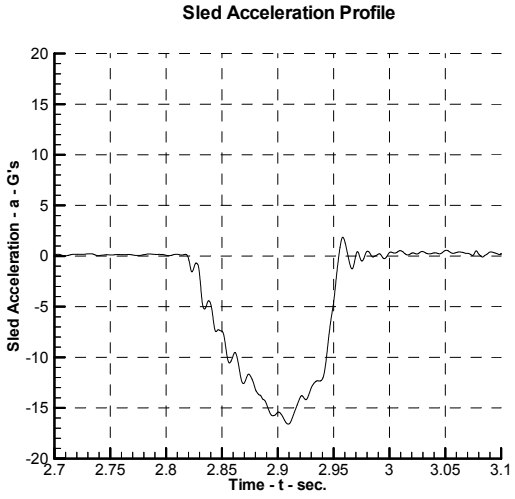

(a)

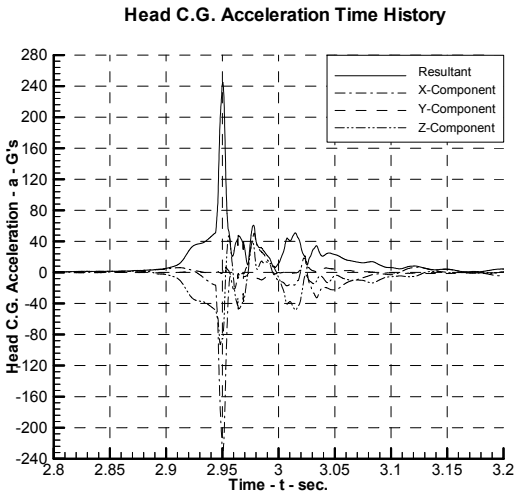

(b)

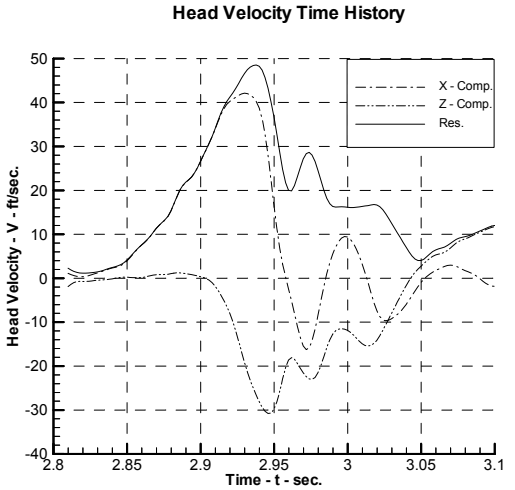

(c)

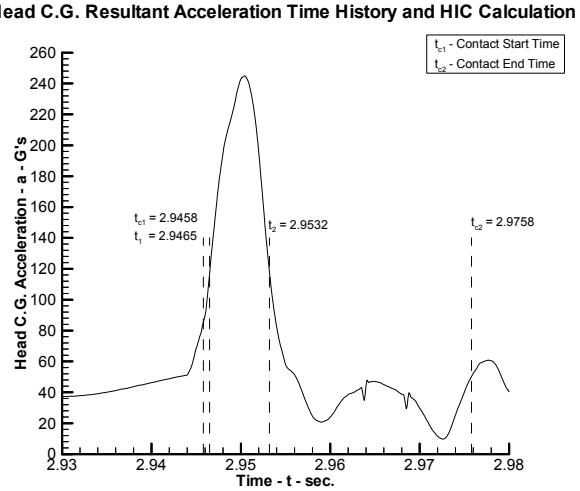

(d)

<u>Results of Sled Test 96127-010</u>

Figure – (a)

Panel – Rigid panel with 3-in. (7.62-cm) Rigid Foam (1 in. FR 3502 & 2 in. FR 3703)
Seat setback – 35 in. (88.9 cm)
Peak sled deceleration – 16.6 g
Rise time – 76.3 ms
Velocity change – 30.2 ft/s (9.20 m/s)
Velocity change total – 45.5 ft/s (13.87 m/s)

Figure – (d)

Head impact velocity – 48.54 ft/s (14.79 m/s)
Head impact angle – 25°
Head c.g. peak acceleration – 244.9 g
HIC – 3709
$\Delta t = t_2 - t_1 = 6.7$ ms

SLED TEST 96127-011

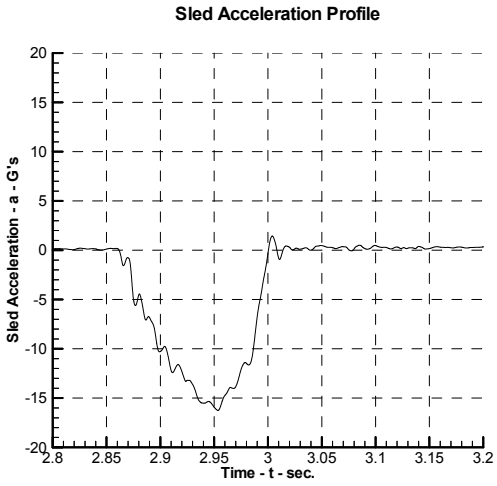

(a)

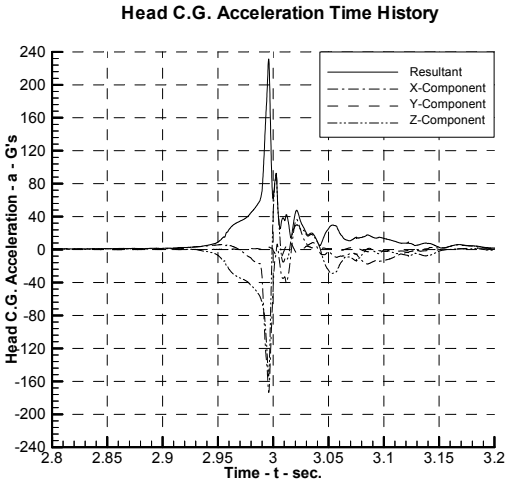

(b)

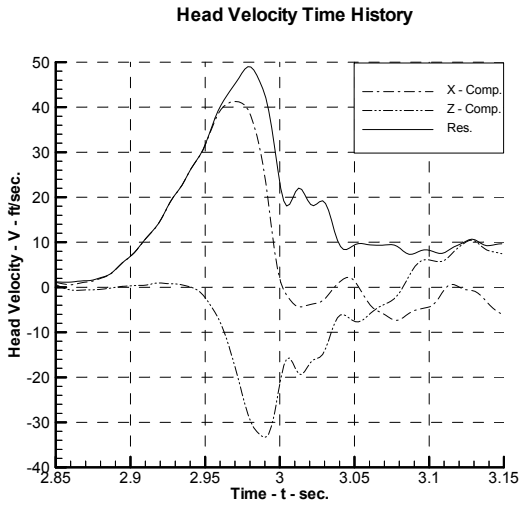

(c)

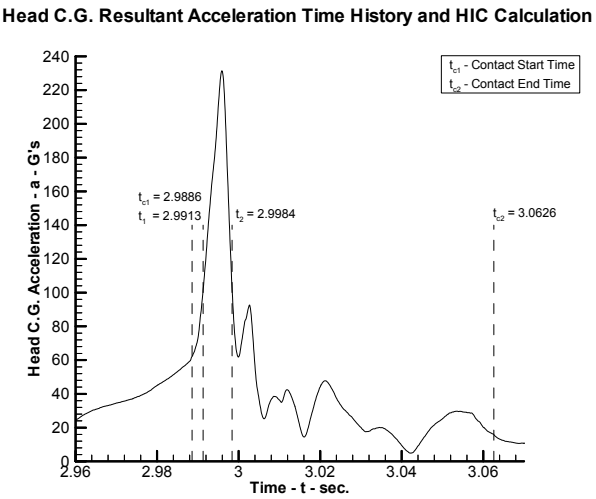

(d)

Results of Sled Test 96127-011

Figure – (a)

Panel – Rigid panel with 2-in. (5.08-cm) Foam (1 in. Ensolite II & 1 in. Ensolite III)
Seat setback – 36 in. (91.44 cm)
Peak sled deceleration – 16.3 g
Rise time – 76.6 ms
Velocity change – 29.8 ft/s (9.08 m/s)
Velocity change total – 45.4 ft/s (13.84 m/s)

Figure – (d)

Head impact velocity – 49.01 ft/s (14.94 m/s)
Head impact angle – 36°
Head c.g. peak acceleration – 231.5 g
HIC – 2715
$\Delta t = t_2 - t_1 = 7.1$ ms

SLED TEST 96127-012

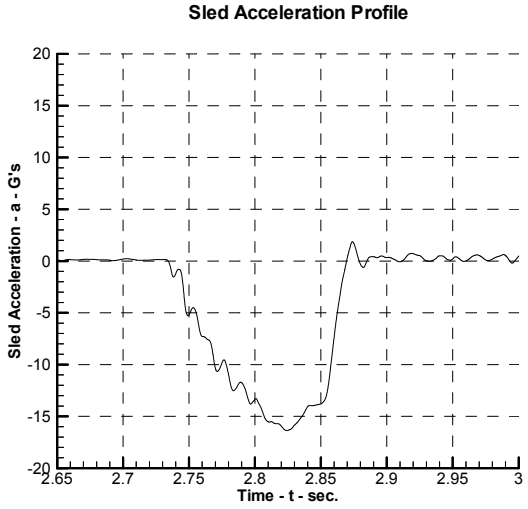

(a)

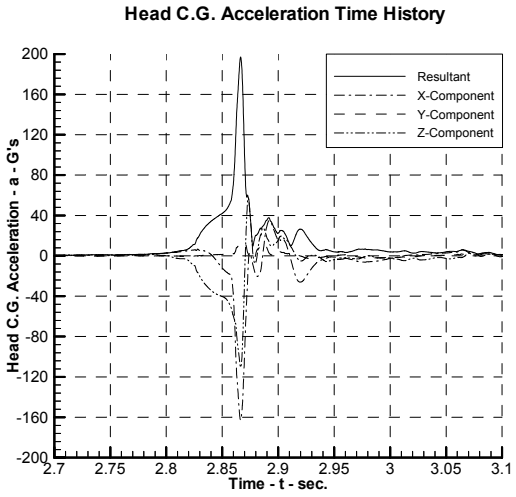

(b)

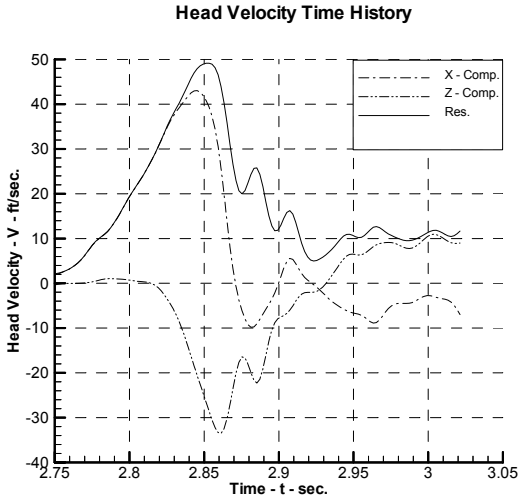

(c)

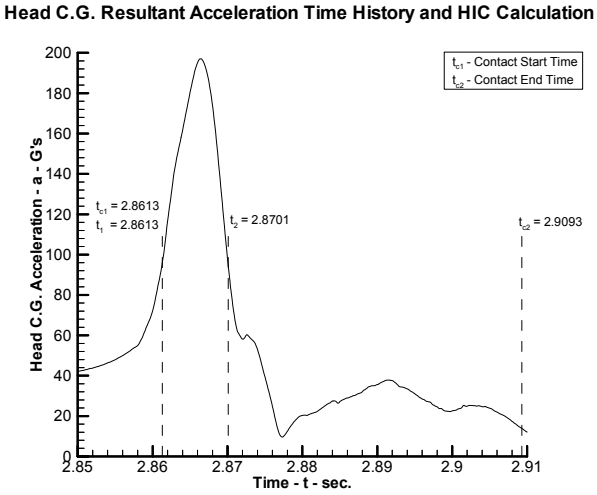

(d)

Results of Sled Test 96127-012

Figure – (a)

Panel – Rigid panel with 3-in. (7.62-cm) Rigid Foam (2 in. Ensolite II & 1 in. Ensolite III)
Seat setback – 35 in. (88.9 cm)
Peak sled deceleration – 16.4 g
Rise time – 76.7 ms
Velocity change – 30.2 ft/s (9.20 m/s)
Velocity change total – 45.7 ft/s (13.93 m/s)

Figure – (d)

Head impact velocity – 49.16 ft/s (14.79 m/s)
Head impact angle – 29°
Head c.g. peak acceleration – 197 g
HIC – 2719
$\Delta t = t_2 - t_1 = 8.8$ ms

SLED TEST 96219-001

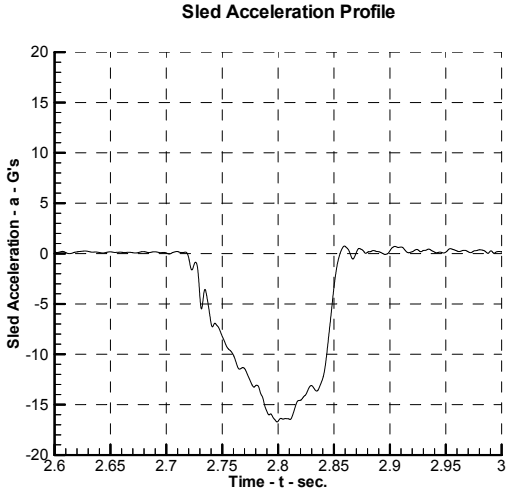

(a)

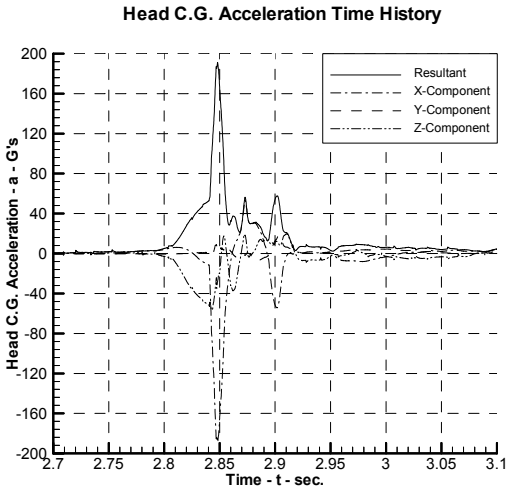

(b)

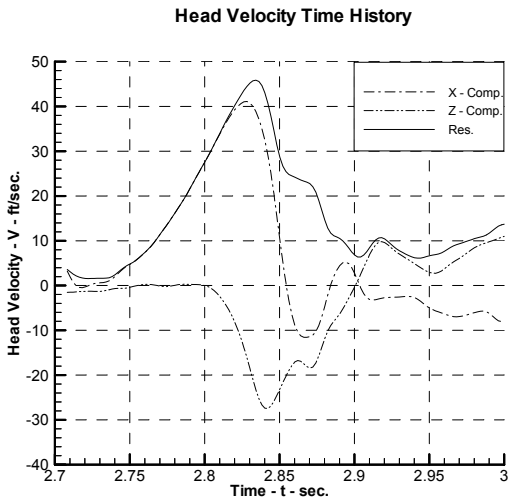

(c)

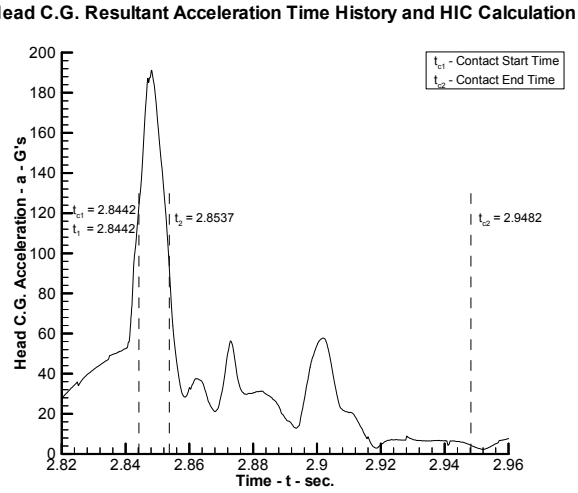

(d)

Results of Sled Test 96219-001

Figure – (a)

Panel – Rigid panel of 0.5-in. (1.27-cm) with 2+2+2 = 6-in. (15.24-cm) Rigid Foam FR 3502
Seat setback – 34 in. (86.36 cm)
Peak sled deceleration – 16.7 g
Rise time – 74.6 ms
Velocity change – 30.5 ft/s (9.30 m/s)
Velocity change total – 46.7 ft/s (14.24 m/s)

Figure – (d)

Head impact velocity – 45.86 ft/s (13.98 m/s)
Head impact angle – 32°
Head c.g. peak acceleration – 191.2 g
HIC – 2850
$\Delta t = t_2 - t_1 = 9.5$ ms

SLED TEST 96219-002

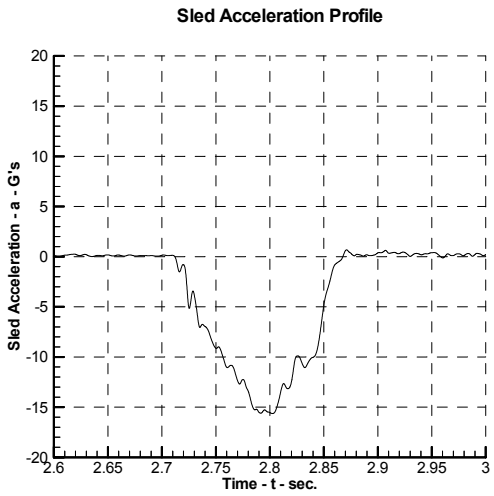

(a)

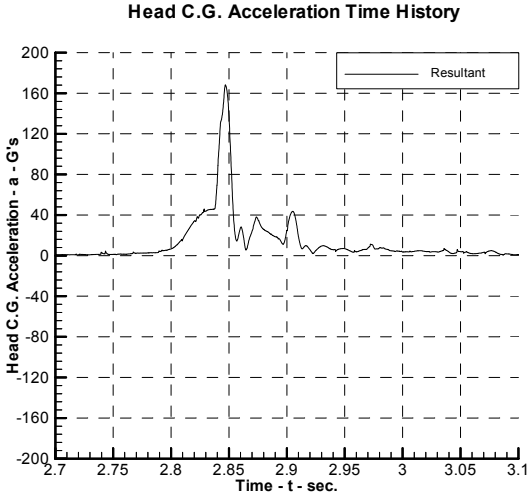

(b)*

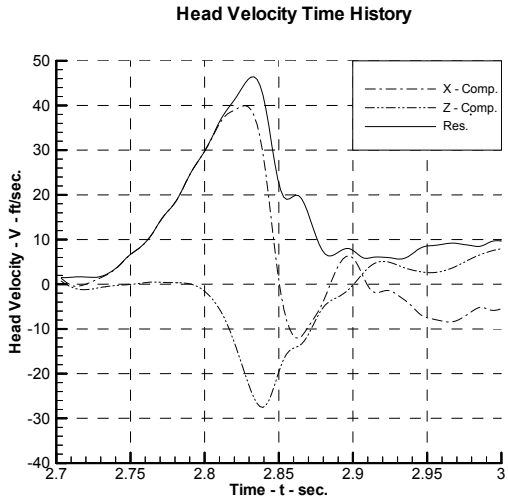

(c)

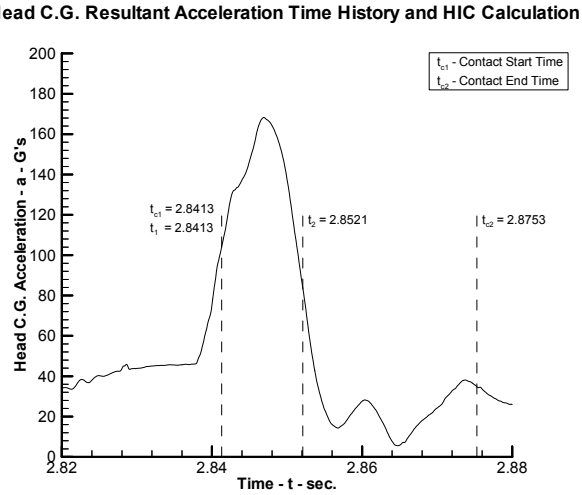

(d)

* Data not available for X, Y & Z component

<u>Results of Sled Test 96219-002</u>

Figure – (a)

Panel – Rigid panel of 0.5 in. (1.27 cm) with 1+2+3 = 6-in. (15.24-cm) Rigid Foam (1+2 in. FR3502 and 3 in. FR3503)
Seat setback – 34 in. (86.36 cm)
Peak sled deceleration – 15.6 g
Rise time – 74.7 ms
Velocity change – 28.7 ft/s (8.75 m/s)
Velocity change total – 45.8 ft/s (13.96 m/s)

Figure – (d)

Head impact velocity – 46.39 ft/s (14.14 m/s)
Head impact angle – 29°
Head c.g. peak acceleration – 168.32 g
HIC – 2481
$\Delta t = t_2 - t_1 = 10.8$ ms

SLED TEST 96219-003

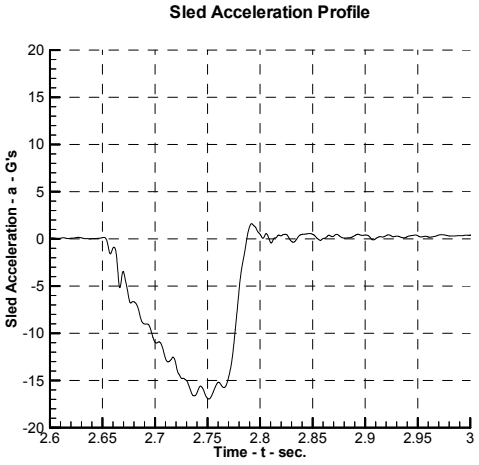

(a)

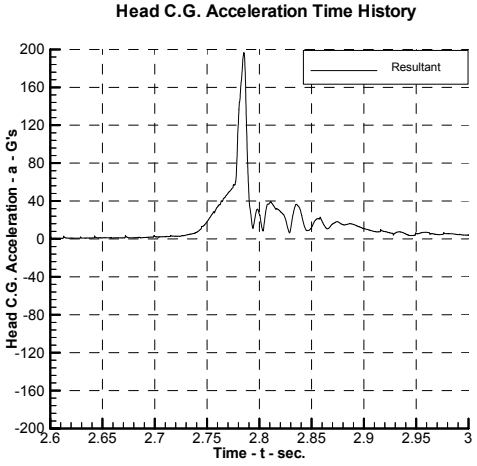

(b)*

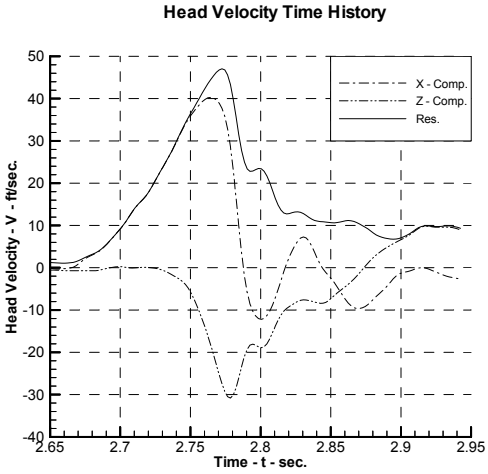

(c)

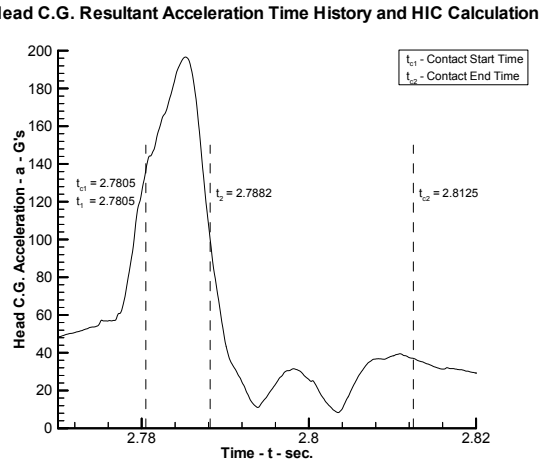

(d)

* Data not available for X, Y & Z component

Results of Sled Test 96219-003

Figure – (a)

Panel – Rigid panel of 0.5 in (1.27 cm) with 1+2 = 3-in (7.62-cm) Rigid Foam FR 3502
Seat setback – 34 in. (86.36 cm)
Peak sled deceleration – 17.0 g
Rise time – 84.9 ms
Velocity change – 28.8 ft/s (8.78 m/s)
Velocity change total – 45.7 ft/s (13.93 m/s)

Figure – (d)

Head impact velocity – 47.08 ft/s (14.35 m/s)
Head impact angle – 29°
Head c.g. peak acceleration – 196.7 g
HIC – 2691
$\Delta t = t_2 - t_1 = 7.7$ ms

SLED TEST 96219-004

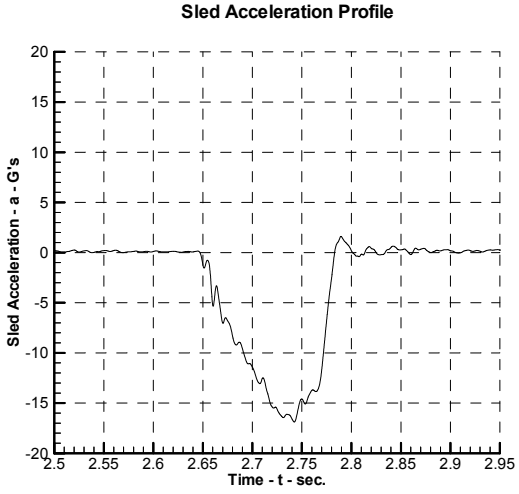

(a)

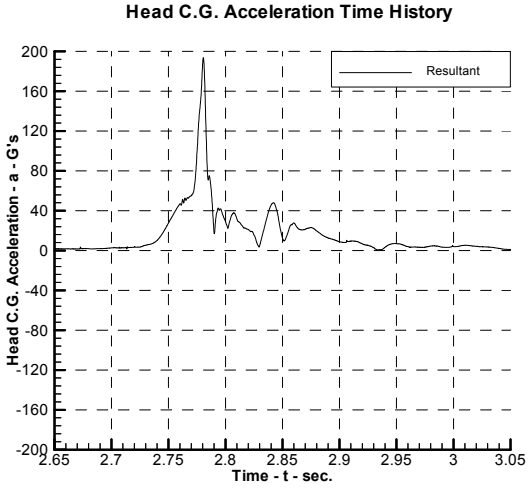

(b)*

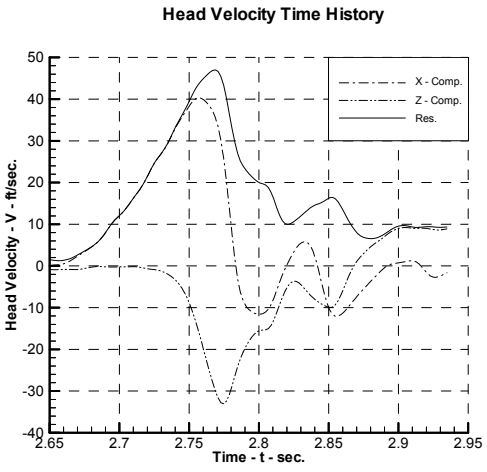

(c)

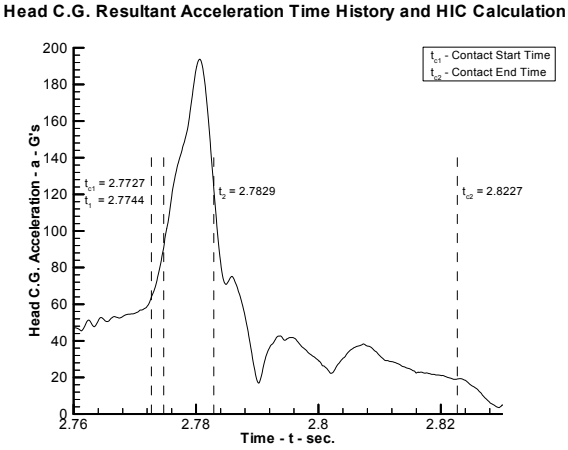

(d)

* Data not available for X,Y & Z components.

<u>Results of Sled Test 96219-004</u>

Figure – (a)

Panel – Rigid panel of 0.5 in (1.27 cm) with 7.62-cm (2+1=3-in.) Rigid Foam (2 in. Ensolite II & 1 in. Ensolite III)
Seat setback – 34 in. (86.36 cm)
Peak sled deceleration – 16.9 g
Rise time – 76.9 ms
Velocity change – 8.96 m/s (29.4 ft/s)
Velocity change total – 14.05 m/s (46.1 ft/s)

Figure – (d)

Head impact velocity – 14.33 m/s (47.03 ft/s)
Head impact angle – 24°
Head c.g. peak acceleration – 193.8 g
HIC – 2352
$\Delta t = t_2 - t_1 = 8.5$ ms

SLED TEST 96219-005

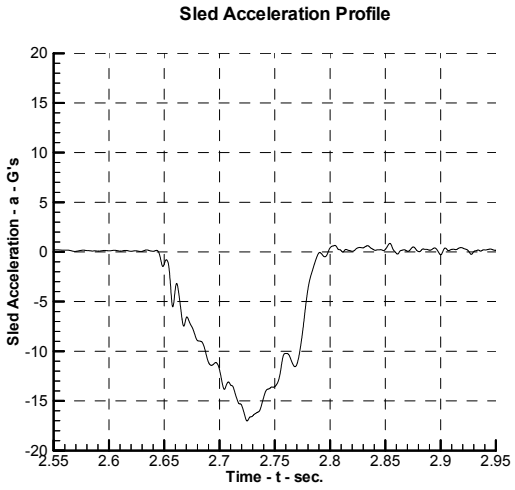

(a)

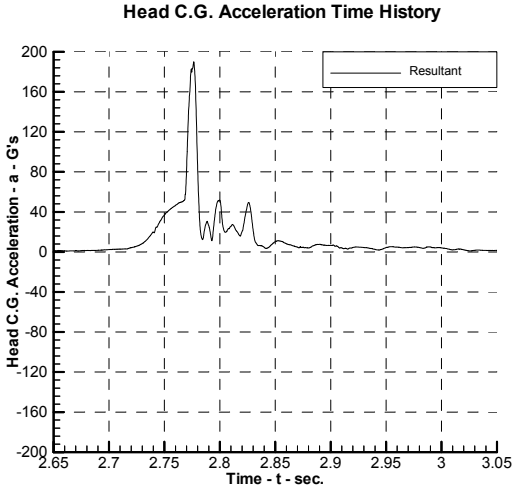

(b)

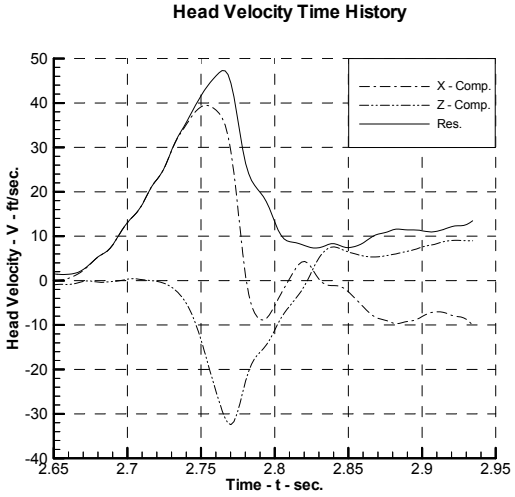

(c)

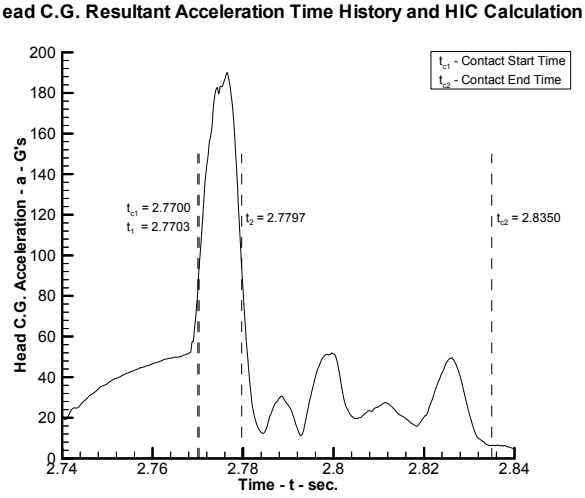

(d)

* Data not available for X, Y & Z components

<u>Results of Sled Test 96219-005</u>

Figure – (a)

Panel – Rigid panel of 0.5 in. (1.27 cm) with 3+3 = 6-in. (15.24-cm) Rigid Foam FR 3703
Seat setback – 34 in. (86.36 cm)
Peak sled deceleration – 17.0 g
Rise time – 81.2 ms
Velocity change – 29.5 ft/s (9.0 m/s)
Velocity change total – 46.3 ft/s (14.16 m/s)

Figure – (d)

Head impact velocity – 47.28 ft/s (14.41 m/s)
Head impact angle – 31°
Head c.g. peak acceleration – 190.0 g
HIC – 2937
$\Delta t = t_2 - t_1 = 9.4$ ms

SLED TEST 96219-006

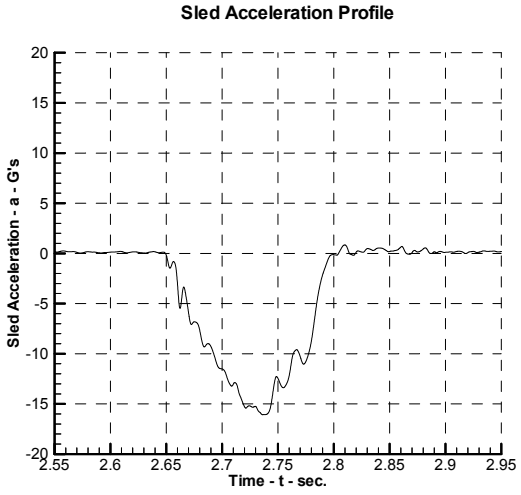

(a)

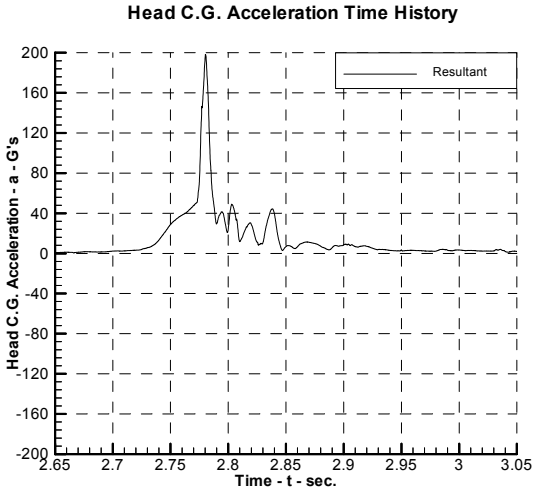

(b)*

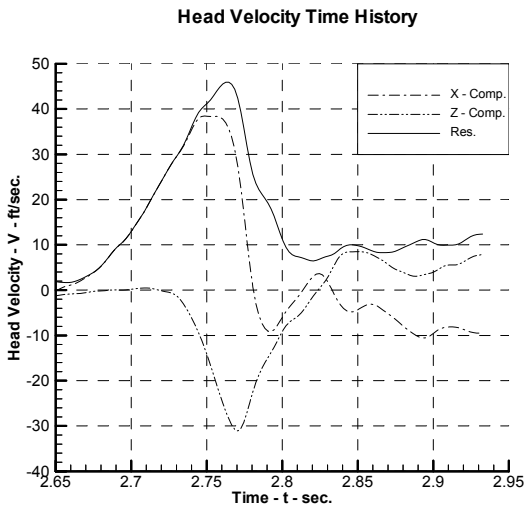

(c)

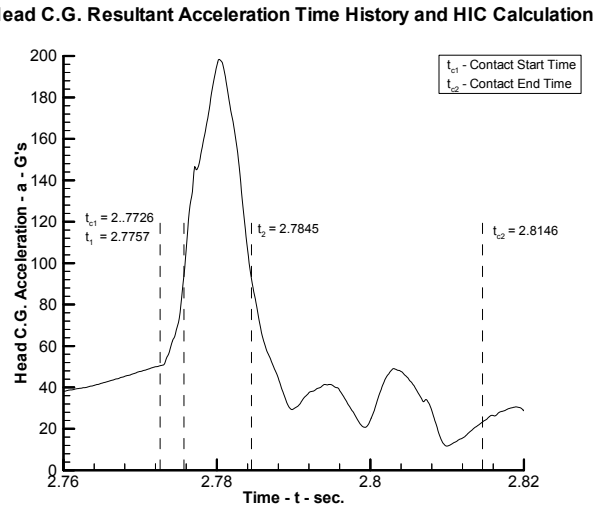

(d)

* Data not available for X, Y & Z components.

Results of Sled Test 96219-006

Figure – (a)

Panel – Rigid panel of 0.5 in (1.27 cm) with 1+3=4 in (10.16-cm) Rigid Foam (1 in. FR 3502 & 3 in. FR 3703)
Seat setback – 34 in. (86.36 cm)
Peak sled deceleration – 16.1 g
Rise time – 72.7 ms
Velocity change – 29.7 ft/s (9.05 m/s)
Velocity change total – 46.1 ft/s (14.05 m/s)

Figure – (d)

Head impact velocity – 45.93 ft/s (14.00 m/s)
Head impact angle – 28°
Head c.g. peak acceleration – 198.4 g
HIC – 2624
$\Delta t = t_2 - t_1 = 8.8$ ms

SLED TEST 96288-001

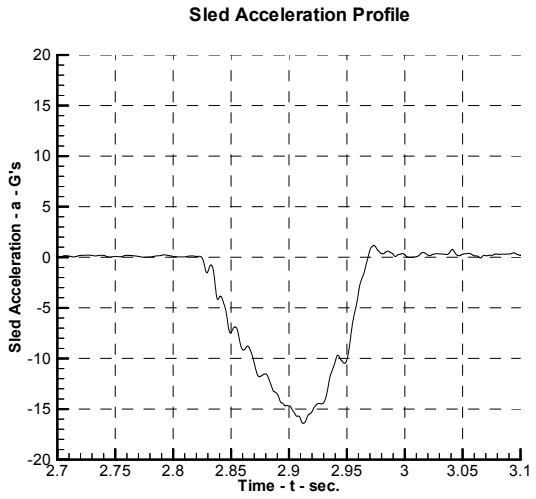

(a)

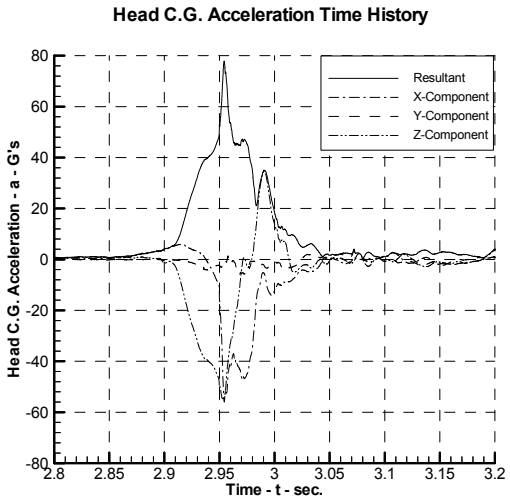

(b)

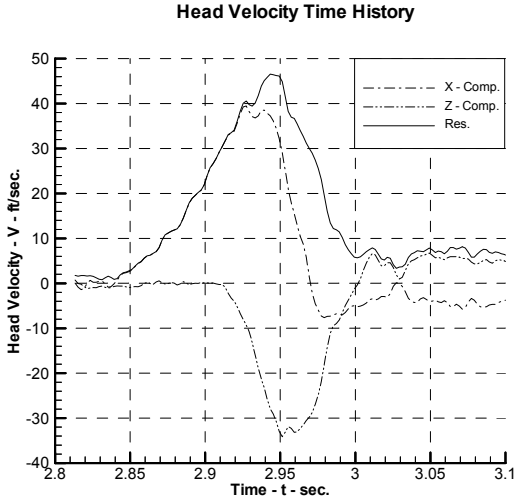

(c)

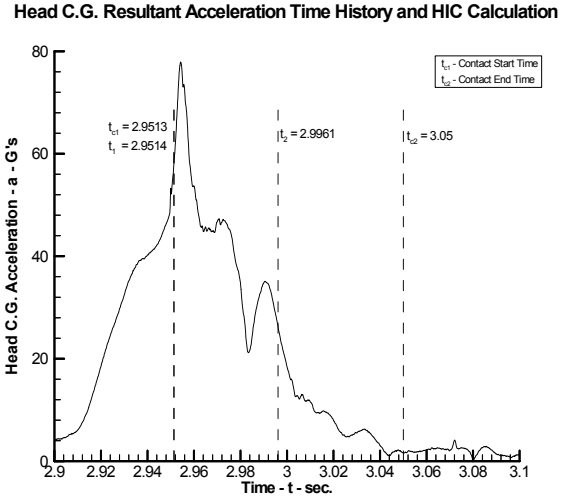

(d)

Results of Sled Test 96288-001

Figure – (a)

Panel – 2024-O aluminum sheet panel of 0.063-in. (0.16-cm) LAST-A-FOAM FR 3502 2 lb/cu.ft thickness 3 in. (7.62 cm)
Seat setback – 34 in. (86.36 cm)
Peak sled deceleration – 16.4 g
Rise time – 82.8 ms
Velocity change – 29.0 ft/s (8.84 m/s)
Velocity change total – 45.0 ft/s (13.72 m/s)

Figure – (d)

Head impact velocity – 46.58 ft/s (14.20 m/s)
Head impact angle – 33°
Head c.g. peak acceleration – 77.9 g
HIC – 559
$\Delta t = t_2 - t_1 = 44.7$ ms

SLED TEST 96288-002

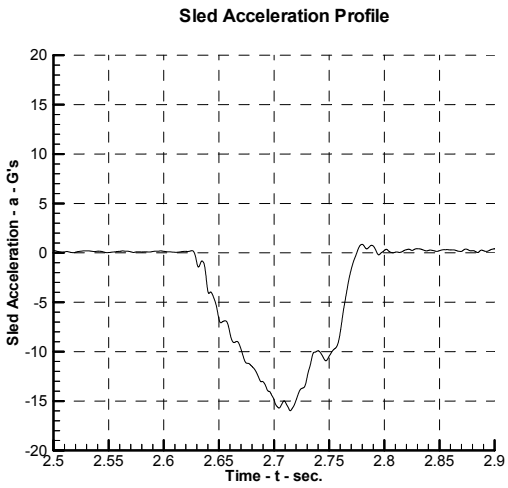

(a)

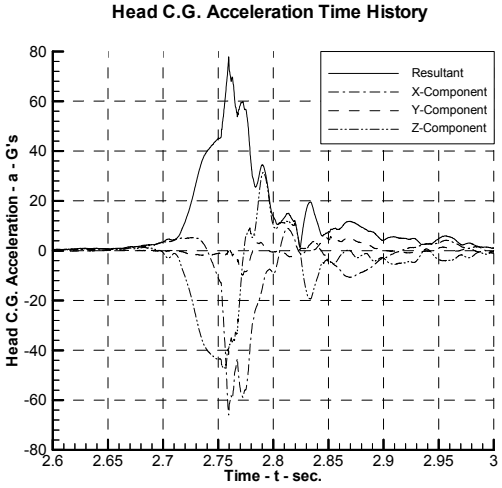

(b)

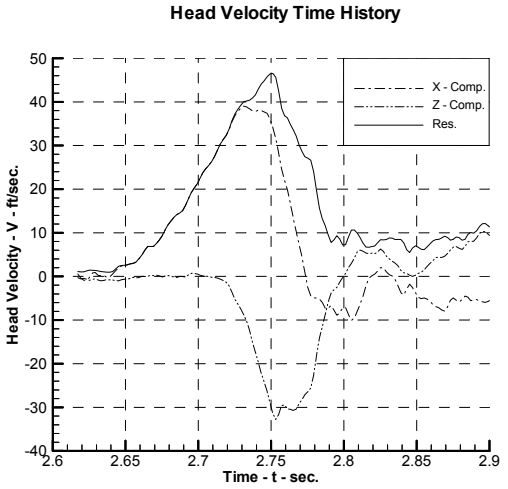

(c)

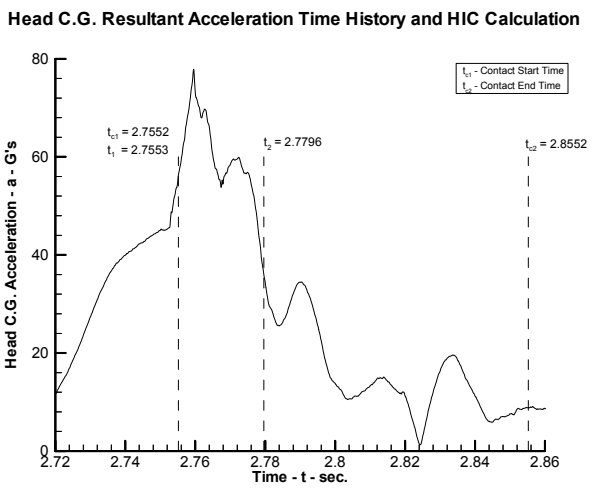

(d)

Results of Sled Test 96288-002

Figure – (a)

Panel – 2024-O aluminum sheet panel of 0.07-in. (0.18-cm) LAST-A-FOAM FR 3502 2 lb/cu.ft thickness 3 in. (7.62 cm)
Seat setback – 34 in. (86.36 cm)
Peak sled deceleration – 16.0 g
Rise time – 75.3 ms
Velocity change – 29.2 ft/s (8.90 m/s)
Velocity change total – 45.1 ft/s (13.75 m/s)

Figure – (d)

Head impact velocity – 46.52 ft/s (14.18 m/s)
Head impact angle – 34°
Head c.g. peak acceleration – 77.8 g
HIC – 674
$\Delta t = t_2 - t_1 = 24.3$ ms

SLED TEST 96288-003

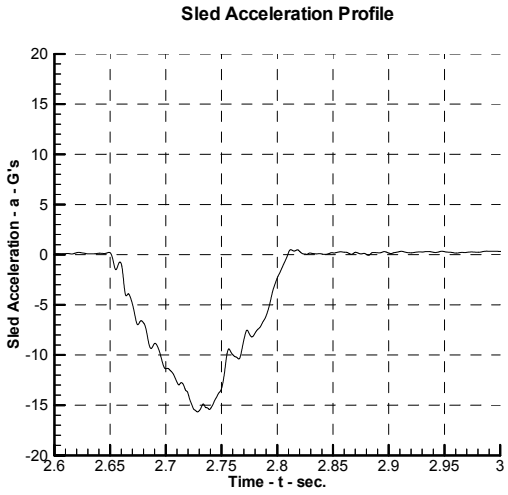

(a)

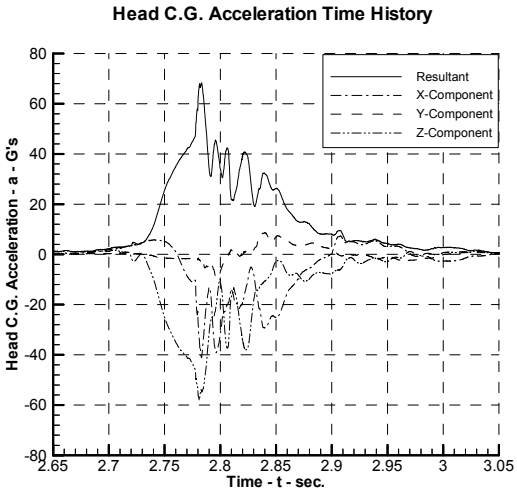

(b)

No video data available

(c)

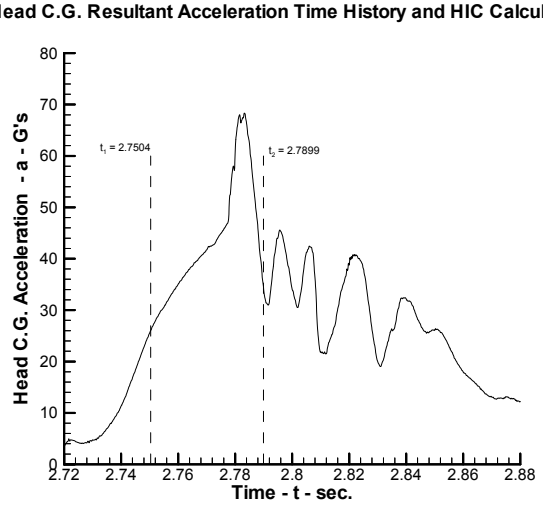

(d)

Results of Sled Test 96288-003

Figure – (a)

Panel – 2024-O aluminum sheet panel of 0.04-in. (0.1-cm) LAST-A-FOAM FR 3502 2lb/cu.ft
thickness 3 in. (7.62 cm)
Seat setback – 34 in. (86.36 cm)
Peak sled deceleration – 15.7 g
Rise time – 74.4 ms
Velocity change – 28.9 ft/s (8.81 m/s)
Velocity change total – 44.9 ft/s (13.69 m/s)

Figure – (d)

Head c.g. peak acceleration – 68.3 g
HIC – 491
$\Delta t = t_2 - t_1 = 39.5$ ms

SLED TEST 96288-004

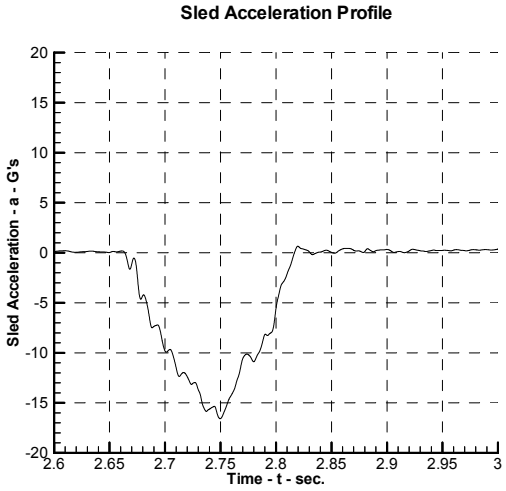

(a)

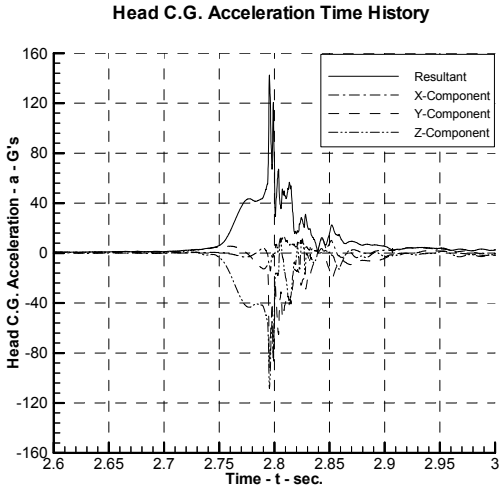

(b)

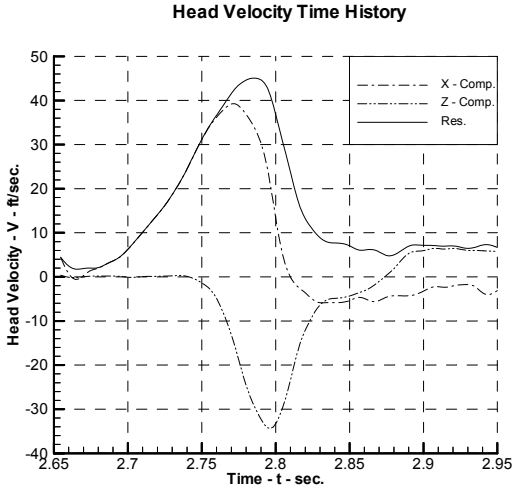

(c)

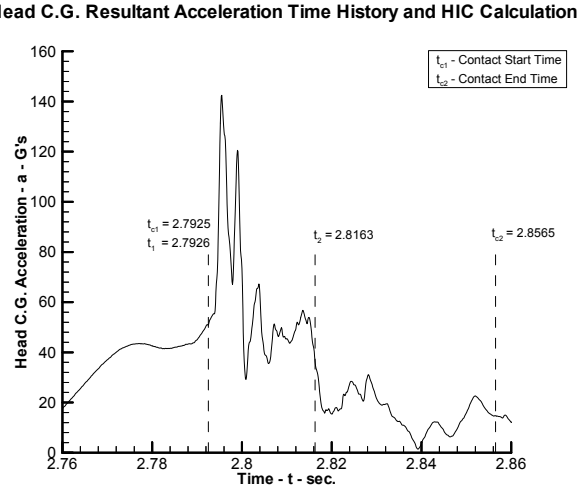

(d)

Results of Sled Test 96288-004

Figure – (a)

Panel – 2024-O aluminum sheet panel of 0.063 in. (0.16 cm)
Seat setback – 34 in. (86.36 cm)
Peak sled deceleration – 16.6 g
Rise time – 73.4 ms
Velocity change – 30.4 ft/s (9.27 m/s)
Velocity change total – 46.1 ft/s (14.05 m/s)

Figure – (d)

Head impact velocity – 45.08 ft/s (13.74 m/s)
Head impact angle – 38°
Head c.g. peak acceleration – 142.5 g
HIC – 694
$\Delta t = t_2 - t_1 = 23.7$ ms

SLED TEST 96288-005

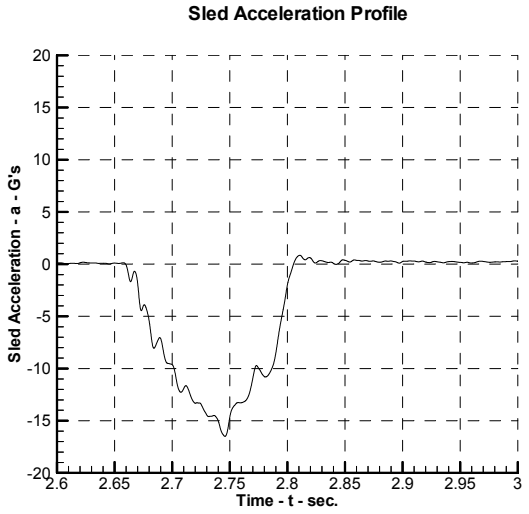

(a)

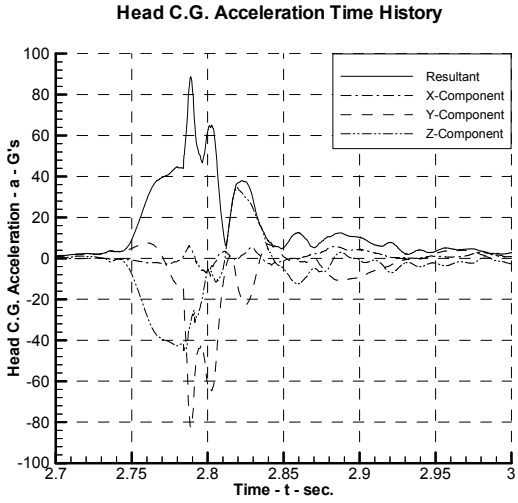

(b)

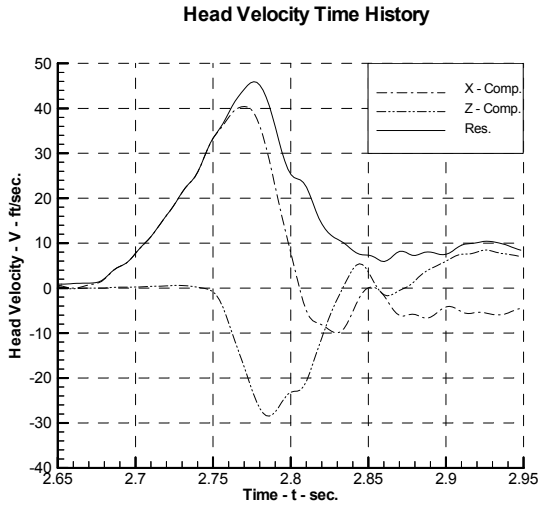

(c)

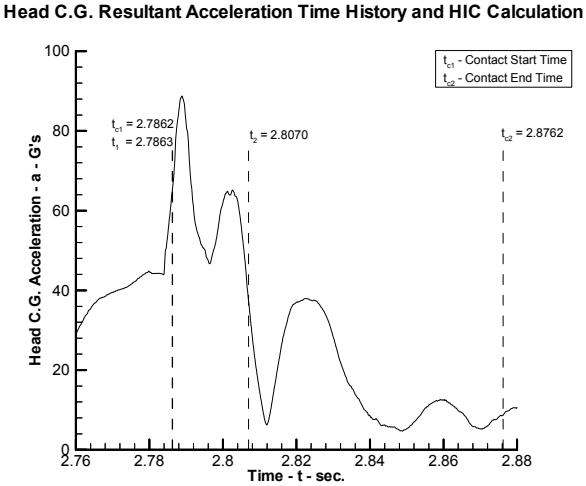

(d)

Results of Sled Test 96288-005

Figure – (a)

Panel – 2024-O aluminum sheet panel of 0.063-in. (0.16-cm) LAST-A-FOAM FR 3502 2 lb/cu.ft thickness 3 in. (7.62 cm)
Seat setback – 34 in. (86.36 cm)
Peak sled deceleration – 16.5 g
Rise time – 86.8 ms
Velocity change – 29.2 ft/s (8.9 m/s)
Velocity change total – 44.8 ft/s (13.65 m/s)

Figure – (d)

Head impact velocity – 45.94 ft/s (14.0 m/s)
Head impact angle – 32°
Head c.g. peak acceleration – 88.75 g
HIC – 619
$\Delta t = t_2 - t_1 = 20.7$ ms

SLED TEST 96288-006

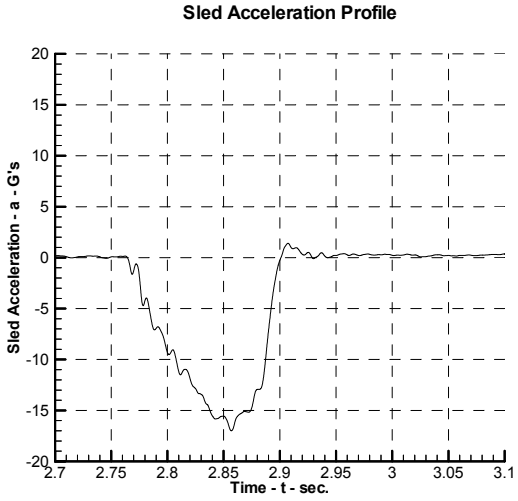

(a)

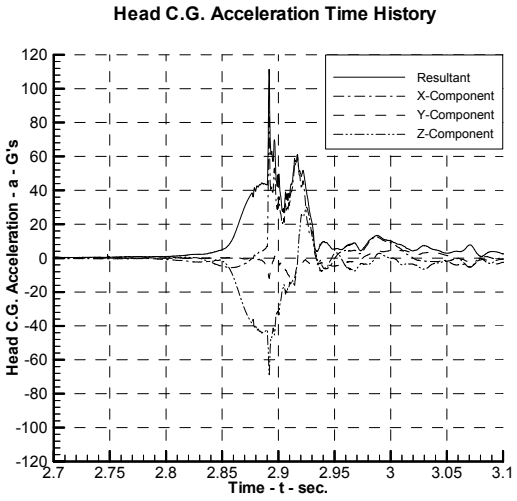

(b)

No Video data is available

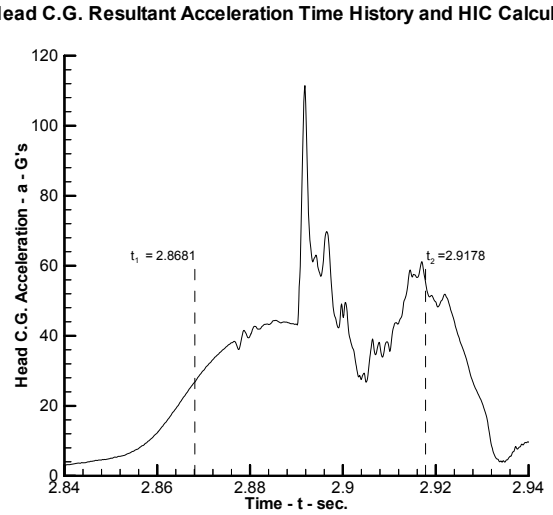

(c)

(d)

Results of Sled Test 96288-006

Figure – (a)

Panel – 2024-O aluminum sheet panel of 0.063 in (0.16 cm)
Seat setback – 34 in. (86.36 cm)
Peak sled deceleration – 17.0 g
Rise time – 79.9 ms
Velocity change – 29.4 ft/s (8.96 m/s)
Velocity change total – 45.2 ft/s (13.78 m/s)

Figure – (d)

Head c.g. peak acceleration – 111.5 g
HIC – 653
$\Delta t = t_2 - t_1 = 49.7$ ms

SLED TEST 96288-007

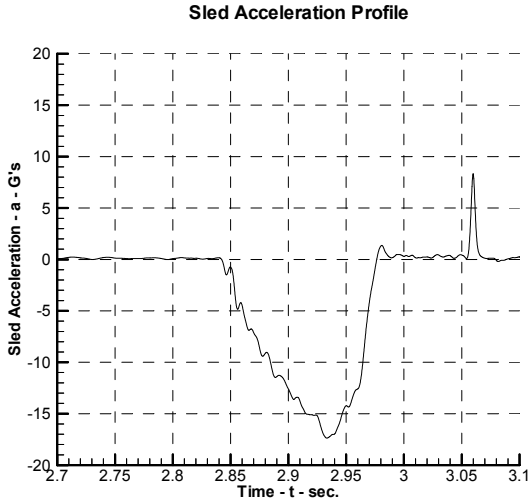

(a)

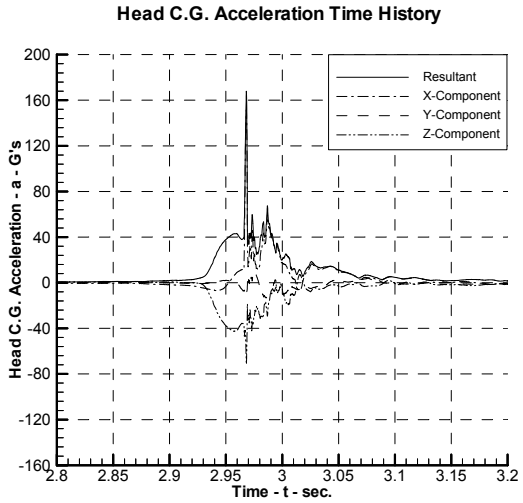

(b)

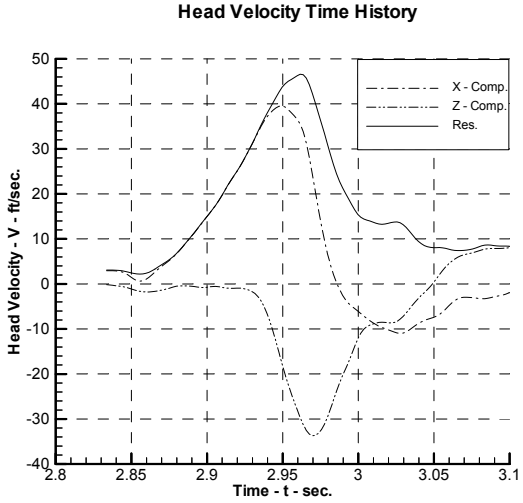

(c)

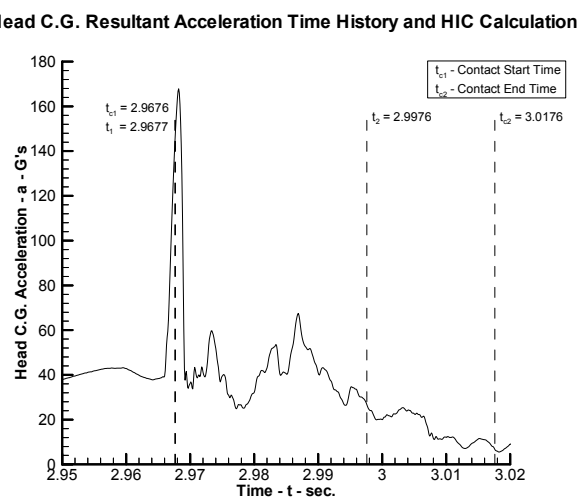

(d)

<u>Results of Sled Test 96288-007</u>

Figure – (a)

Panel – Aluminum sheet panel of 0.063 in. (0.16 cm)
Seat setback – 34 in. (86.36 cm)
Peak sled deceleration – 17.3 g
Rise time – 92.6 ms
Velocity change – 29.0 ft/s (8.84 m/s)
Velocity change total – 45.3 ft/s (13.81 m/s)

Figure – (d)

Head impact velocity – 46.59 ft/s (14.2 m/s)
Head impact angle – 33°
Head c.g. peak acceleration – 167.8 g
HIC – 397
$\Delta t = t_2 - t_1 = 29.9$ ms

SLED TEST 96288-008

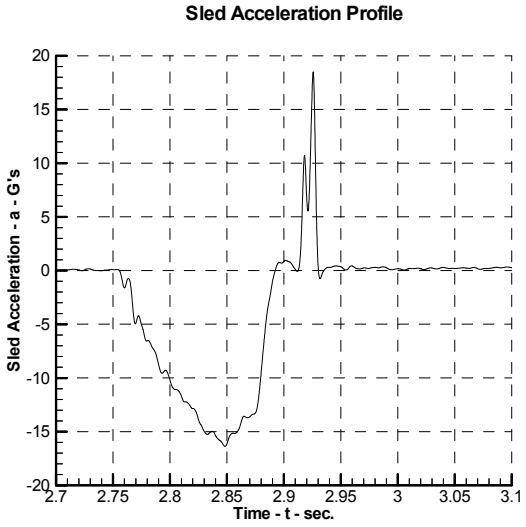

(a)

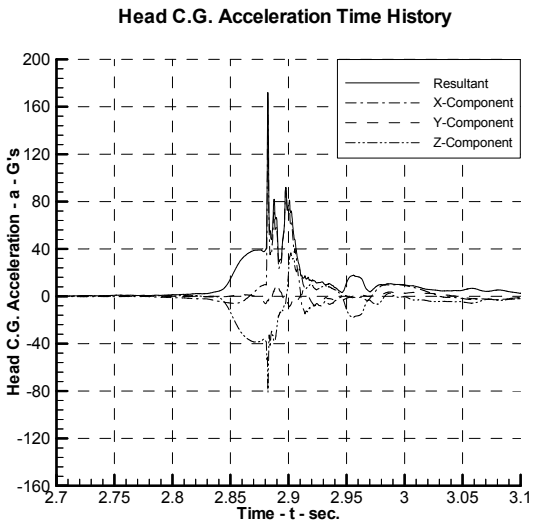

(b)

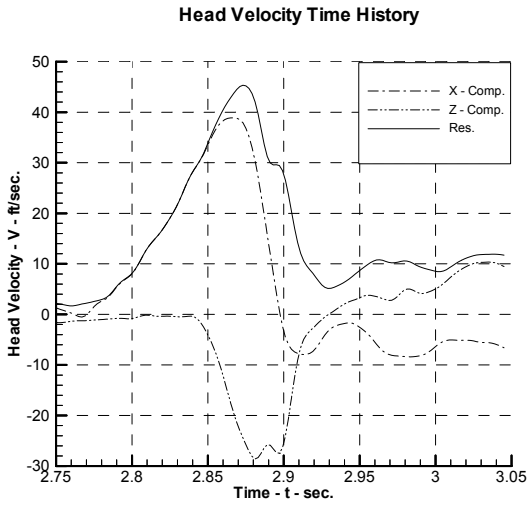

(c)

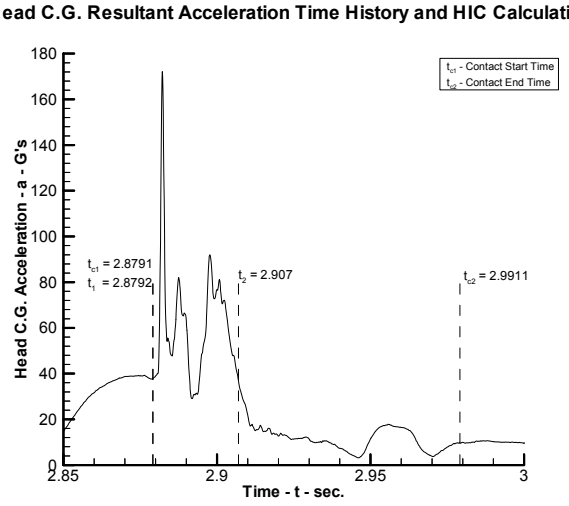

(d)

Results of Sled Test 96288-008

Figure – (a)

Panel – Aluminum sheet panel of 0.063 in. (0.16 cm)
Seat setback – 32 in. (81.28 cm)
Peak sled deceleration – 16.4 g
Rise time – 78.8 ms
Velocity change – 28.8 ft/s (8.78 m/s)
Velocity change total – 44.7 ft/s (13.62 m/s)

Figure – (d)

Head impact velocity – 45.33 ft/s (14.05 m/s)
Head impact angle – 32°
Head c.g. peak acceleration – 171.8 g
HIC – 832
$\Delta t = t_2 - t_1 = 27.8$ ms

SLED TEST 96288-009

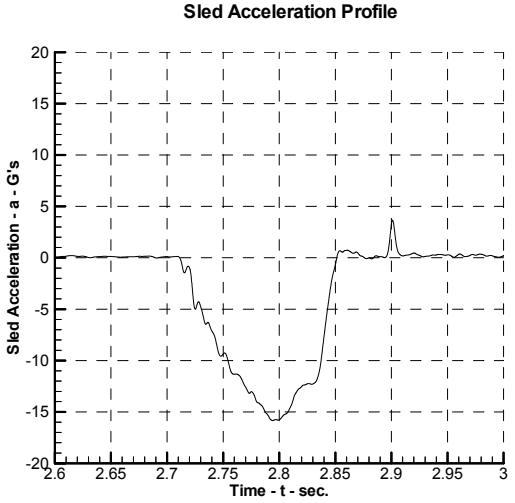

(a)

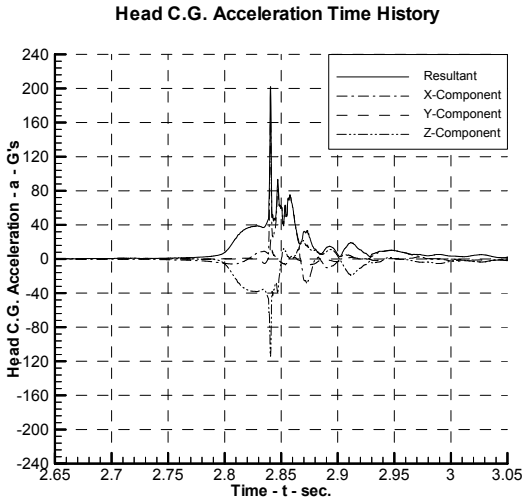

(b)

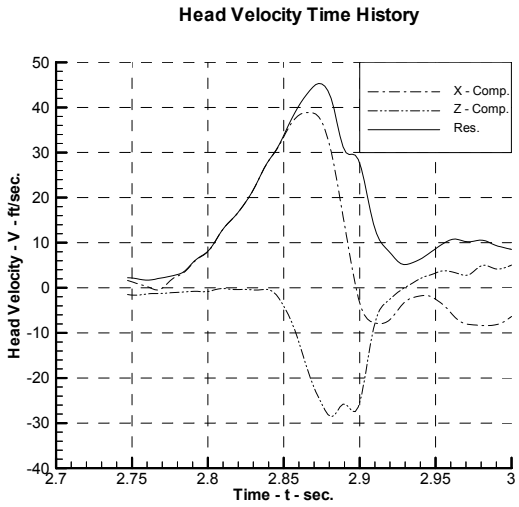

(c)

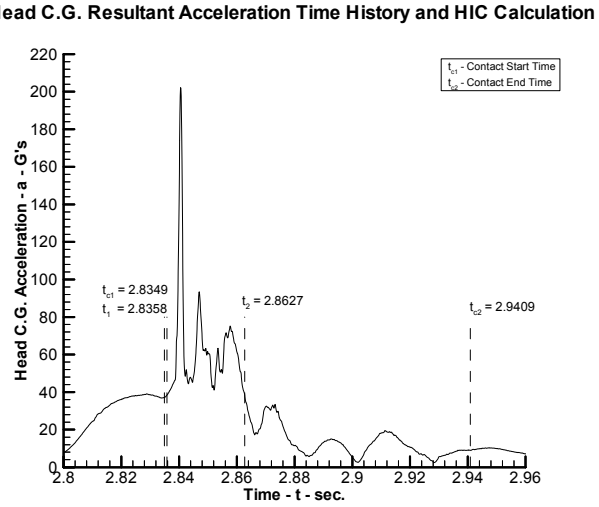

(d)

Results of Sled Test 96288-009

Figure – (a)

Panel – Aluminum sheet panel of 0.063 in. (0.16 cm)
Seat setback – 32 in. (81.28 cm)
Peak sled deceleration – 15.9 g
Rise time – 78.3 ms
Velocity change – 29.1 ft/s (8.87 m/s)
Velocity change total – 45.1 ft/s (13.75 m/s)

Figure – (d)

Head impact velocity – 46.09 ft/s (14.05m/s)
Head impact angle – 32°
Head c.g. peak acceleration – 201.7 g
HIC – 882
$\Delta t = t_2 - t_1 = 26.9$ ms

SLED TEST 96288-010

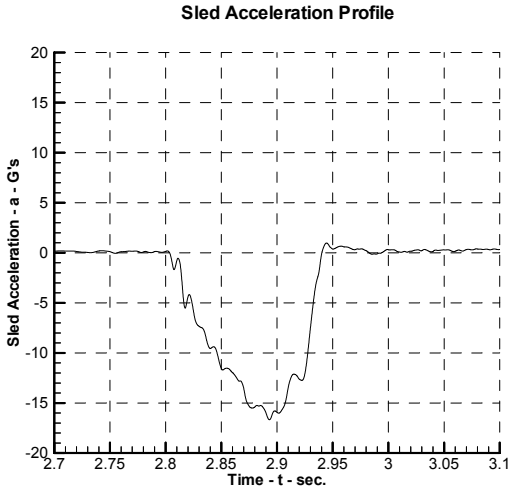

(a)

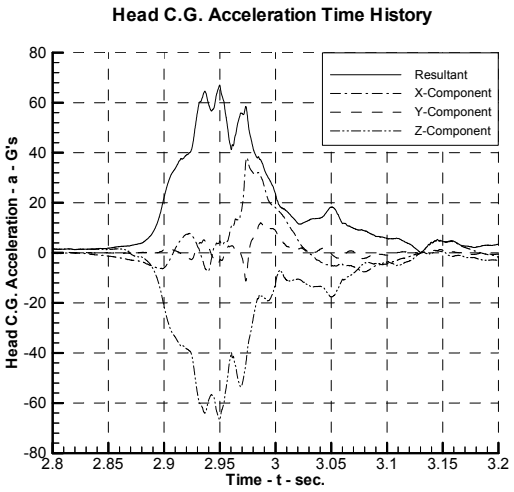

(b)

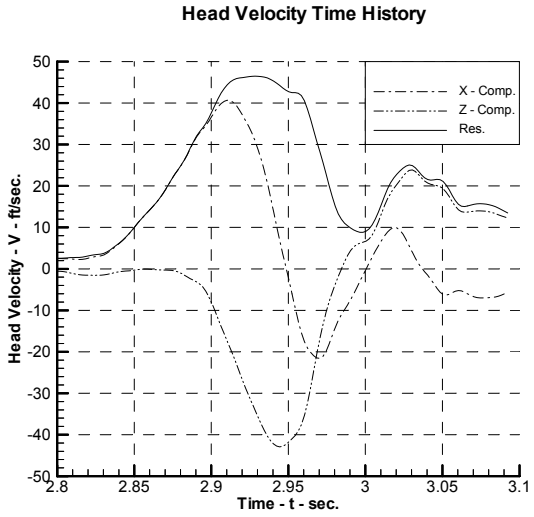

(c)

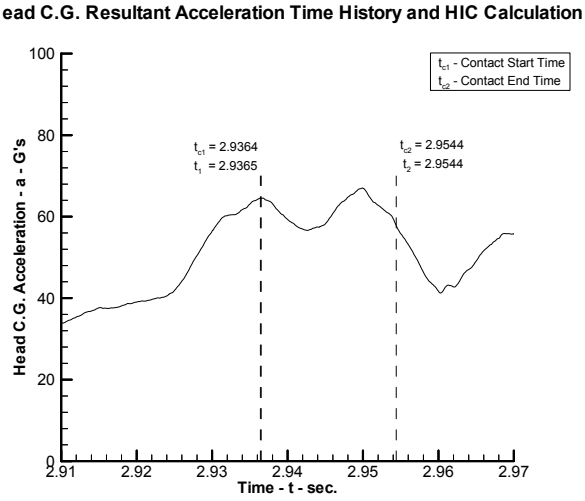

(d)

Results of Sled Test 96288-010

Figure – (a)

Panel – Aluminum sheet panel of 0.063 in. (0.16 cm)
Seat setback – 37 in. (93.98 cm)
Peak sled deceleration – 16.7 g
Rise time – 82.4 ms
Velocity change – 26.1 ft/s (7.95 m/s)
Velocity change total – 45.4 ft/s (13.84 m/s)

Figure – (d)

Head impact velocity – 46.49 ft/s (14.18 m/s)
Head impact angle – 67°
Head c.g. peak acceleration – 66.5 g
HIC – 528
$\Delta t = t_2 - t_1 = 17.9$ ms

SLED TEST 96288-011

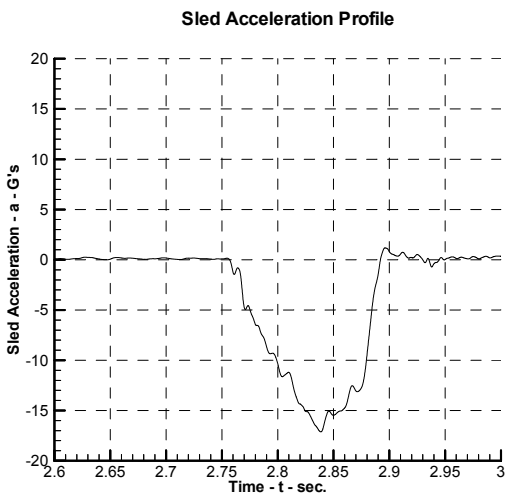

(a)

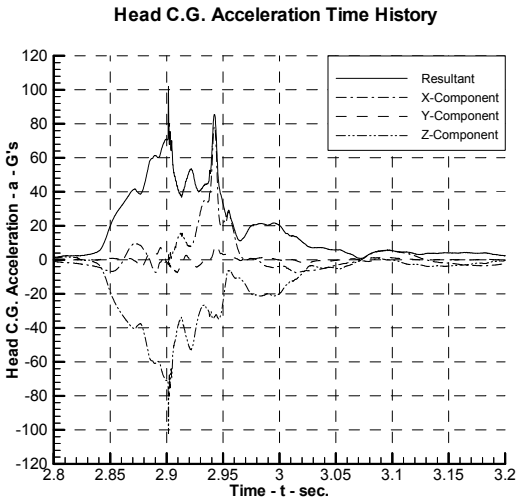

(b)

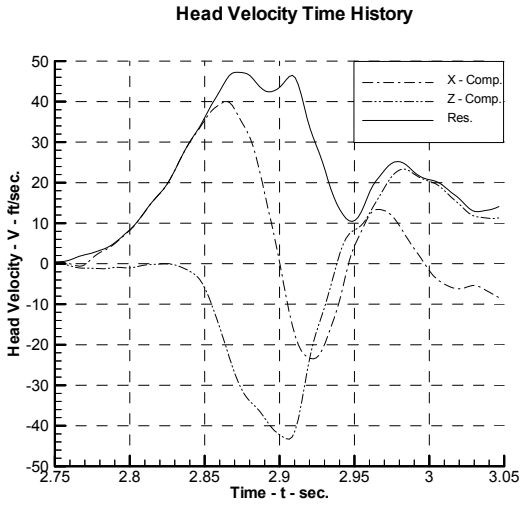

(c)

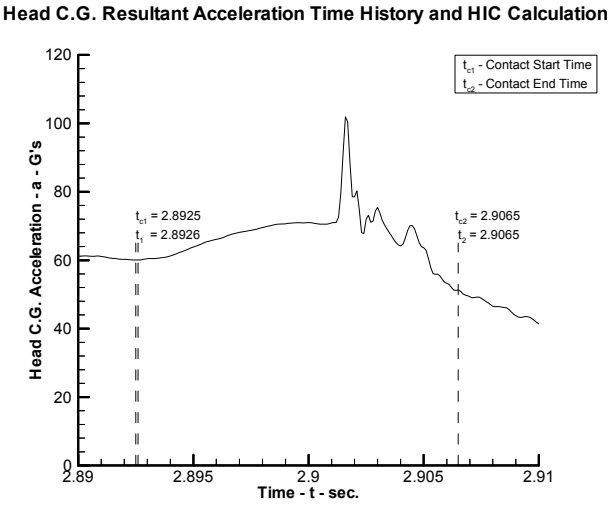

(d)

<u>Results of Sled Test 96288-011</u>

Figure – (a)

Panel – Aluminum sheet panel of 0.063 in. (0.16 cm)
Seat setback – 37 in. (93.98 cm)
Peak sled deceleration – 17.1 g
Rise time – 77.1 ms
Velocity change – 30.3 ft/s (9.24 m/s)
Velocity change total – 45.4 ft/s (13.84 m/s)

Figure – (d)

Head impact velocity – 47.26 ft/s (14.4 m/s)
Head impact angle – 67°
Head c.g. peak acceleration – 101.7 g
HIC – 515
$\Delta t = t_2 - t_1 = 13.9$ ms

SLED TEST 96288-012

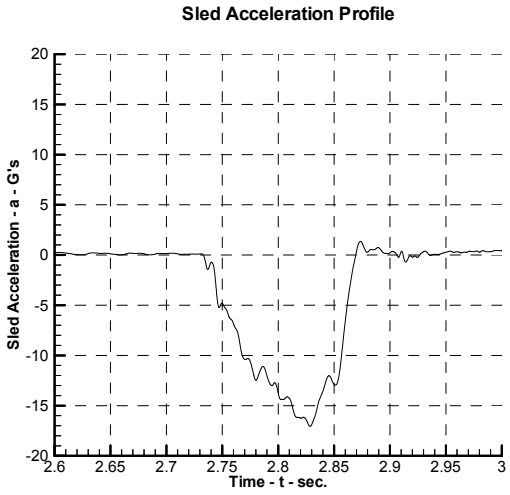

(a)

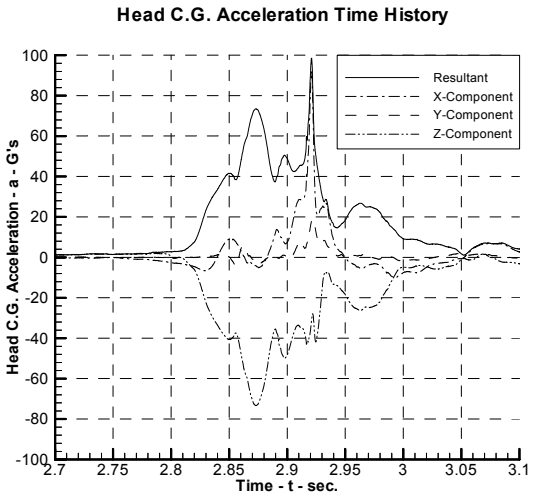

(b)

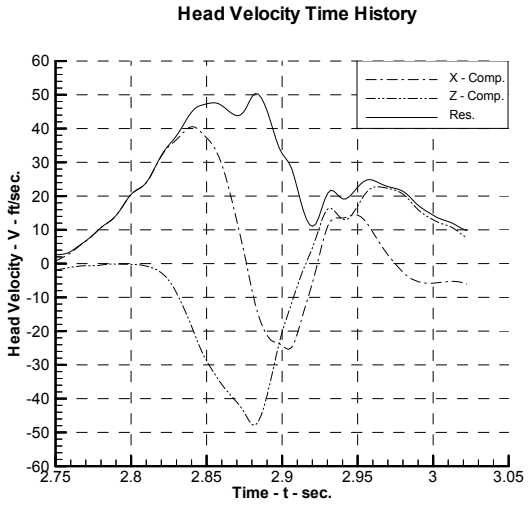

(c)

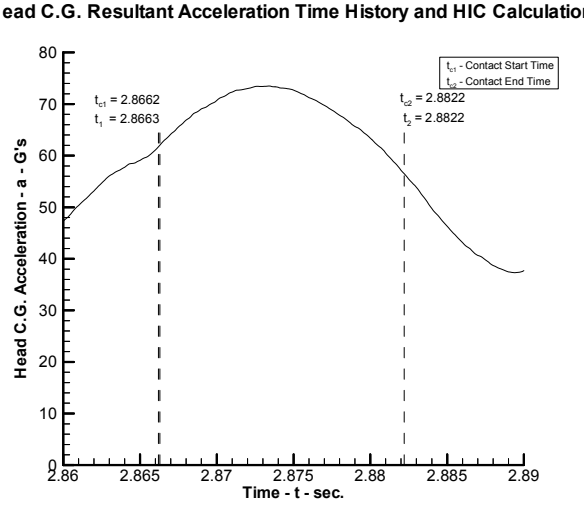

(d)

Results of Sled Test 96288-012

Figure – (a)

Panel – Aluminum sheet panel of 0.063 in. (0.16 cm)
Seat setback – 37 in. (93.98 cm)
Peak sled deceleration – 17.1 g
Rise time – 87.7 ms
Velocity change – 29.2 ft/s (8.9 m/s)
Velocity change total – 45.5 ft/s (13.87 m/s)

Figure – (d)

Head impact velocity – 50.38 ft/s (15.35 m/s)
Head impact angle – 67°
Head c.g. peak acceleration – 73.6 g
HIC – 614
$\Delta t = t_2 - t_1 = 15.9$ ms

SLED TEST 96288-013

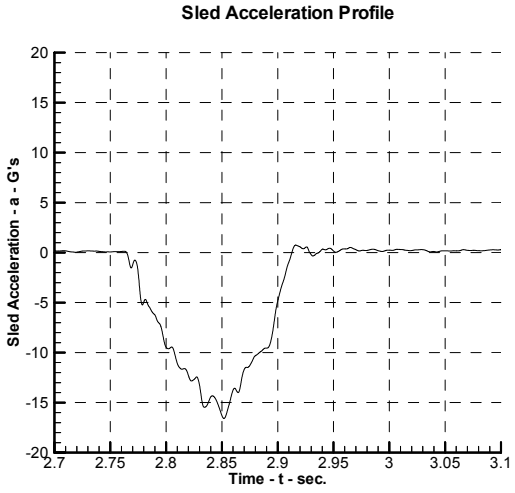

(a)

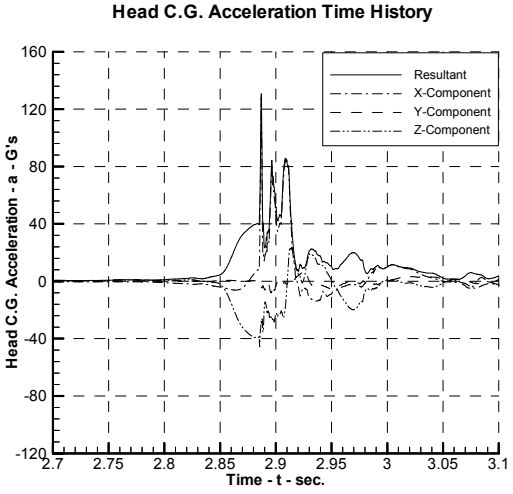

(b)

No Video data is available

(c)

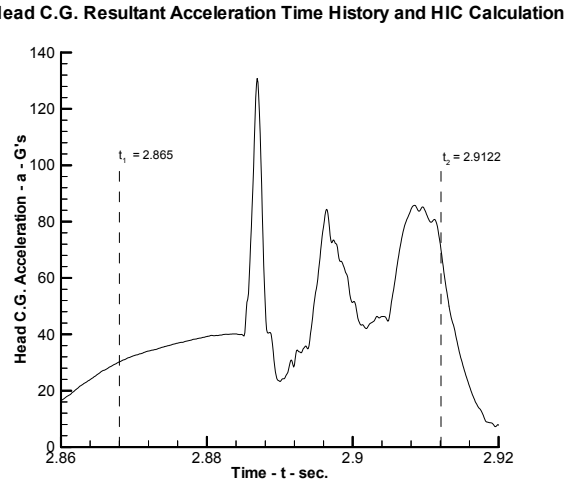

(d)

Results of Sled Test 96288-013

Figure – (a)

Panel – 2024-O aluminum panel of 0.063 in. (0.16 cm)
Seat setback – 32 in. (81.28 cm)
Peak sled deceleration – 16.6 g
Rise time – 71.9 ms
Velocity change – 29.7 ft/s (9.05 m/s)
Velocity change total – 45.3 ft/s (13.81 m/s)

Figure – (d)

Head c.g. peak acceleration – 130.8 g
HIC – 792
$\Delta t = t_2 - t_1 = 47.2$ ms

APPENDIX B—DATA ANALYSIS FOR BULKHEAD SLED TEST SERIES 97191 AND 97204

SLED TEST 97191-001

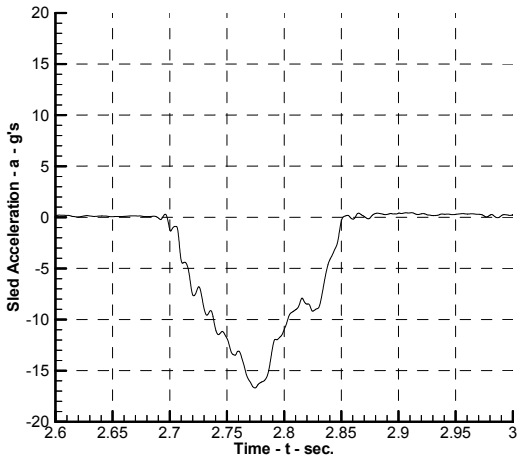

(a)

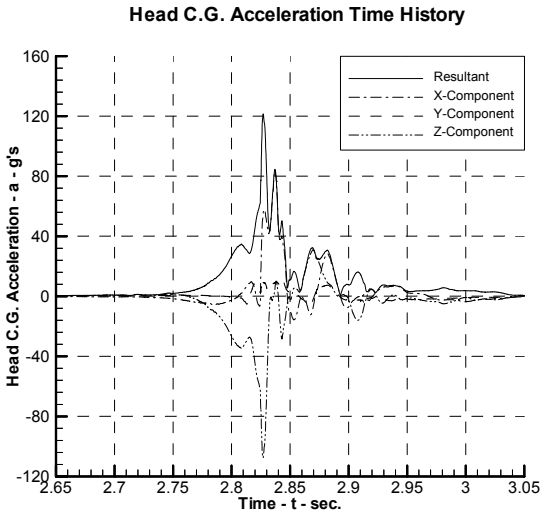

(b)

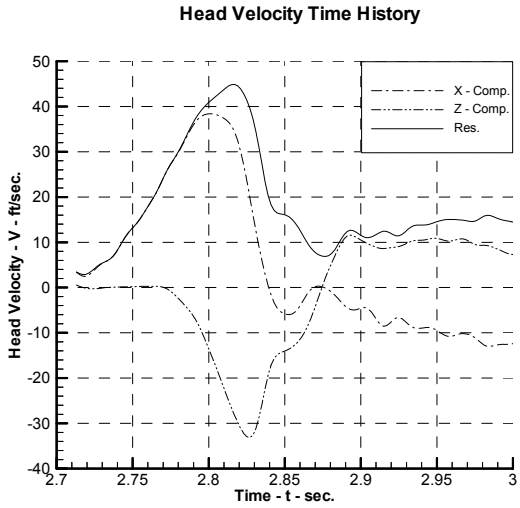

(c)

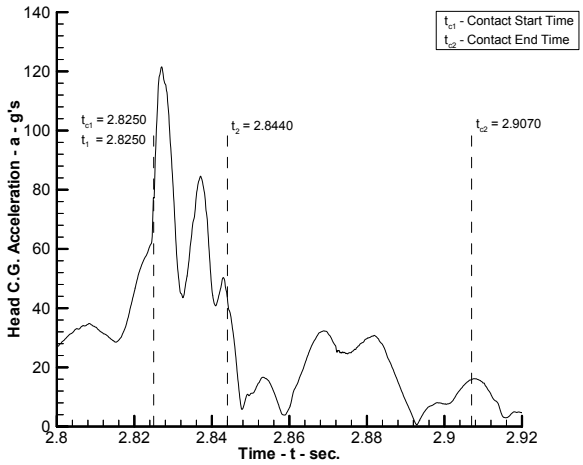

(d)

Results of Sled Test 97191-001

Figure – (a)

Panel – Cabin class divider panel type 2 (unmodified)
Seat setback – 35 in. (88.9 cm)
Peak sled deceleration – 16.7 g
Rise time – 73.3 ms
Velocity change – 30.5 ft/s (9.30 m/s)
Velocity change total – 45.8 ft/s (13.96 m/s)

Figure – (d)

Head impact velocity – 44.87 ft/s (13.68 m/s)
Head impact angle – 53°
Head c.g. peak acceleration – 121.5 g
HIC – 823
$\Delta t = t_2 - t_1 = 19.0$ ms

SLED TEST 97191-002

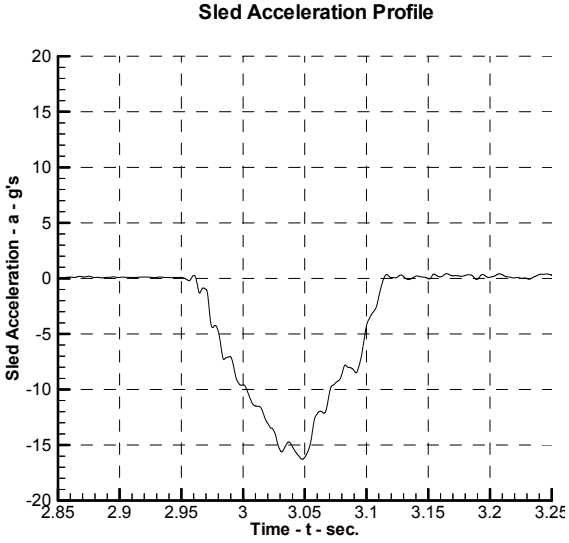

(a)

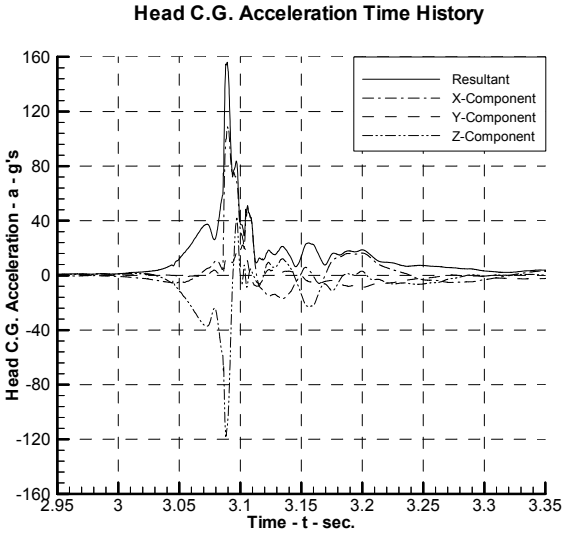

(b)

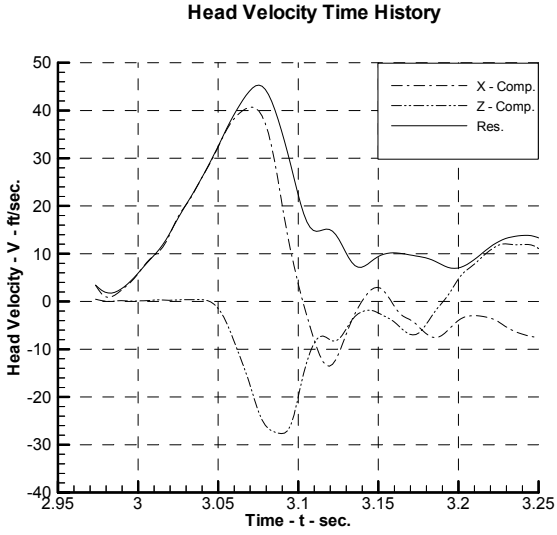

(c)

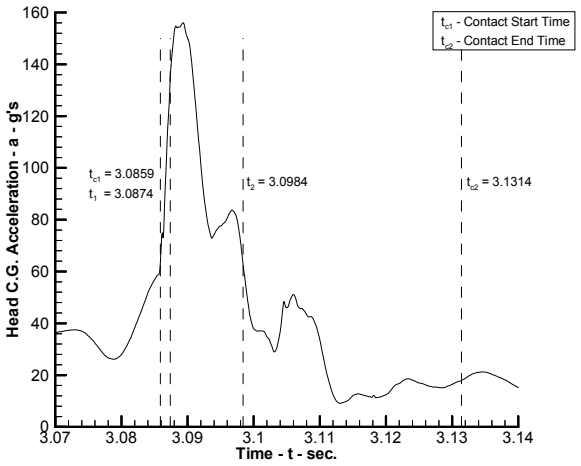

(d)

Results of Sled Test 97191-002

Figure – (a)

Panel – Cabin class divider panel type 2 (unmodified)
Seat setback – 34 in. (86.36 cm)
Peak sled deceleration – 16.3 g
Rise time – 69.8 ms
Velocity change – 30.4 ft/s (9.27 m/s)
Velocity change total – 45.4 ft/s (13.85 m/s)

Figure – (d)

Head impact velocity – 45.32 ft/s (13.82 m/s)
Head impact angle – 42°
Head c.g. peak acceleration – 156 g
HIC – 1394
$\Delta t = t_2 - t_1 = 12.5$ ms

SLED TEST 97191-003

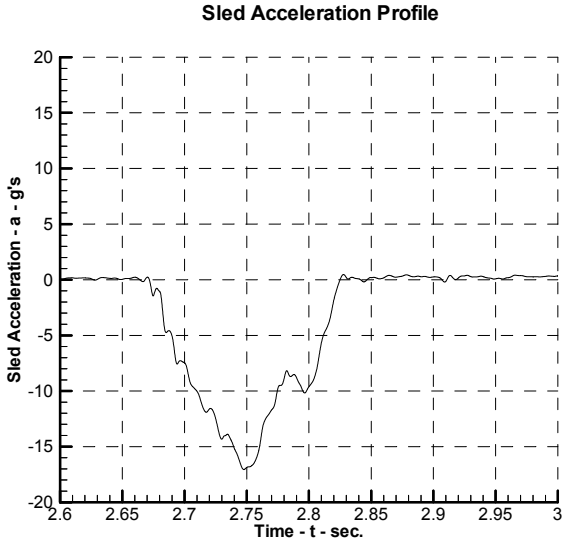

(a)

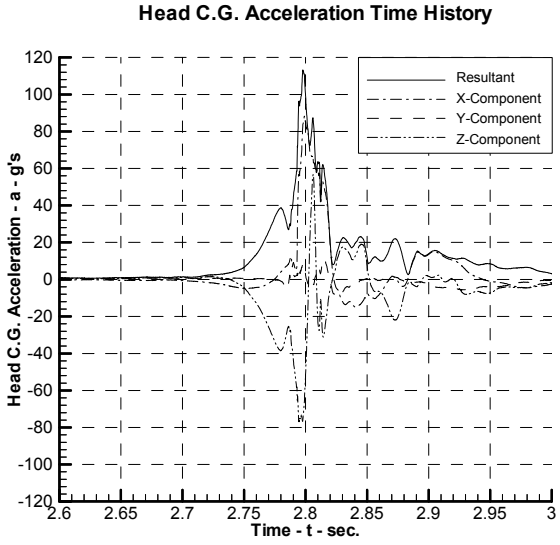

(b)

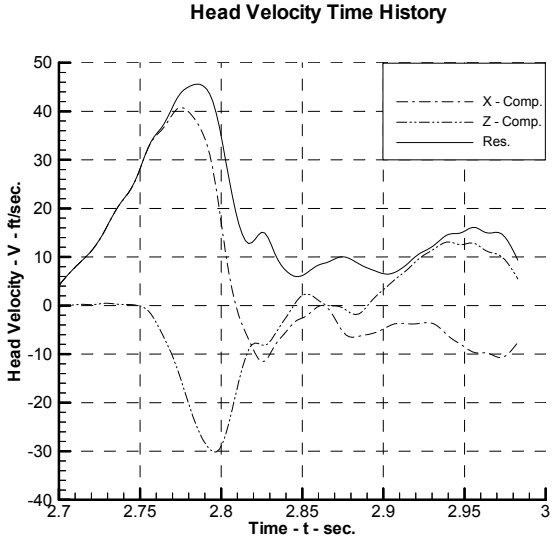

(c)

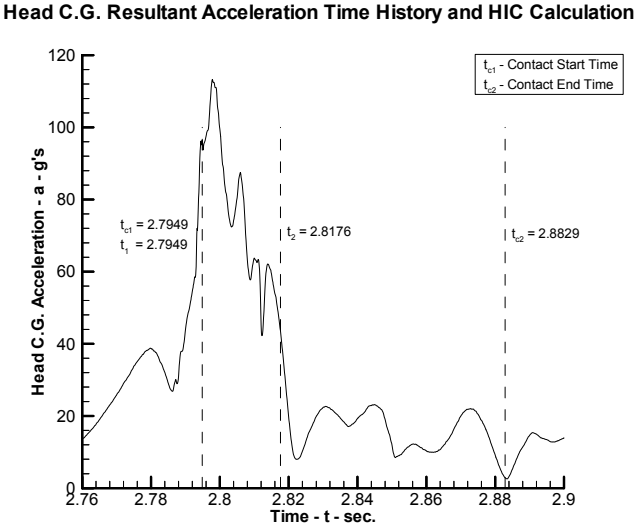

(d)

Results of Sled Test 97191-003

Figure – (a)

Panel – Cabin class divider panel with vertical slits at 4 in. (10.16 cm)
Seat setback – 33 in. (83.82 cm)
Peak sled deceleration – 17.1 g
Rise time – 74.2 ms
Velocity change – 31.3 ft/s (9.54 m/s)
Velocity change total – 46.8 ft/s (14.27 m/s)

Figure – (d)

Head impact velocity – 45.61 ft/s (13.90 m/s)
Head impact angle – 40°
Head c.g. peak acceleration – 113.2 g
HIC – 1132
$\Delta t = t_2 - t_1 = 22.7$ ms

SLED TEST 97204-002

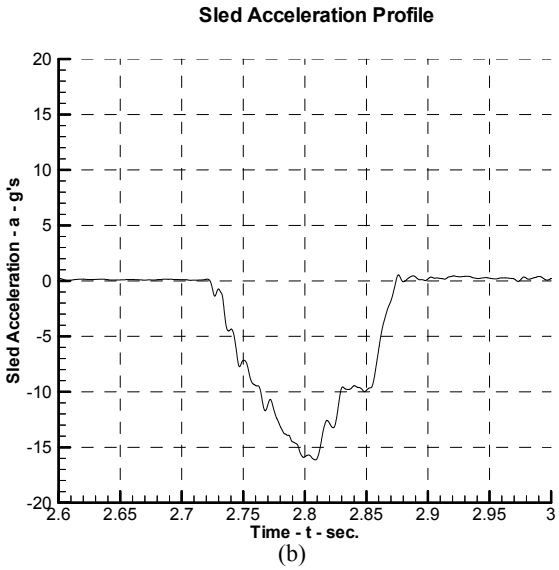

(b)

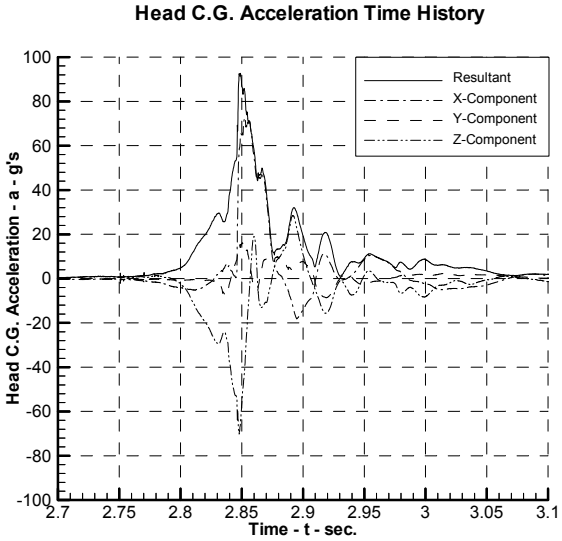

(b)

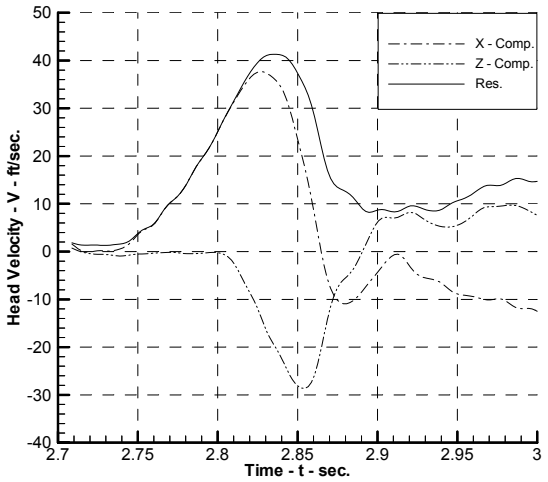

(c)

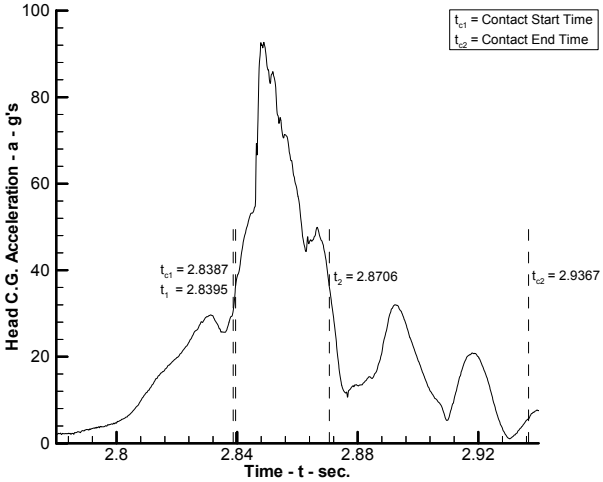

(d)

Results of Sled Test 97204-002

Figure – (a)

Panel – Cabin class divider panel with vertical slits at 4 in. (10.16 cm)
Seat setback – 34 in. (86.36 cm)
Peak sled deceleration – 16.2 g
Rise time – 65.3 ms
Velocity change – 27.73 ft/s (8.45 m/s)
Velocity change total – 42.01 ft/s (12.81 m/s)

Figure – (d)

Head impact velocity – 41.3 ft/s (12.59 m/s)
Head impact angle – 44°
Head c.g. peak acceleration – 93 g
HIC – 882
$\Delta t = t_2 - t_1 = 31.1$ ms

APPENDIX C—DATA ANALYSIS FOR THE BULKHEAD SLED TESTS

Accelerometer and video data for each test is recorded onto a compact disc. For each test, a summary of the data is represented on one page in appendices A and B. The following summarizes the procedure adopted in the data analysis for each test and in calculating the different parameters.

C.1 SLED DECELERATION PROFILE.

For each test, the sled acceleration data, obtained from the Impact Dynamics Laboratory at NIAR, is plotted against time. In the summary page for each test, this is shown in figure (a).

C.2 HEAD c.g. ACCELERATION TIME HISTORY.

The head c.g. acceleration data is obtained from the tri-axis accelerometer placed at the c.g. of the anthropomorphic test dummy (ATD) head. From this, the acceleration time histories in x, y, z and the resultant are obtained. Note that the y axis component is negligible as all the sled tests were conducted with no yaw. In the summary page for each test, this is shown in figure (b).

C.3 HEAD VELOCITY PROFILE.

The head velocity is obtained from the video data. The paths of two target points on the head, one on the top and one on the bottom of the ATD, are tracked. The Impact Dynamic Laboratory calculates the velocities of these target points for each frame. The velocities are calculated from the target point positions using the central difference method. The average position of the two points is used as the position of the head c.g. In the plot, a 10-point moving average smoothing algorithm is used. In the summary page for each test, this is shown in figure (c).

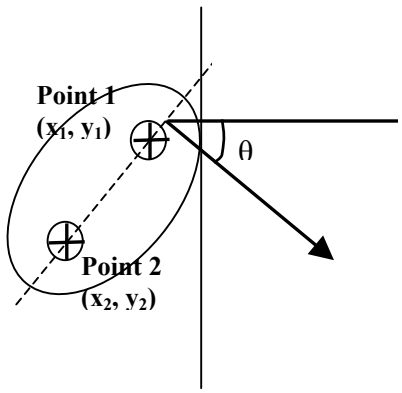

$$X = \frac{x_1 + x_2}{2} \qquad Y = \frac{y_1 + y_2}{2}$$

$$Vx = \frac{X(t + \Delta t) - X(t - \Delta t)}{2\Delta t}$$

$$Vy = \frac{Y(t + \Delta t) - Y(t - \Delta t)}{2\Delta t}$$

$$V = \sqrt{Vx^2 + Vy^2}$$

C.4 CONTACT TIME.

The instants of initial head contact and also departure are noted from the video data and shown in figure (d) of the summary of each test. The video time zero is correlated to the

actual sled time based on the data obtained from the Impact Dynamics Lab. This is done by correlating the video time zero, which is triggered manually, and the time of triggering.

From this, the contact start time and end time are obtained by adding the time obtained from the video with the video time zero.

$$t_{c1} = t_{0v} + t_{vc1}$$
$$t_{c2} = t_{0v} + t_{vc2}$$

where

t_{c1} Contact start time
t_{0v} Video time zero
t_{vc1} Contact start time from video
t_{vc2} Contact end time from video
t_{c2} Contact end time

C.5 HEAD VELOCITY AT THE INITIAL CONTACT TIME.

The head velocity at the contact start time is evaluated following the same procedure of section 3. The resolution of the video data is 2 ms. The velocity at the contact start time and one step prior to it are calculated. The head impact velocity is taken as the average of the two velocities calculated at these two time steps.

C.6 HEAD IMPACT ANGLE.

The head impact angle is calculated using the video data. The slope of the line joining the two target points on the ATD head is calculated. From the slope, the head impact angle is calculated.

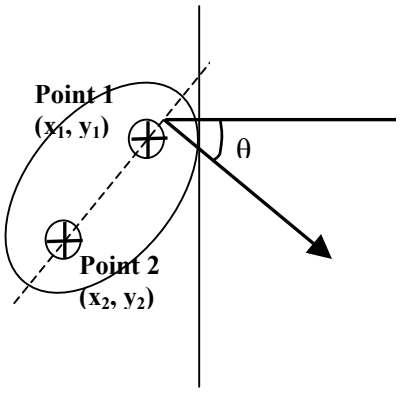

$$\theta = \frac{\pi}{2} - \tan^{-1}\left(\frac{y_2 - y_1}{x_2 - x_1}\right) \quad \text{(Radians)}$$

θ is converted to degrees and this gives the head impact angle. The head angle at the contact start time and one step prior to it are calculated. The head impact angle is taken as the average of the angles calculated at these two time steps.

C.7 HEAD IINJURY CRITERIA.

According to the FAR, the head injury criteria (HIC) is calculated for the duration of the head contact only, not the entire head acceleration profile. Note that HIC is quite sensitive to small variations in the window size.